THE UNIVERSITY OF QUEENSLAND

AUSTRALIA

Functional and comparative studies of members of the genus *Methanosphaera*, and their adaptations to the gut environment

Emily Cornelia Hoedt

Bachelor of Biotechnology

Major in Microbiology Biotechnology

Honours Class I

A thesis submitted for the degree of Doctor of Philosophy at

The University of Queensland in 2016

School of Chemistry and Molecular Biosciences

Abstract

The methanogenic archaea are responsible for maintaining an efficient scheme of fermentation in many environments and habitats, including the gastrointestinal tracts of animals and humans. The principal members of gut methanogenic communities are members of the *Methanobrevibacter* genus, with lesser numbers of *Methanosphaera* and *Methanomassiliicoccus* spp. Much of our understanding of gut methanogens has been produced using axenic cultures and genomic data for ~30 *Methanobrevibacter* spp. but the functional relevance of these other archaeal lineages to digestive function remains poorly understood. With this background, the goals of my PhD research are: i) to increase the biotic representation of the *Methanosphaera* genus through the recovery of axenic isolates from different environments; ii) characterise the metabolic properties of these isolates in terms of their methanogenic pathways and; iii) expand our functional understanding of this genus via reconstruction of "population genomes" from existing metagenomic datasets and comparative genome analyses. During the latter stages of my PhD, I chose to make a transition in my research activities to include some biomedical focus and take advantage of my relocation to the University of Queensland Diamantina Institute. Here, I have examined variations in methanogenic archaeal populations in some clinical studies, as well as evaluated the immunostimulatory properties of some gut archaea.

Chapter Two describes the enrichment, isolation, and pathways of methane formation by a strain of *Methanosphaera* sp. (WGK6) recovered from the Western Grey kangaroo (*Macropus fulginosus*). In contrast with the human isolate, strain WGK6 was found to utilize ethanol to support growth, but principally as a source of reducing power. Both the WGK6 and *Msp. stadtmanae* DSMZ 3091^{T} genomes are very similar in terms of their size (~1.7 Mbp), synteny, and G:C content. However, the WGK6 genome was found to encode contiguous genes encoding putative alcohol- and aldehyde- dehydrogenases, which are absent from the *Msp. stadtmanae* genome. These two genes provide a plausible explanation for the ability of WGK6 to utilize ethanol for methanol reduction to methane. Furthermore, my *in vitro* studies suggest that ethanol supports a greater cell yield per mol of methane formed compared to hydrogen-dependent growth. Taken together, this expansion in metabolic versatility can explain the persistence of these archaea in the kangaroo foregut, and their abundance in these "low methane emitting" herbivores.

Chapter Three describes the isolation of a hydrogen-dependent methylotrophic archaeon assigned to the *Methanosphaera* genus from bovine animals in northern Australia (strain BMS). The BMS genome was sequenced to closure and surprisingly, found to be substantially larger (2.9 Mbp) than the WGK6 and *Msp. stadtmanae* genomes (~1.8 Mbp). I then interrogated metagenomic datasets produced from human stool and ruminant digesta samples, to recover 7 "population genomes" assigned to the *Methanosphaera* genus, with 5 of these genomes also predicted to be large (> 2.1 Mbp). The *Methanosphaera* pan-genome consists of 5321 genes and 305 of these were assigned to the core-genome, which principally consists of the genes coordinating methanogenesis, anaerobic metabolism, and related functions. The whole genome phylogeny analysis of all genomes suggests a monophyletic origin for the genus *Methanosphaera*, with those isolates possessing smaller genomes being the most recently evolved lineages.

Chapter Four investigates whether and how the composition of the methanogenic archaea in patients with chronic kidney disease is altered in response to synbiotic administration, as an intervention designed to mitigate uremic toxin production. The synbiotic intervention was found to have no measurable impact on the methanogen profiles of the patients, with *Methanobrevibacter smithii* the predominant archaeon and an infrequent occurrence of *Methanomassiliicoccus*, but no detectable populations of *Methanosphaera* spp. I also have assessed the immunogenic properties of *Mbb. smithii* DSMZ 861^T, *Msp. stadtmanae* DSMZ 3091^T, *Mbb. ruminantium* DSMZ 1093^T, and my new *Methanosphaera* isolates, using human peripheral blood mononuclear cells (PBMC) and a mouse macrophage cell line. I first showed that *Msp. stadtmanae* DSMZ 3091^T cell preparations produce a stronger TNF-α response from PBMC than *Mbb. smithii* DSMZ 861^T, as well as the other *Methanosphaera* isolates WGK6 and BMS, but *Mbb. ruminantium* DSMZ 1093^T cells produced the strongest TNF-α response. In subsequent studies using methanogen cell preparations and different sources of PBMC (also from healthy subjects) I measured the release of a broader range of cytokines, using a multi-bead array and flow cytometry techniques. In these studies, *Mbb. smithii* DSMZ 861^T was more immunogenic compared to *Msp. stadtmanae* DSMZ 3091^T, but both types of cells induce a similar cytokine profile from the PBMC preparations. Last, I used a murine macrophage cell line bearing a reporter gene activated by the NF-κB transcription system, which further confirmed that cell preparations of all these archaea induce reporter gene activation via this important pathway of stress response. Collectively, these results suggest all these methanogens possess immunostimulatory properties that remain cell

associated, and the findings are discussed with respect to gastrointestinal inflammation and also the development of anti-methanogen vaccines.

Chapter 5 provides an integrative overview of the findings arising from my research, which provide a deeper understanding into the genus *Methanosphaera*, in terms of its evolutionary development, nutritional ecology, and host adaptation. I believe my findings are novel and provide new insights into the role of methanogenic archaea in gut function; and this knowledge will be useful to address key challenges facing agriculture (e.g. methane abatement strategies) and human health (e.g. as triggers of inflammation and immune response in gut and respiratory disease).

Declaration by author

This thesis is composed of my original work, and contains no material previously published or written by another person except where due reference has been made in the text. I have clearly stated the contribution by others to jointly-authored works that I have included in my thesis.

I have clearly stated the contribution of others to my thesis as a whole, including statistical assistance, survey design, data analysis, significant technical procedures, professional editorial advice, and any other original research work used or reported in my thesis. The content of my thesis is the result of work I have carried out since the commencement of my research higher degree candidature and does not include a substantial part of work that has been submitted to qualify for the award of any other degree or diploma in any university or other tertiary institution. I have clearly stated which parts of my thesis, if any, have been submitted to qualify for another award.

I acknowledge that an electronic copy of my thesis must be lodged with the University Library and, subject to the policy and procedures of The University of Queensland, the thesis be made available for research and study in accordance with the Copyright Act 1968 unless a period of embargo has been approved by the Dean of the Graduate School.

I acknowledge that copyright of all material contained in my thesis resides with the copyright holder(s) of that material. Where appropriate I have obtained copyright permission from the copyright holder to reproduce material in this thesis.

Publications during candidature

Published peer-reviewed papers

Hoedt EC, Ó Cuív P, Evans PN, Smith WJM, McSweeney C, Denman SE, and Morrison M (2016). Differences down-under: alcohol-fuelled methanogenesis by archaea present in Australian macropodids. *ISME Journal* DOI: 10.1038/ismej.2016.41. Writing from this manuscript has been incorporated into Chapter 2.

Published peer-reviewed literature reviews

Hoedt EC, Evans PN, Denman SE, McSweeney C, Ó Cuív P, and Morrison M (2015). Methane matters in animals and man: from beginning to end. *Microbial Australia* 36:4 DOI: 10.1071/MA15003. Writing from this manuscript has been incorporated into Chapter 1.

Hoedt EC, Ó Cuív P, and Morrison M (2016). Methane Matters: from blue-tinged moos, to boozy roos, and the health of humans too. *Animal Frontiers* 6:3 DOI 10.2527/af.2016-0029. Writing from this manuscript has been incorporated into Chapter 1, 4 and 5.

Conference abstracts

Hoedt EC, Smith W, Evans P, Ó Cuív P and Morrison M: An ethanol-dependent pathway of methanol reduction to methane in a newly isolated *Methanosphaera* sp. from the Western Grey kangaroo. 4th ASM Conference on Beneficial Microbes, 2012 Oct. 22 – 26; San Antonio, TX, USA.

Hoedt EC, Ó Cuív P, and Morrison M: Newly isolated *Methanosphaera* sp. and *Methanoplasmatales sp.* from Australian bovine. CGIF Congress on Gastrointestinal Function, 2013 April 15-17; Chicago, USA. QAAFI Animal Science Olympics, 2013 July 26; Brisbane, Australia.

Hoedt EC, Ó Cuív P, and Morrison M: Newly isolated *Methanosphaera* sp. and *Methanoplasmatales sp.* from Australian bovine. MLA postgraduate student conference, 2013 October 4-7; Coffs Harbor, Australia.

Hoedt EC, Ó Cuív P, Evans P, Denman SE, Smith W, and Morrison M: The foregut microbiota of kangaroos include methylotrophic methanogens that can also use ethanol to

support methanogenesis and growth. ISME 15 conference, 2014 August 24-29; Seoul, South Korea.

Hoedt EC, Ó Cuív P, Wheeler L, Lacaze P, and Morrison M: A novel isolate of *Methanosphaera* sp. isolated from cattle possesses a large genome compared to methanogens isolated from other gut environments. MLA postgraduate student conference, 2014 November 2-6; Manly, NSW, Australia.

Hoedt EC, Ó Cuív P, Park DH, Tyson GW and Morrison M, Expansion of the genus *Methanosphaera* reveals a greater metabolic versatility relevant to host adaptation. MLA postgraduate student conference, 2015 November 1-5; Manly, NSW, Australia.

Publications included in this thesis

Hoedt EC, Evans PN, Denman SE, McSweeney C, Ó Cuív P, and Morrison M (2015). Methane matters in animals and man: from beginning to end. *Microbial Australia* 36:4 doi: 10.1071/MA15003. Writing from this manuscript has been incorporated into Chapter 1.

Contributor	**Statement of contribution**
Author Hoedt EC (Candidate)	Wrote the paper (50%)
Author Evans PN	Edited paper (5%)
Author Denman SE	Edited paper (5%)
Author McSweeney C	Edited paper (5%)
Author Ó Cuív P	Edited paper (5%)
Author Morrison M	Wrote and edited paper (30%)

Hoedt EC, Ó Cuív P, Evans PN, Smith WJM, McSweeney C, Denman SE, and Morrison M (2016). Differences down-under: alcohol-fuelled methanogenesis by archaea present in Australian macropodids. *ISME Journal* doi: 10.1038/ismej.2016.41. Writing from this manuscript has been incorporated into Chapter 2.

Contributor	**Statement of contribution**
Author Hoedt EC (Candidate)	Designed experiments (60%)

	Wrote the paper (70%)
Author Ó Cuív P	Designed experiments (5%)
Author Evans PN	Designed experiments (5%)
Author Smith WJM	Illumina 454 genome preparation
Author McSweeney C	Supported research
Author Denman SE	Assembled Illumina 454 output
Author Morrison M	Designed experiments (30%) Wrote and edited paper (30%)

Hoedt EC, Ó Cuív P, and Morrison M (2016). Methane Matters: from blue-tinged moos, to boozy roos, and the health of humans too. *Animal Frontiers* 6:3 DOI 10.2527/af.2016-0029. Writing from this manuscript has been incorporated into Chapter 1, 4 and 5.

Contributor	**Statement of contribution**
Author Hoedt EC (Candidate)	Wrote the paper (60%)
Author Ó Cuív P	Edited paper (10%)
Author Morrison M	Wrote and edited paper (30%)

Contributions by others to the thesis

Dr Paul Evans collected Western Grey kangaroo digesta samples in 2008 used for isolation work, Wendy Smith assisted with the 454 sequencing of *Methanosphaera* sp. WGK6 and Dr Stuart Denman assembled the resulting genomic data in Chapter 2. Dr Páraic Ó Cuív assembled the PacBio sequence data for *Methanosphaera* sp. BMS genome in Chapter 3. Dr Anh Do assisted with the calibration of the BD LSR II fluorescence-assisted cell sorter and Sian Pottenger cultured the RAW264.7 macrophage cell line in preparation for assay work detailed in Chapter 4. All work presented here was critically revised by my primary supervisor Prof. Mark Morrison.

Statement of parts of the thesis submitted to qualify for the award of another degree

The content presented in Chapter Two, page 17 paragraph 3 to page 21 paragraph 1 has also been presented as part of a BSc Honours at the University of Queensland with the degree awarded on the 19th December 2011.

Acknowledgements

To my supervisors, I am so grateful for all the guidance and support given to me over the years. Words cannot express how grateful I am to my primary supervisor Professor Mark Morrison for accepting me into his group when I was just an undergraduate and providing me invaluable mentorship over the years, I couldn't have achieved what I have without it. To Dr Phil Hugenholtz and Dr Gene Tyson I'm very grateful for their support and openness to discuss any new ideas as well as their invaluable scientific experience.

To the people working at CSIRO, thank you all for your support and friendship over the years. Special mentions to go to Dr Stuart Denman for advice on many different technical aspects; Chris McSweeney for allowing me to stick around the lab even after my move to UQ Diamantina Institute at the Translational Research Institute. Jane Cheung, Wendy Smith and Leanne Dierens also deserve honourable mentions for their friendship, help and chocolate over the years.

To everyone within Diamantina Institute I am very grateful for your support, but a special mention goes to Dr Páraic Ó Cuív for the many discussions of scientific ideas over the years. This thank you also extends to Dr Erin Shanahan, Dr Anh Do, Dr Ashok Raj and Sian Pottenger for jumping into the world of immunology with me. I would also like to thank everyone at Australian Centre for Ecogenomics for teaching me the computational aspects of biology, in particular Donovan Parks, Rochelle Soo, Caitlin Singleton and Nancy Lachner. Paul Evans deserves an extra special mention for teaching me anaerobic techniques and remaining sane after all the years of questions.

To my family and friends all of your love, support and food over the years are responsible for keeping me on track during this emotional rollercoaster; I couldn't have done it without all of you. From the very bottom of my heart thank you.

Finally, I gratefully acknowledge the scholarships provided by the University of Queensland Australian Postgraduate Award system as well as the Meat and Livestock Industry for also providing a top-up and technical assistances grant without which my PhD would not have been possible.

Keywords

methanogen, methane, macropodid, ruminant, human, Methanosphaera, population genome, pan-genome, immunostimulatory

Australian and New Zealand Standard Research Classifications (ANZSRC)

ANZSRC code: 060503 Microbial Genetics, 20%

ANZSRC code: 060309 Phylogeny and Comparative Analysis, 30%

ANZSRC code: 060599 Microbiology not elsewhere classified, 50%

Fields of Research (FoR) Classification

FoR code: 0603 Evolutionary Biology, 20%

FoR code: 0604 Genetics, 20%

FoR code: 0605 Microbiology, 60%

Table of contents

List of figures in the thesis

List of tables in the thesis

List of abbreviations used in the thesis

ΔG°’	Gibbs free energy
µ	specific growth rate
µg	microgram
µL	microliter
μ_{max}	maximal growth rate
16S rRNA	16S ribosomal RNA
AA	auxiliary activity
alc	alcohol dehydrogenase
ald	aldehyde dehydrogenase
ANI	average nucleotide identity
asd	aspartate dehydrogenase
BLASTn	basic local alignment search tool- nucleotide
BLASTp	basic local alignment search tool- protein
BMS	Brahman *Methanosphaera* isolate
bp	base pair
BRN-RF10	Balch – 10% rumen fluid medium
BRN-RF30	Balch – 30% rumen fluid medium
BSA	bovine serum albumin
CAZyme	carbohydrate-active enzymes
CBM	carbohydrate-binding module
cDNA	complementary DNA
CE	Carbohydrate esterase
CH_3CH_2OH	ethanol
CH_3CHO	acetaldehyde
$CH_3CO_2^-$	acetate
CH_3OH	methanol
CH_3-S-CoM	2-(methylthio)ethanesulfonic acid
CH_4	methane
CKD	chronic kidney disease
COG	clusters of orthologous groups
CoM-S-S-CoB	coenzyme M-HTP heterodisulfide
CSIRO	Commonwealth scientific and industrial research organisation
DEW79	diabetic European women *Methanosphaera* population genome 79

DGGE	denaturing gradient gel electrophoresis
DSMZ 1093^T	*Methanobrevibacter ruminantium* strain M1
DSMZ 3091^T	*Methanosphaera stadtmanae*
DSMZ 861^T	*Methanobrevibacter smithii* strain PS
e^-	electron
EDGAR	efficient database framework for comparative genome analyses using BLAST score ratios
EDTA	ethylenediaminetetraacetic acid
ehaRST	energy conserving hydrogenase
ESRD	end stage renal disease
fno	F_{420}:NADP oxidoreductase
frhADGB	F_{420}-reducing hydrogenase complex
GC	gas chromatograph
GDH	glutamate dehydrogenase
GH	glycoside hydrolase
GS1	glutamine synthetase gene Type 1
GS-GOGAT	glutamine synthetase-glutamate synthase pathway
GT	glycosyltransferase
H^+	hydrogen proton
H_2	hydrogen
H_2O	water
HdrABC	heterodisulfide reductase
HS-CoB	coenzyme B
HS-CoM	coenzyme M
hyp	hypothetical protein
IBD	inflammatory bowel disease
IBS	irritable bowel syndrome
IBS-C	irritable bowel syndrome- constipation
IBS-D	irritable bowel syndrome- diarrhoea
IBS-M	irritable bowel syndrome- both constipation and diarrhoea
IFNα	interferon alpha
IFNγ	interferon gamma
IgG	immunoglobulin G
IHT	interspecies hydrogen transfer

IL-10	interleukin-10
IL-12p70	interleukin-12 p70
IL-17A	interleukin-17A
IL-18	interleukin-18
IL-1β	interleukin-1β
IL-23	interleukin-23
IL-33	interleukin-22
IL-6	interleukin-6
IL-8	interleukin-8
JTT	Jones-Taylor-Thornton
Kb	kilo bases
KEGG	Kyoto Encyclopedia of Genes and Genomes
KJ/mol	kilo joules per mole
kPa	kilo pascal
K_S	substrate affinity
LPS	lipopolysaccharide
map	methionine aminopeptidase
Mbb.	*Methanobrevibacter*
Mbp	mega base pair
MCP-1	monocyte chemoattractant protein-1
mL	millilitre
mM	millimolar
Mms.	*Methanomassiliicoccus*
moDCs	monocyte-derived dendritic cells
mrtABG	methyl-coenzyme M reductase
Msp.	*Methanosphaera*
MtaABC	coenzyme M methyltransferase
mtaB1	methanol-cobalamin methyltransferase
MvhADG	non-F420-reducing hydrogenase
NADPH	nicotinamide adenine dinucleotide phosphate-oxidase
NAFLD	non-alcoholic fatty liver disease
NCBI	national centre for biotechnology information
NF-κB	nuclear factor- kappa beta
nifH	nitrogenase reductase

nm	nanometres
OD_{600}	optical density at 600nm
omp	outer membrane protein
PBMC	peripheral blood mononuclear cells
PBS	phosphate-buffered saline
PCR	polymerase chain reaction
PL	polysaccharide lyase
qPCR	quantitative polymerase chain reaction
RAST	rapid annotation using subsystem technology
RBB+C	repeated bead beating plus column
rholeuAM130	Rhodes and leucine bovine *Methanosphaera* population genome 130
rholeuAM270	Rhodes and leucine bovine *Methanosphaera* population genome 270
rholeuAM6	Rhodes and leucine bovine *Methanosphaera* population genome 6
rholeuAM74	Rhodes and leucine bovine *Methanosphaera* population genome 74
RNA	ribonucleic acid
rRNA	ribosomal ribonucleic acid
S	concentration of the limiting substrate for growth
SEM	standard error of mean
SHI1033	ovine *Methanosphaera* population genome 1033
SHI613	ovine *Methanosphaera* population genome 613
SRA	sequence read archives
Tg	trillion grams
TMAO	trimethylamine-oxide
TNF-α	tumour necrosis factor alpha
UV	ultra violet
vol	volume
WGK6	Western Grey kangaroo isolate 6

Chapter 1 Introduction and Literature Review

1.1 Methanogenic archaea, their niche and biochemistry

The world's societies are being challenged to reduce their greenhouse gas emissions, in response to global concerns about our impacts on the environment and climate change. Methane is recognized to be a potent greenhouse gas, and much of it arises during anaerobic decomposition of organic matter by the microbial world. The processes governing methanogenesis reside within members of the Archaea and more specifically, the phylum Euryarchaeota. Five orders of methanogens have long been recognized: Methanopyrales, Methanococcales, and Methanobacteriales (class I); the Methanomicrobiales (class II) (Bapteste et al., 2005); and the Methanosarcinales (class III) (Anderson et al., 2009). However, this has since expanded to recognise Methanocellales (Sakai et al., 2008) as well as the recently proposed seventh order of methanogens Methanomassiliicoccales (Paul et al., 2012, Oren and Garrity, 2013). The role methanogens play within microbial communities supports the recycling of complex organic materials through a 'three-step process' of bioconversion (Fig. 1.1) in which methanogenesis is the final step (Liu and Whitman, 2008).

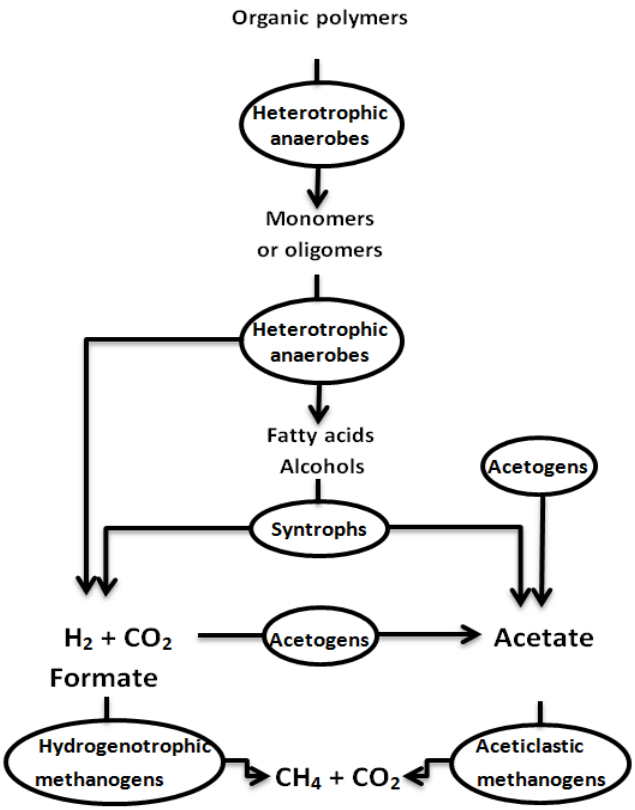

Figure 1.1. An extract from Liu and Whitman (2008) demonstrating the 'three step process' for the anaerobic breakdown of complex organic matter within a methanogenic microbial community.

While the metabolic versatility of the members of each order of methanogens may differ, methanogenesis is only known to occur through three different processes: the carbon dioxide-reduction, methyl-group reduction and acetic acid cleavage (acetoclastic) reactions (Fig. 1.2 (Liu and Whitman, 2008, Thauer et al., 2008)). Not surprisingly then, methanogens are found in many environments, especially those where sulphate is limiting; including fresh water sediments and rice paddies, landfills, moist soil biomes, the human, animal and some insect gastrointestinal tracts and their waste streams (Edwards and McBride, 1975, Liu and Whitman, 2008, Evans et al., 2009). Although the presence and role of methanogenic archaea in gut environments has long been recognized, greater attention has been directed to studying methanogens from other environments. It is only in recent years that there has been a renewed interest in gut methanogens, driven in part by the desire to reduce livestock methane emissions, as well as the possibility that methanogens might influence human gut function and health.

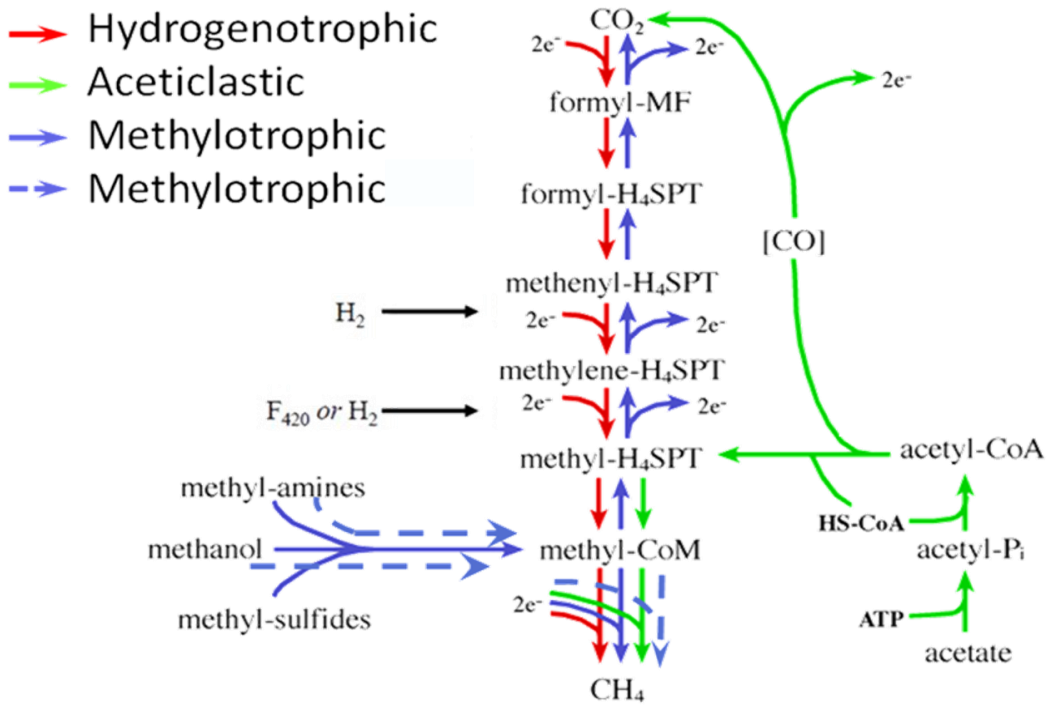

Figure 1.2. The three different metabolic schemes for methanogenesis: hydrogenotrophic (carbon dioxide or formate reduction, red arrows); acetoclastic (green arrows); methyl group reduction (disproportionate reaction solid blue arrows or hydrogen-dependant reduction broken blue arrows). Modified from Professor Dr. Michael Rother, Dresden University of Technology and Welander and Metcalf (2005).

1.2 Methane emissions, methanogenic archaea and the ruminant host

Various studies have reported that the global annual methane production ranges from 500-600 Tg (trillion grams); as much as 20% of this amount is currently attributed to ruminant livestock such as cattle, sheep, deer and goats (Lowe, 2006). The global demand for meat and milk is predicted to increase by 60% before 2050, in response to the world's growing human population (2012). Australia in particular has been identified as one of the world's largest producers of greenhouse gases on a per-capita basis (Garnaut, 2008) and methane emissions from ruminant livestock are now being targeted as a critical control point. There is an increased focus on the development of novel approaches and technologies to manage livestock methane emissions, so it seems logical that without a thorough characterisation of the gut methanogenic archaea responsible, it will be difficult to achieve success. Ruminants rely upon their microbial community to breakdown plant biomass in a manner that is

consistent with that illustrated in Figure 1 (13, 14). Upon ingestion of plant biomass by the host, it is initially broken down by hydrolytic enzymes, then fermented by a diverse community of prokaryote and eukaryote microbes (Bryant, 1979); subsequently synthesizing short chain fatty acids, hydrogen and carbon dioxide (Karasov and Carey, 2009). Within this community hydrogen accumulation can result in the inhibition of further metabolism of certain microorganisms (Hobson, 1988); so hydrogen utilising microbes are very important, as they allow the rest of the rumen microbial community to function most efficiently (Hobson and Stewart, 1997). Within the rumen, this niche is most often filled by methanogens; demonstrating this symbiotic relationship, of "interspecies hydrogen transfer" (IHT) as first described by Bryant and Wolin (1975). Since that time, much of the research has focused on confirming the class I methanogens, and especially the autotrophic *Methanobrevibacter* spp. are numerically most predominant (~6.0 x 10^8 cells per gram of sample) (Janssen and Kirs, 2008, Evans et al., 2009). These archaea are best known for their use of the hydrogenotrophic pathway for methanogenesis, which involves the use of either CO_2 or formate as the principal C-sources for reduction with H_2 gas and methane formation (Miller et al., 1982, Miller and Lin, 2002). Accordingly, *Mbb.* spp. have been the primary focus of cultural, biochemical and genomic methods of analysis (Samuel et al., 2007, Leahy et al., 2010) with either draft or closed genome sequences publically available for no less than 41 axenic isolates from both the rumen and human digestive tracts. Despite the current research interests seeking abatement of livestock methane emissions in total only seven types of rumen methanogens (*Mbb.* spp., *Methanobacterium* spp., *Methanomicrobium* sp., and *Methanoculleus* sp.) have been described in any detail (Attwood et al., 2011, Janssen and Kirs, 2008) and relatively little attention has been paid to the heterotrophic members of the community.

In recent years, the application of "omics" approaches has provided new insights into the roles the archaea might play in rumen function. Poulsen *et al.* (2013) showed that the reduced methane emissions from dairy cows fed rapeseed oil could be attributed to a selective suppression of the "*Methanomassiliicoccus",* with coincident decreases in transcripts encoding for methylotrophic methanogenesis from the rumen contents of these animals (Poulsen et al., 2013). New Zealand and US-DOE researchers have also studied the rumen microbiota of sheep stratified with respect to methane production, and demonstrated that the trait is heritable (Shi et al., 2014). Using a combination of metagenomic and metatranscriptomic methods they found no significant differences in total methanogen numbers between the "low" and "high" methane producers, although there were differences

in the relative abundances of the methylotrophic *Methanosphaera* spp. (increased in "low methane" sheep) and the hydrogenotrophic *Mbb. gottschalkii* clade (increased in "high methane" sheep). The metatranscriptomic data revealed that 7/10 genes coordinating the hydrogenotrophic pathway were significantly increased in high methane producing sheep. Additionally, New Zealand researchers have used metagenomics to build a comparative profile of methanogenic diversity across 252 sampled animals (eight cohorts of sheep and cows) from around New Zealand (Seedorf et al., 2015). While *Mbb.* and *Mms.* spp. dominate the communities of all the cohorts sampled, the less abundant *Msp.* spp. were also consistently identified within the sampled animals. Parallel studies in Europe with beef cattle produced similar findings with respect to higher numbers of *Mbb.* spp. in the "high" emitters, while changes in the bacterial population favouring the succinate-producers like *Succinivibrionaceae* were found in the "low" emitting animals. Furthermore, these variations in metagenomic data between the "high" and "low" emitters have been proposed as biomarkers for animal selection and breeding strategies that seek to reduce methane emissions and/or improve feed efficiency (Wallace et al., 2015). Indeed, it would seem that the alterations in methanogen profiles observed among animals stratified by their methane emissions involves genotype x environment interactions that affect rumen fermentation and gaseous hydrogen formation (Kittelmann et al., 2014). Collectively, these findings suggest that while the inhibition of select populations of methanogens can mitigate livestock methane emissions, it is also a heritable trait, suggesting host-mediated effects on the rumen microbiota. In that context, "high methane" emitting animals have been postulated to possess a longer retention of feed within the rumen as well as alterations in the bacterial "ruminotype" increasing the levels of ruminal hydrogen, with coordinate elevated expression of genes encoding the hydrogenotrophic pathway and greater methane yield (Janssen, 2010, Kittelmann et al., 2014) . It seems intuitive then to further suggest that the increased relative abundance of hydrogen-dependent methylotrophic methanogens in "low methane" animals relates to their capacity for growth when the bacterial ruminotype favours less hydrogen production during fermentation (Janssen and Kirs, 2008, Attwood et al., 2011).

1.3 Australia's macropodids as the "low" methane agricultural model

Australia's native herbivores macropodids (kangaroos and wallabies) are similar to ruminants in that they rely on a fore stomach colonized by microbes for the breakdown of plant material, and production of protein- and energy-yielding nutrients. Interestingly, two studies in the late 70's suggested the scheme of anaerobic digestion in macropodids results in

relatively low methane emissions per unit of digestible energy intake compared to sheep (Engelhardt et al., 1978, Dellow et al., 1988). These earlier observations have recently been validated using a colony of kangaroos and wallabies from a zoo in Denmark (Madsen and Bertelsen, 2012). Macropodids have been shown to harbour methanogenic archaea in their foregut; with Evans et al. (2009) demonstrating the methanogen-specific 16S rRNA gene clone libraries produced from macropodids are taxonomically similar to those produced from numerous rumen and human microbiota, namely *Mbb.*, *Msp.*, and uncultured *Mms.* archaea. However, their qPCR analyses established that the abundance of methanogens were substantially less in macropodids (7.0×10^5 to 3.9×10^6 cells per gram of sample) than that of ruminant livestock (~9.8×10^8 cells per gram of sample) (Evans et al., 2009). Additionally, the recent identification of both acetogenic bacteria (Ouwerkerk et al., 2009) and Succinivibrionaceae WG-1 (Pope et al., 2011) suggests these bacteria could act as hydrogen sinks and effectively compete with methanogens for hydrogen, in a manner similar to that observed with some species of termites, and ostriches (Breznak and Switzer, 1986, Fievez et al., 2001). So how and why do methanogenic archaea colonise and persist in the foregut of these animals? Have at least some of these methanogens evolved to survive by using H_2-independent pathways for methane production and growth? These questions can be addressed by isolating methanogens from native Australian herbivores, in addition to comparing them with strains from other gut environments.

1.4 Interactions between methanogenic archaea and the human host

The last decade has also seen the emergence of widespread public interest in the human "microbiome" and its effects on our health and well-being, driven in large part by the technological advances in DNA/RNA sequencing technologies and related computational tools for data analysis (Eckburg et al., 2005, Dridi et al., 2011). Recently, IHT driving methane formation has been proposed as a mechanism positively affecting calorie release in the large bowel, and a possible contributing factor to adiposity (Samuel et al., 2007, Mathur et al., 2013, Gaci et al., 2014). Certainly there is evidence to suggest that this is not true for all races, there is an increased incidence of breathe methane in African rural and urban black populations in comparison to European Americans (Nava et al., 2012). Supported by another study which sampled and compared Native and American Africans in comparison with Caucasian Americans, again demonstrating that there was a significantly higher parts per million reading of methane for Native Africans and an average BMI of 28 (O'Keefe et al., 2007). Nottingham and Hungate (1968) first isolated methanogens from human faeces in the

late 1960's and the links between methane, methanogens and human gut function have been reported since the early 1970's (Haines et al., 1977, Bond et al., 1971). The early studies suggested familial-based environmental (rather than genetic) effects influenced prevalence, with about one-third of "healthy persons" found to be methane excretors. Subsequent studies have suggested a higher prevalence of methane excretors (and when measured, methanogen abundance in faeces) among persons suffering from organic gastrointestinal disorders, including colorectal cancer and diverticulosis (Conway de Macario and Macario, 2009). Irritable bowel syndrome (IBS) is categorised by episodes of diarrhoea (IBS-D), constipation (IBS-C), or both (IBS-M), and breath methane measurement of IBS patients has been reported to be greater in IBS-C and lower or not detectable in IBS-D patients (Chatterjee et al., 2007). It has been demonstrated in animal and human models that methane can influence the intestinal motor function, with an abundance of methane resulting in a slow intestinal transit time as a result of augmented small bowel contractile activity (Pimentel et al., 2006).

Since the pioneering efforts from the early-1980s by Miller and Wolin, which include the isolation and characterization of *Mbb. smithii* and *Msp. stadtmanae* DSMZ 3091^{T} (Miller et al., 1982, Miller and Wolin, 1985), the cultured lineages of human methanogens and rRNA–based microbiota studies have expanded their prevalence to other body sites (e.g. oral cavity and vagina) and the hydrogenotrophic methanogens were again linked with alterations in anaerobic schemes of metabolism associated with disturbances to tissue homeostasis and inflammation (see Chaudhary et al. (2015) for a recent review). In recent years, the analysis of human microbiota samples from subgingival, intestinal or vaginal mucosae has further expanded the diversity of methanogenic archaea to include a new species of *Mbb. (Mbb. oralis),* as well as two isolates of methylotrophic archaea (*Candidatus* 'Methanomethylophilus alvus' and *Mms. luminyensis)* affiliated with the newly defined seventh order *Mms.* (Dridi et al., 2012, Borrel et al., 2012, Borrel et al., 2013, Borrel et al., 2014), which also includes the often referenced "rumen cluster C" from livestock surveys (Janssen and Kirs, 2008). A combination of both culture-based and genomic studies have characterised the narrow substrate range used by members of this order (methanol and/or methylated amines) and found that members of this order appear to be more prevalent in mature age persons (Borrel et al., 2014, Vanderhaeghen et al., 2015, Gaci et al., 2014). In addition to pectins being a source of methanol, other food components such as choline, lecithin and L-carnitine can be transformed by bacterial fermentation into methylated amines. The capacity of these "new" methanogens to utilize such products takes on added

significance given the growing evidence that trimethylamine production by the gut microbiota, and its subsequent oxidation in the liver to an oxide (trimethylamine-oxide: TMAO), is a primary contributor to cardiovascular disease pathogenesis and uremic toxin load in chronic kidney disease (CKD) patients (Tang et al., 2014, Wang et al., 2011). In summation, the links between gut methanogens and a person's health and well-being has principally focused on their syntrophic associations and physiological ecology. In other words, their relative abundance is predicated on the fermentative activities of the gut bacteria providing substrates in support of their growth, and/or alterations in gastrointestinal motility, influencing their relative abundance. In that context, Conway de Macario and Macario (2009) proposed that their role in pathogenesis is largely indirect, and a better understanding of the metabolic interactions involving the methanogenic archaea are relevant in combating many non-communicable diseases, from periodontitis to obesity. For instance, efforts are now underway that parallel those with livestock: to identify specific methanogen inhibitors as a treatment for GI disorders (e.g. Gottlieb et al. (2016); the use of statins to inhibit archaeal membrane synthesis), as well as suggestions that the methylamine-utilizing archaea might be used prophylactically and therapeutically as probiotics to mitigate TMAO production (Brugere et al., 2014, Morrison, 2013, Gaci et al., 2014). In these respects, there are many correlates to draw, and lessons to be learned, from the studies of methanogenic archaea in ruminant livestock and potential interventions in humans positively affecting health.

In their review, Conway de Macario and Macario (2009) also raised the spectre that the methanogenic archaea might also possess a more direct role in pathogenesis, via their interaction with the immune system, and outlined the differentiation of *Mbb. smithii* strains into no less than 7 "immunotypes". Similarly, Horz and Conrads (2011) described the findings by Yamabe et al. (2008) of humoral (IgG) responses to the oral methanogens present in periodontal lesions. More recently, Blais Lecours et al. (2011) reported that *Msp.* spp. are a predominant form of bioaerosols in animal houses, and using a mouse model showed that *Msp. stadtmanae* provokes a stronger immune response within the lung tissue (including stimulation of macrophage, lymphocyte, neutrophil, and eosinophil recruitment to lung tissue) than mice exposed to preparations of a *Mbb. smithii* strain. In a subsequent report by the same group Blais Lecours et al. (2014), the abundances of *Mbb.* and *Msp.* spp. present in stool samples were determined from healthy control subjects and patients suffering from IBD. While the "total methanogen" count was dramatically decreased in IBD patients, there was a measurable and significant increase in both the prevalence and abundance of *Msp.* spp.

observed. Such findings suggest that the production of short chain alcohols (often observed during "dysbiosis") might promote the growth of *Msp.* spp. and an expansion of their niche. Importantly, these authors also reported that not only does *Msp. stadtmanae* DSMZ 3091^T provoke a stronger inflammatory response from the peripheral immune system than *Mbb. smithii*, but the archaeon also elicits a strong IgG response in IBD patients, compared to the humoral response found towards *Mbb. smithii* in either IBD patients or healthy control subjects. Further investigations by Bang et al. (2014) have also identified the expression of CD197 and CD86 cell-surface receptors by monocyte-derived dendritic cells (moDCs) after stimulation of cells with either *Mbb. smithii* DSMZ 861^T or *Msp. stadtmanae* DSMZ 3091^T, providing further confirmation of earlier findings.

1.5 Summary and research goals

Despite the widespread recognition of the roles methanogenic archaea may play in gut environments, very little is known about their metabolic versatility, host adaptation, and immunogenic properties relevant to host health and nutrition. With the exception of some detailed examination of the physiological and genetic potential of the autotrophic *Mbb.* spp. (Leahy et al., 2010), much of the past efforts have been directed towards examining the ecological and taxonomic variations among these microbes in gut environments. To date, little is understood about the methylotrophic methanogens present in these environments (ie: *Msp.* spp.); I believe that these methylotrophic archaea may possess novel metabolic features associated with host adaptation. The fields of microbial genomics and metagenomics offer the potential to examine, and obtain a better understanding of the many microbes present in complex microbial communities, like those present in the bovine rumen, macropodid foregut and large bowel of humans.

The overall goal for my PhD program was to gain a detailed understanding of heterotrophic methanogens, especially members of the genus *Msp.*, by examining isolates recovered from the bovine, macropodid and human digestive tracts; and using biochemical, genomics, and cell biology approaches. While more specific aims of my project included:

1. The isolation of 'new' heterotrophic methanogenic archaea from domesticated Australian livestock and native Australian herbivores, through a combination of culture dependant and independent approaches.

2. Develop a deeper understanding of the metabolic versatility of culture dependent isolates using biochemical and/or genetic strategies.

3. Complete a comparative "pan-genome" analysis to identify core, shared and unique genes of macropodid, ruminant and human derived heterotrophic methanogenic archaea; in order to establish the links between genome variation and habitat adaptation/specificity.

4. Investigate the variations in *Mbb.* and *Msp.* spp. populations in CKD clinical studies and perform an assessment of their immunomodulatory properties.

This research should not only provide a stronger understanding of methanogen-host interactions, but should also aid in future research that seeks to find novel targets to manipulate these archaea in either agricultural or clinical scenarios.

Chapter 2 Differences down-under: alcohol-fuelled methanogenesis by archaea present in Australian macropodids

2.1 Introduction

Methane emissions from anthropogenic sources are viewed as a significant contributing factor to climate change and global warming and ruminant livestock populations are estimated to contribute between 13-19% of these emissions (IPCC, 2007, Leahy et al., 2010, Lowe, 2006, Johnson and Johnson, 1995, Lassey, 2007), which is a driving force behind global research efforts to productively alter livestock methane emissions. Recent studies have demonstrated that methane emissions by ruminant livestock is a heritable trait (Lassey et al., 1997, Pinares-Patino et al., 2013, Pinares-Patiño et al., 2011b, Pinares-Patiño et al., 2011a) and that animals selected for a "low methane" phenotype do develop and sustain an altered rumen bacterial population (Shi et al., 2014). Interestingly, although the structure of the methanogenic community changes in these animals, metagenomic and other cultivation-independent methods suggest the abundance of methanogens remains largely unchanged. Instead, there appears to be a reduction in the expression of genes that coordinate the hydrogenotrophic (autotrophic) pathway of methanogenesis in the "low emitters" suggesting that the archaeal populations need to adapt to changing environmental conditions via metabolic niche expansion.

Kangaroos and wallabies are the most numerous members of the Macropodidae and produce substantially less methane per unit of digestible organic matter intake than ruminant livestock when fed the same diet (Engelhardt et al., 1978), and this difference was recently confirmed with captive zoo populations in Europe (Madsen and Bertelsen). Although both are foregut digesters the digestive anatomy and associated physiology of macropodids and ruminants is quite different (Hume, 1984), and as expected the microbial communities that have evolved to colonize and persist in these digestive chambers are also different.

In that context, recent applications of metagenomic methods have revealed novel insights into the macropodid foregut microbiota that further explain their "low methane" emissions (Morrison, 2013). Evans et al. (2009) were the first to show that the macropodid foregut is colonized by methanogenic archaea, albeit at numbers substantially less than typically reported in ruminants (10^5 to 10^6 cells per gram of macropodid digesta as compared to 10^8 to 10^9 cells per gram of ruminant digesta). Although the taxonomic assignments of the macropodid archaeal populations are largely similar to those from ruminant livestock

virtually nothing is known about their metabolic capabilities and adaptations to the different gut environments. Here, I show that a *Msp.* sp. isolated from the Western Grey kangaroo (*Macropus fuliginosus*) expands the metabolic versatility of this genus, to include the utilization of short-chain alcohols in the absence of hydrogen gas, to fuel carbon reduction and methanogenesis.

2.2 Materials and Methods

2.2.1 Animal sampling protocol and digesta preservation.

The digesta samples used were collected from 17 Western Grey kangaroos (estimated to be between 1 month and 5 years of age, see section 6.1) during a culling exercise in 2008 by licensed hunters, as part of the state's control procedures, on a CSIRO managed farm in Yallenbee (Western Australia). Digesta samples were collected from the anterior region of the sacciform forestomach, and representative contents were added directly to completely fill a 50 ml sterile Falcon tube and stored at -80 ºC. The remainder of the digesta sample was strained through muslin cloth, with ~2 ml of the strained liquid immediately mixed with 2 ml of an anaerobic, pre-sterilized solution of 30% (vol/vol) glycerol (see section 6.2). These samples were all stored at -80 ^{o}C and used for the subsequent PCR-DGGE and cultivation based studies.

2.2.2 DNA extraction and PCR-DGGE analysis of Western grey kangaroo digesta samples.

Samples of whole digesta (~0.5 g) were mixed with a disassociation buffer (see section 6.3, Whitehouse et al., 1994) to desorb the microbial cells adherent to plant particles, and the resulting liquid was used for total DNA extraction by the RBB+C method (see section 6.4, Yu and Morrison, 2004). The DNA was used as a template for nested PCR, with the initial PCR amplification performed using the Archaea-specific primers (see section 6.5 Table 6.1) 86F/1340R (Wright and Pimm, 2003). The second, nested PCR was performed using 2 µl aliquots of the primary amplification mixture; combined with touchdown PCR amplification (Hwang et al., 2008) using primers 344F (Raskin et al., 1994) and 519R (Lane et al., 1985). The primer 344F was also contained a 38 nt G:C "clamp" (1999) for DGGE analyses (see section 6.6). Of the original 17 samples only 14 yielded PCR products which were subjected to DGGE using the Bio-Rad D-code System (Ouwerkerk et al., 2008) and the gel images were captured using a Typhoon scanner and Typhoon TRIO Variable Mode Imager (GE Healthcare Life Sciences, Parramatta, NSW, Australia).

2.2.3 Enrichment and isolation of *Methanosphaera* sp. WGK6

The glycerol stock from two animals (#2 and #6) was selected for culture work, based on their distinctive PCR-DGGE patterns (see Results section 2.3.1). The isolation process was conducted over a period of two months, and was initiated by setting up enrichment cultures based on BRN-RF30 medium (see section 6.7, Joblin et al., 1990) with a mixture of hydrogen and carbon dioxide gases (80:20 vol/vol) added to the headspace within each tube to a final pressure of 150 kPa. In addition, a selection of these starter cultures were also supplied with methanol (1% vol/vol). Penicillin and streptomycin were added to final concentrations of 600 µg/mL and 200 µg/mL, respectively (see section 6.8), and were incubated at 39^{o}C. Samples were taken aseptically from the cultures every 2 or 3 days, to check for methane in headspace gases and the presence of autofluorescent cells, as biomarkers of methanogen enrichment. Positive cultures were then further treated with erythromycin (100 µg/mL final concentration) and serially diluted to extinction. The highest dilutions still exhibiting autofluorescent growth and methane production were then serially diluted and used to inoculate BRN-RF30 agar roll tubes for the generation of single colonies. Several colonies were picked using a sterile glass pipette and then transferred to fresh medium and incubated at 39^{o}C. Following growth, each culture was confirmed to produce methane and to contain autofluorescent cells. Cell biomass from the candidate axenic cultures was harvested by centrifugation and DNA extracted using the RBB+C method (Yu and Morrison, 2004). The DNA samples were then used as templates for PCR amplifications with either Archaea- (86F/1340R) or Bacteria-specific (27F/1492R) primers (see section 6.5 Table 6.2) (Wright and Pimm, 2003) and the products were cleaned (see section 6.9) and sequenced using an Applied Biosystems 3130xl Genetic Analyser.

2.2.4 Substrate utilization tests for strain WGK6 and *Methanosphaera stadtmanae* DSMZ 3091^{T}

A basal medium of BRN-RF10 "medium 1" (see section 6.10, Balch et al., 1979) was used for these studies, with the headspace purged with oxygen-free N_2 gas to remove any carryover H_2, and with the various substrates aseptically added to individual tubes. The individual and substrate combinations tested were: ethanol alone, ethanol and H_2:CO_2 (80:20 vol/vol), methanol alone, methanol and H_2:CO_2 (80:20 vol/vol), methanol and ethanol, 20 mM each of mono-, di- and trimethylamine, propanol alone, and H_2:CO_2 (80:20 vol/vol). In all cases, the

alcohols were added to give a final concentration of 1% (vol/vol), and when required the tubes were pressurized to 202 kPa with H_2:CO_2 (80%:20%). The two strains were also evaluated for growth and methane formation with acetate or formate as the principal carbon sources. Here, basal BRN-RF10 "medium 1" lacking these substrates was prepared and they were subsequently added as sterilized solutions post autoclaving to a final concentration of 20 mM. For all these studies, culture tubes containing the different media were inoculated in triplicate with 0.1 mL aliquots of 6 day old cultures of either WGK6 or DSMZ 3091^T, both of which possessed an optical density at 600 nm (OD_{600}) ~1.0. Growth was monitored over time by measuring OD_{600} of all the cultures at fixed intervals over a 24 hour period (alternating between 9 and 15 hours apart) for 7 days. At the end of the incubation period a sample of the headspace gases were collected from all the cultures and subjected to GC analysis (Gagen et al., 2014).

2.2.5 Comparative growth studies with *Methanosphaera stadtmanae* strain DSMZ 3091^T

The growth yields, substrate utilization and methane production profiles of WGK6 and DSMZ 3091^T were then examined in more detail using large scale batch fermentations. Here, the medium was prepared in custom made 1.2 L serum bottles with a H_2-free headspace, as described above. The bottles were modified with a Balch tube fused to the wall of the bottle, so that the OD_{600} measurements could be made. Each bottle also contains a serum bottle closure to support aseptic sampling from the cultures. Each bottle was prepared to contain 500 mL of BRN-RF10 medium and was inoculated with 2 day old diluted cultures of either WGK6 or DSMZ 3091^T to give a starting optical density at 600 nm (OD_{600}) of ~0.02. The alcohols were added to these media to a final concentration of 1% (vol/vol), and when necessary, pressurized to 202 kPa with the H_2:CO_2 gas mix. The bottles were placed within a shaking incubator cabinet and agitated at 100 rpm for 6 days. Growth was monitored by OD_{600} measurements, taken at fixed intervals over each 24 hour period (5, 5, and 14 hours apart) using SPECTRAmax Plus 384 spectrophotometer. Samples (2 ml) were taken daily (at the time of the second OD_{600} measurement) from which cell biomass was harvested by centrifugation. Cell yields were calculated according to dry weight of cells per mol of methane measured at the peak of the exponential phase of growth (Miller and Wolin, 1985). The supernatants from these samples were stored at -80°C prior to their analyses for methanol, ethanol and short chain fatty acids, using published GC procedures (Pontes et al.,

2009), with the exception that the column temperature gradient was altered slightly to improve peak separation. Samples of the headspace gases were also removed each day, and the hydrogen, CO_2 and methane concentrations were also measured by GC analysis (Gagen et al., 2014).

2.2.6 Taxonomic assignment of strain WGK6, genome sequencing and analysis

WGK6 cells were harvested after 5 days growth and the DNA was extracted using the RBB+C method (Yu and Morrison, 2004). The DNA was then quantified using the Quant-iT dsDNA BR Assay Kit according to the manufacturer's instructions (Invitrogen); and the integrity of the DNA was determined by agarose gels and electrophoresis. The gene encoding 16S rRNA was amplified with primers 86F and 1340R using methods as described above. The individual sequence reads were trimmed and assembled using Vector NTI to produce a near complete 16S rRNA gene sequence and used for phylogenetic analysis using MEGA5 (Tamura et al., 2011). The stability of the neighbour-joining tree was evaluated by 1000 bootstrap replications and Kimura 2-parameter modelling (Kimura, 1980).

Genomic DNA from strain WGK6 was subjected to shotgun sequencing at the Australian Centre of Ecogenomics (ACE) using a 454 Roche GS-FLX system with titanium chemistry. The sequence data was quality checked, filtered and then *de novo* assembled using the Velvet assembler (Zerbino and Birney, 2008). The WGK6 contigs were re-ordered using Mauve (Darling et al., 2010) and with the DSMZ 3091^T genome sequence as a reference. Mauve is a genome alignment algorithm that allows an anchored (and rapid) alignment of two or more genomes, but also supports the rearrangement of these alignment anchors to support the identification of any genome rearrangements. By doing so, it provides information relating to genome synteny, xenologous regions, and genome rearrangements as evolutionary marks. The Mauve-generated assembly was submitted to the xBASE annotation pipeline (Chaudhuri et al., 2008), and the resulting output files examined using the Artemis genome browser (Rutherford et al., 2000). The WGK6 draft genome was further examined using JGI IMG/ER see Appendix 6.11, Table 6.3(Markowitz et al., 2012) which facilitated more genes being assigned to Kyoto Encyclopedia of Genes and Genomes (KEGG) pathways and orthologous groups (Kanehisa and Goto, 2000, Kanehisa et al., 2010, Kanehisa et al., 2006). The draft genome has been deposited at JGI IMG/ER under the accession 2595698213 and the whole genome shotgun project has also been deposited at DDBJ/EMBL/GenBank under the

accession JRWK00000000. The version described in this paper with regards to annotations and locus tags is JGI IMG/ER version 2595698213.

2.2.7 RT-PCR analysis of WGK6 alcohol (*walc*) and aldehyde (*wald*) dehydrogenase gene expression

Strain WGK6 was cultured for 48 hours (OD_{600} ~0.6) with BRN-RF30 medium supplemented with either methanol and hydrogen, or methanol and ethanol, as previously described. The cells were harvested by centrifugation and subjected to phenol:choloroform treatment and bead beating to lyse the cells, followed by RNA purification with the Qiagen RNeasy mini kit. Residual DNA was removed from the extracts with the Ambion Turbo DNase "rigorous" protocol. The quality of the RNA was determined using Agilent RNA 6000 Nano Kit and those samples with a RNA Integrity Number (RIN) >9 were reverse transcribed using Invitrogen Superscript III reverse transcriptase and random hexamers, according to manufacturer's specifications. The cDNA was then used as a template for qPCR, with primers targeting either the candidate alcohol (*walc*) or aldehyde (*wald*) dehydrogenase genes, as well as the intergenic transcribed space (Table S1). The primers were all designed using the online software Primer3 (Rozen and Skaletsky, 2000), and were cross checked to ensure non-specific binding to other regions of the WGK6 genome by using NCBI BLAST and pDRAW32. The cDNA was also used with 16S rRNA gene-specific primers. All these reaction mixtures were treated with RNaseH at 37ºC for 20 minutes, and aliquots (1 µL) were added to 12.5 µL of power SYBR green PCR Master Mix (Applied Biosystems), 0.25 µL each of forward and reverse primer pair, and then made up to a final volume of 25 µL. The PCR conditions used were one hold at 50 °C for 2 minutes, and then one hold at 95 °C for 2 minutes, followed by 40 cycles at 95 °C for 15 seconds, and a 60 °C elongation for 1 minute. The real-time PCR efficiency (*E*) was calculated for all three primer sets, by setting up qPCR reactions with varying amounts of cDNA added to the reaction mixtures (0.016, 0.08, 0.4 and 2 ng, each done in triplicate). The *E* values were calculated as described by Rasmussen where $E = (10^{[-1/\text{slope}]}) - 1) * 100$ (Rasmussen, 2001), and for both dehydrogenase primer sets was 90%, and 102% for 16S rRNA gene. Then, the fold-change for each of the dehydrogenase gene transcripts was calculated using (Pfaffl, 2001):

$$\text{Fold change} = \frac{E_{target}^{[\text{Ct target (control} - \text{treated)}]}}{E_{reference}^{[\text{Ct reference (control} - \text{treated)}]}}$$

Here, "target" refers to either the *walc*- or *wald*-derived transcript, and "reference" refers to the 16S rRNA-derived cDNA. "Control" and "treated" conditions were growth of strain WGK6 with methanol:H_2 and methanol:ethanol, respectively.

2.2.8 Taxonomic assignment of WGK6 alcohol and aldehyde dehydrogenase genes

The phylogeny of protein coding sequences for WGK6 alcohol and aldehyde dehydrogenase genes was constructed with sequences recovered from the NCBI and JGI databases. MEGA5 (Tamura et al., 2011) was used to construct phylogeny for each dehydrogenase gene respectively, ClustalW (Thompson et al., 1994) aligned the sequences, the stability of the Poisson modelled (Rosset, 2007) neighbour-joining tree was evaluated by 1000 bootstrap replications.

2.3 Results

2.3.1 Analysis of foregut digesta samples and isolation of *Methanosphaera* sp. WGK6

The PCR-DGGE analysis of the digesta samples showed there were two dominant profiles (Fig. 2.1) and based on these results, digesta samples from two animals (#2 and #6 in Fig. 2.1) were selected for methanogen enrichment and isolation. The digesta sample from animal #2 produced cultures with only weak growth (OD_{600} < 0.2) and a small amount of methane could only be measured in headspace gases when H_2 and CO_2 were provided for growth and without antibiotic additions, so were not pursued further. However, the sample from animal #6 produced more actively growing cultures and more methane in headspace gases when H_2 and methanol were provided for growth; and autofluorescent cells were also present upon UV-transilluminated microscopy. Interestingly, the addition of erythromycin solubilised in ethanol appeared to further improve growth of the culture. Upon microscopic examination, the culture appeared to be comprised exclusively of coccoid-shaped cells forming clumps, which were autofluorescent during UV-transillumination (Fig. 2.2). Four single colonies were propagated in broth cultures and were confirmed to share the same morphology, autofluorescence, and growth characteristics. Furthermore, each of these four cultures produced amplicons with Archaea-domain specific primers, with no detectable amplicon produced with Bacteria-domain specific primers. The PCR amplicon produced with Archaeal primers was sequenced and found to be 100% identical to each other, and share 97% sequence identity with the 16S rRNA gene sequence of *Msp. stadtmanae* (DSMZ 3091^T). At

this stage the individual cultures were presumed to be axenic and siblings of each other, so only one of these cultures, hereafter referred to WGK6, was selected for further study.

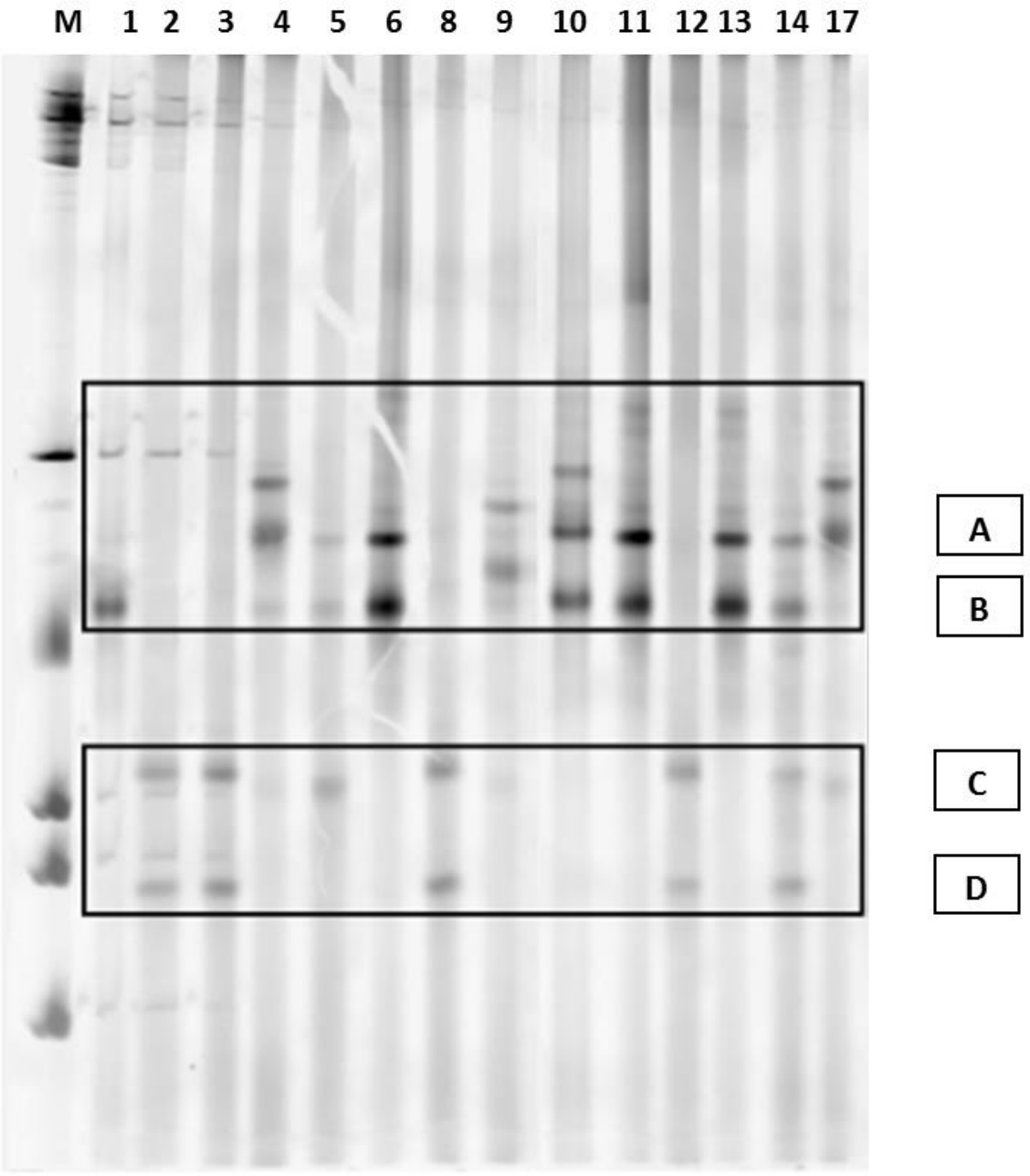

Figure 2.1. Nested PCR-DGGE analysis of the archaeal populations recovered from sacciform foregut digesta samples collected from 14 Western Grey kangaroos, as described in the Materials and Methods. Lane M contains 2.5 µg of 100bp ladder, and lane numbers represent individual animal samples. Two profiles appear to dominate the samples: 8/14 animals possess amplicons marked A and/or B, and 5/14 animals possess amplicons marked C and/or D. Strain WGK6 was recovered from digesta sample 6, which possesses both amplicons A and B.

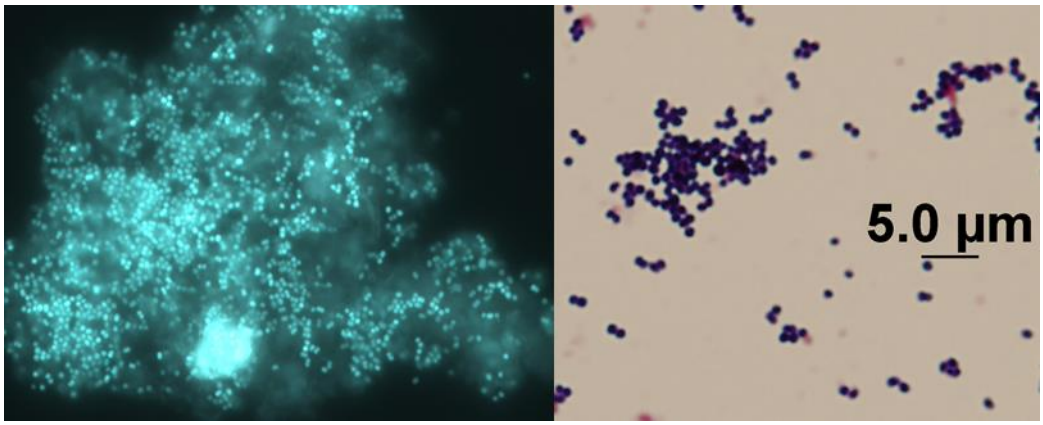

Figure 2.2. Photomicrographs of *Msp.* sp. WGK6 upon UV-transillumination (left), or following Gram staining (right). Both images were produced from WGK6 cultures following growth with BRN-RF30 medium containing methanol and erythromycin.

Cell biomass was harvested from a WGK6 culture to provide template DNA for 16S rRNA gene-specific PCR analysis. The phylogenetic analysis of the WGK6 and gut methanogen sequences shows that it is assigned to a cluster containing DSMZ 3091^T, with other sequences recovered from the rumen microbiomes of cattle in North America (Wright et al., 2007) and China (Pei et al., 2009), as well as other macropodids (Evans et al., 2009) (Fig. 2.3). Of these, DSMZ 3091^T and *Msp. cuniculi* (DSMZ 4103^T, originally isolated from rabbit rectum) appear to be the only members of this cluster that are available as axenic cultures; and to my knowledge DSMZ 3091^T is the only one to have its genome sequenced and publically available.

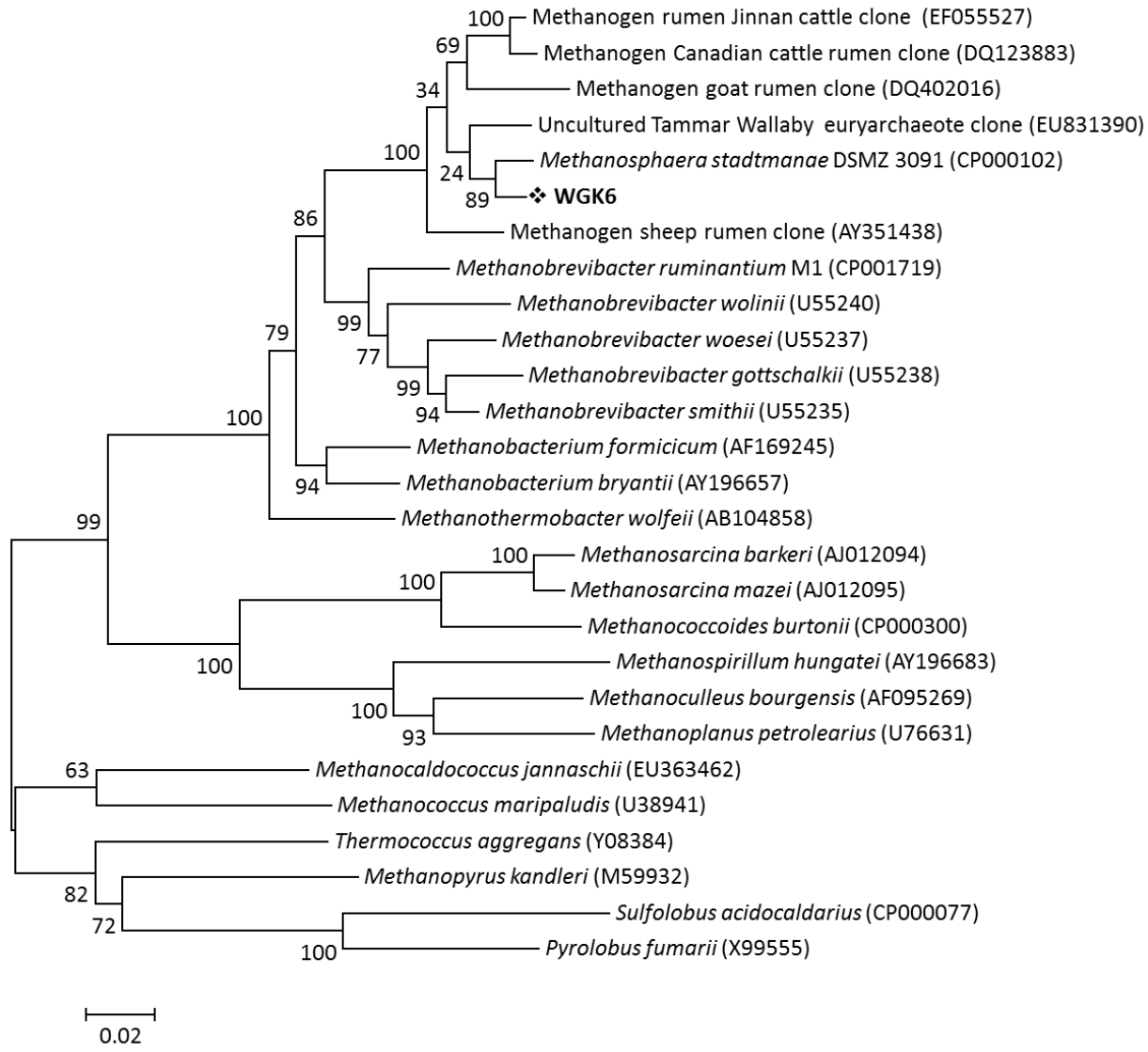

Figure 2.3. Phylogenetic analysis of the 16S rRNA gene sequence for strain WGK6 shows it is most similar to the human gut isolate *Msp. stadtmanae* DSMZ 3091^T and both are clustered with other clone sequences representing uncultured methanogens derived from ruminant and macropodid sources. Only bootstrap values greater than 50% are shown and the scale bar represents 2% sequence divergence, with *S. acidocaldaricus and P. fumarii* used as the outgroups.

2.3.2 Alcohol-fuelled methanogenesis by *Methanosphaera* sp. WGK6

Msp. stadtmanae DSMZ 3091^T has been shown by a combination of culture based and genomic methods to be a hydrogen-dependent methylotroph restricted to using methanol and H_2 (Miller and Wolin, 1985, Fricke et al., 2006, Miller and Wolin, 1983), and incapable of

autotrophic growth. Conversely, growth of the WGK6 enrichment culture appeared to be stimulated by the addition of ethanol (and/or erythromycin), suggesting the strain may possess a greater metabolic versatility compared to that of DSMZ 3091^T. Substrate utilization tests confirmed that neither strain WGK6 nor DSMZ 3091^T was capable of growth when methylated amines, acetate, formate, ethanol, propanol, or CO_2 were provided as carbon sources in the presence of hydrogen (data not shown). However, differences between the two strains were observed in terms of their ability to utilise combinations of methanol, ethanol and hydrogen to support growth (Fig. 2.4). As expected, both strain DSMZ 3091^T and WGK6 grew well when provided with both methanol and H_2. Furthermore, neither strain was capable of growth with ethanol alone, nor with ethanol and H_2. However, growth of strain WGK6 with the combination of short-chain alcohols occurred sooner than in cultures provided methanol:H_2 and the headspace gas pressure was also higher (280 kPa c.f. 145 kPa at 120 hours growth). As anticipated, strain DSMZ 3091^T was not capable of growth under these conditions. Based on these results, I hypothesized that strain WGK6 can use ethanol as a source of reducing power coupled to methanol reduction and methane formation.

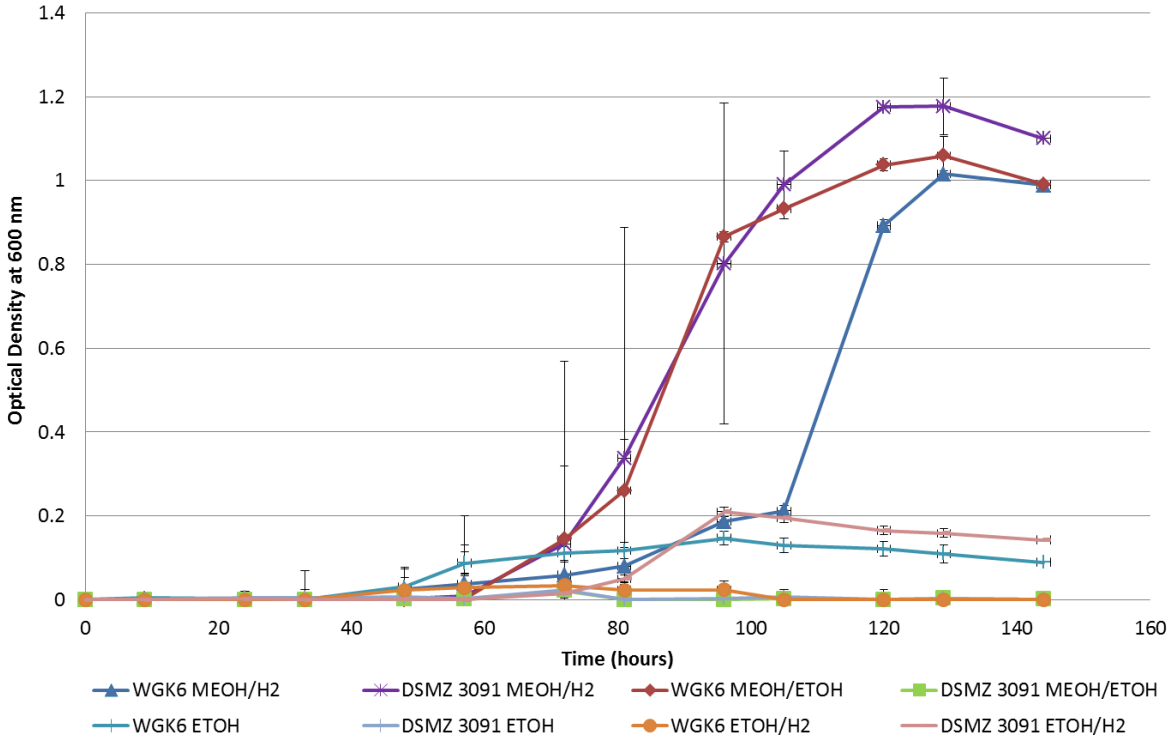

Figure 2.4. Growth of *Msp.* sp. WGK6 and *Msp. stadtmanae* DSMZ 3091^T when provided with different combinations of methanol, ethanol and H_2 added to BRN-RF10 basal medium, as described in the materials and methods. Note that measurable growth is only apparent for strain DSMZ 3091^T when provided with a combination of methanol and hydrogen, whereas growth of strain WGK6 can be supported by methanol and ethanol, as well as methanol and hydrogen. Individual values represent the mean (± SEM) produced from triplicate cultures.

2.3.3 Alcohol-fuelled methanogenesis is coupled with ethanol utilization and acetate formation by *Methanosphaera* sp. WGK6

Next, large-volume batch cultures of both WGK6 and DSMZ 3091^T provided with either methanol:H_2 or methanol:ethanol were sampled longitudinally to determine substrate utilization, product (methane and acetate) formation, and growth kinetics, and the results of these experiments are illustrated in Fig. 2.5. Methanol utilization, methane formation and growth was observed for strain WGK6 under both conditions and the cell yields were estimated to be 2.4 and 4.0 g/mol methane produced with methanol:H_2 and methanol:ethanol, respectively. Additionally, ethanol utilization by strain WGK6 (Fig. 2.5A) was coupled with the accumulation of acetate in these cultures only (Fig. 2.5C) suggesting strain WGK6 has the capacity to coordinate a two-stage oxidation of ethanol to provide the reducing power used

for methanol reduction and methanogenesis. As expected, methanol utilization, methane formation and growth of strain DSMZ 3091^T occurred only with methanol:H_2 with a cell yield of 4.0 g/mol methane, which is virtually identical to the findings reported by Miller and Wolin (Miller and Wolin, 1985). Taken together, these results suggested that strain WGK6 has an expanded metabolic versatility compared to strain DSMZ 3091^T via a capacity to catalyse ethanol oxidation via acetaldehyde to acetate.

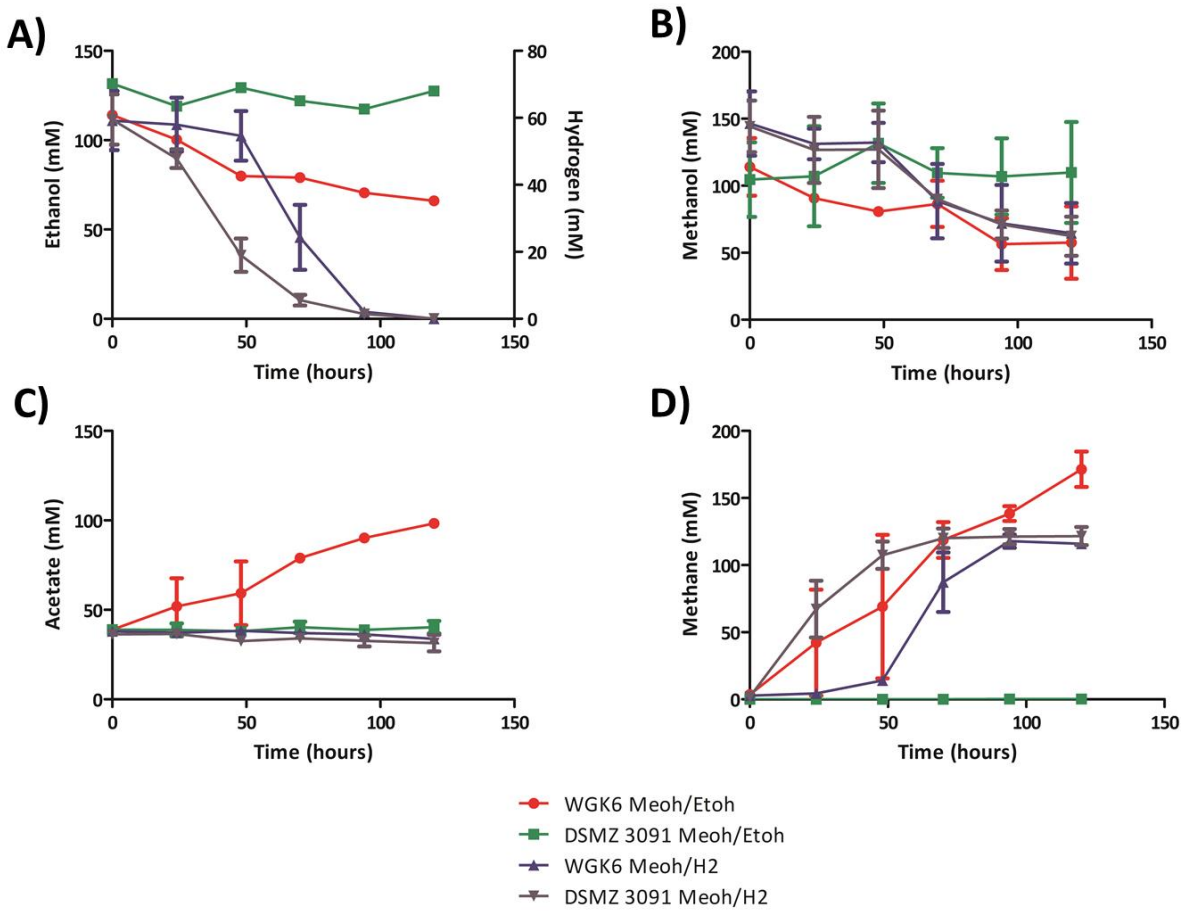

Figure 2.5. Longitudinal monitoring of the utilization of ethanol or H_2 (A), and methanol (B), as well as the formation of acetate (C) and methane (D) in batch cultures of *Msp.* sp. WGK6 and *Msp. stadtmanae* DSMZ 3091^T when provided with either methanol and hydrogen or methanol and ethanol. As expected methanol and hydrogen utilization, as well as methane formation, was observed for both WGK6 and DSMZ 3091^T, when cultured using this substrate combination (▲ and ▼ for WGK6 and DSMZ 3091^T, respectively). However, only strain WGK6 (●) and not DSMZ 3091^T (■) demonstrated an ability to utilize both methanol and ethanol to support methane formation (and growth, as depicted in Fig. 2.3). Additionally, acetate accumulation over time was only evident when strain WGK6 was cultured with both methanol and ethanol, suggesting a two-step oxidation of ethanol can provide the reducing power required for methanol reduction and methanogenesis (and growth) in the absence of H_2. With the exception of the results for ethanol measurements presented in Fig. 2.5A, the results represent the mean values obtained from duplicate experiments.

2.3.4 The WGK6 genome encodes dehydrogenase genes that are absent from the DSMZ 3091^T genome

The WGK6 genome was assembled into 37 large contiguous sequences at 68x coverage, with its genome size estimated to be 1.732 Mbp. The WGK6 draft genome sequence was then further assessed for both genome completeness and contamination using CheckM v1.0.3, an automated method which examines a draft genome against a broad set of marker genes, specific to an inferred lineage within a reference genome tree (Parks et al., 2015). These analyses suggested the WGK6 draft genome sequence is 96.8% complete and has a contamination level of 0%. In comparison, CheckM analysis of the DSMZ 3091^T closed genome produced values of 97.6% completeness and 0% contamination. Additionally both genomes are calculated to possess G:C content of 28% and are also very similar in size, with the closed DSMZ 3091^T genome being 1.767 Mbp (Fricke et al., 2006). The basic annotation tables for both WGK6 and DSMZ 3091^T are provided in section 6.11 Table 6.3, and with the exception of the number of 16S rRNA genes found (1 copy in strain WGK6 c.f. 4 copies in DSMZ 3091^T) the relative proportions of protein coding sequences with (and without) function predictions and/or KEGG pathway designations, are virtually identical. However the Mauve alignment of the two genomes, while showing there is extensive amount of synteny with only a few genome rearrangements between the WGK6 and DSMZ 3091^T genomes did reveal a region of genomic difference and found only in the WGK6 genome (Fig. 2.6). A closer examination of the annotation results for this region produced by JGI IMG/ER pipeline and KEGG-based pathway analysis showed this region to encode genes encoding putative alcohol (*walc)* and aldehyde *(wald)* dehydrogenases, and are positioned contiguously within this region. No orthologs of these genes could be identified anywhere else within the DSMZ 3091^T genome. The *walc* and *wald* sequences were then used to query the NCBI non redundant BLAST databases, to find their closest matches with biochemically validated gene products. The closest for the *walc* gene product is with the NADPH-dependent butanol dehydrogenase from *Clostridium saccharobutylicum* (63% amino acid identity and 100% coverage, (Youngleson et al., 1989)); and the *wald* gene product best matches with an aldehyde dehydrogenase from *Alcaligenes eutrophus* (47% amino acid identity and 99% coverage, (Priefert and Steinbuchel, 1992)).

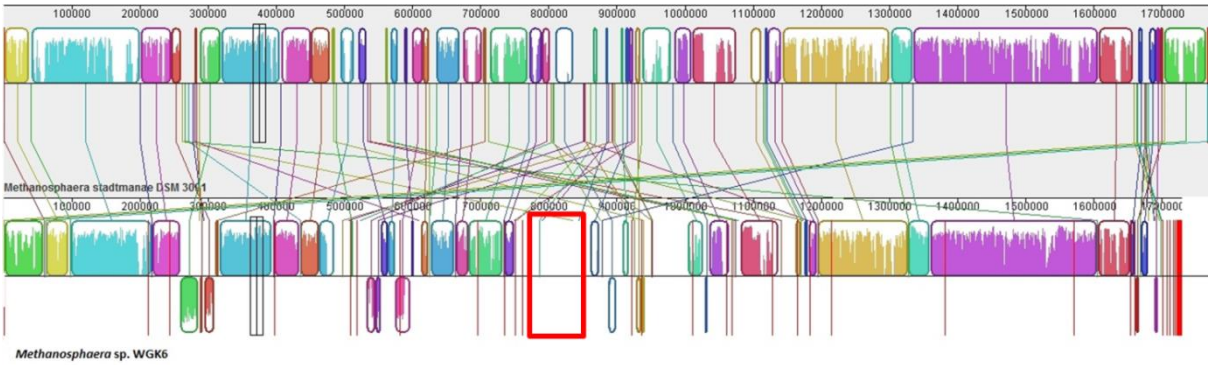

Figure 2.6. Alignment of the *Msp. stadtmanae* DSMZ 3091^T and *Msp*.sp. WGK6 genomes using the Mauve alignment software. In brief detail, the alignment algorithm facilitates the depiction of genome synteny (illustrated by the size and the colouring scheme used for the identified locally collinear blocks), regions of genome rearrangement (illustrated via the lines connecting locally collinear blocks between the two genome models) and any xenologous regions (illustrated by blank spaces). The region encoding the cotranscribed dehydrogenase genes in WGK6 is annotated by the red rectangle, and is notably different to the DSMZ 3091^T genome in this region.

Based on these comparative genome-wide analyses, I conclude that strain WGK6 is capable of utilizing ethanol as a source of reducing power because it possesses genes encoding for an alcohol and aldehyde dehydrogenase, whereas DSMZ 3091^T lacks both these genes and thereby is incapable of utilizing ethanol to support methanol reduction, methanogenesis and growth.

2.3.5 The *walc* and *wald* genes are constitutively expressed and cotranscribed by *Methanosphaera* sp. WGK6.

The expression of the *walc* and *wald* genes was assessed by qRT-PCR following growth of strain WGK6 with either methanol and hydrogen or methanol and ethanol, and the results are shown in Fig. 2.7. Both genes are expressed constitutively (Fig. 2.7A and B) and are also co-transcribed under both growth conditions (Fig. 2.7C). The qPCR analyses showed there was a ~2-fold increase in transcript abundance in response to growth with methanol and ethanol, when using cDNA produced from 16S rRNA as a reference. Based on these results, I conclude these genes can support ethanol oxidation and alcohol-fuelled methanogenesis by strain WGK6 and underpin its growth in the presence of both methanol and ethanol.

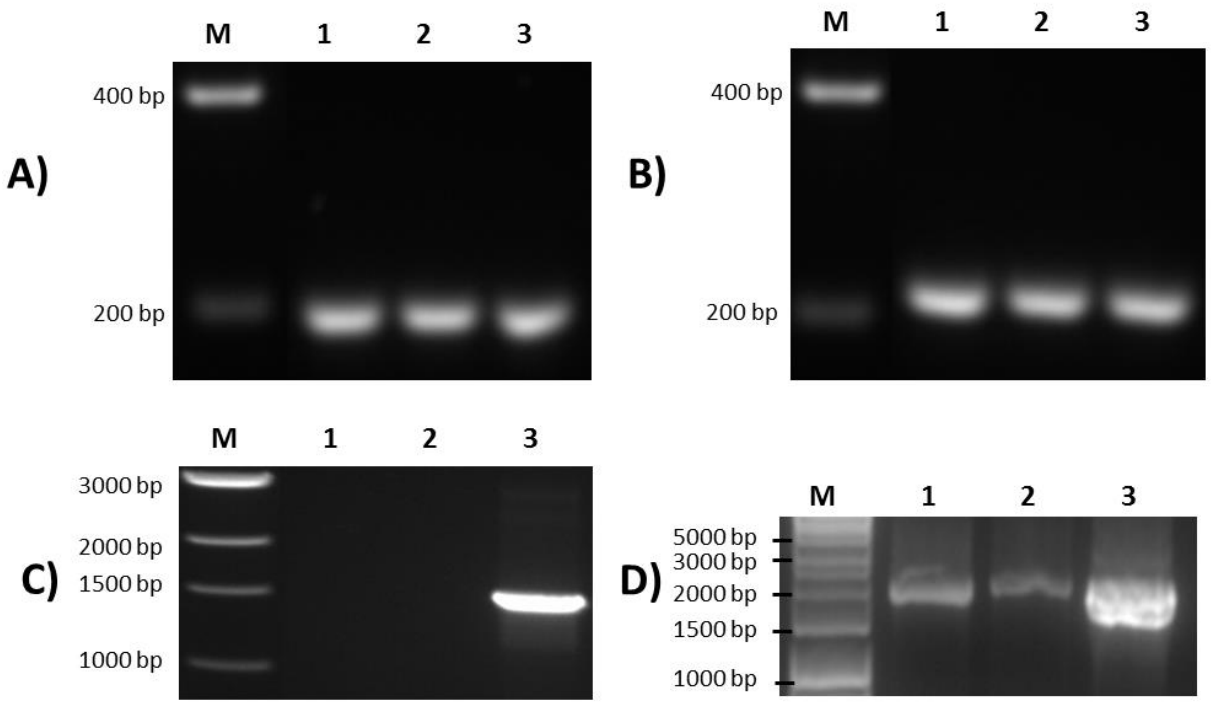

Figure 2.7. RT-PCR analysis of the *walc* and *wald* transcripts from *Msp.* sp. WGK6 during growth with either methanol and hydrogen, or methanol and ethanol, as described in the materials and methods. Both the *walc* transcript (panel A) and *wald* transcript (panel B) are detectable with both growth conditions. An amplicon was also produced using the *walc*-F and *wald*-R primers (panel C), suggesting the two genes are co-transcribed. In panels A-C, lane M shows a DNA standard ladder (sizes annotated), lanes 1 and 2 use cDNA produced from the RNA extracted from cultures provided with ethanol, or hydrogen, respectively; and lane 3 shows the results of PCR only, using genomic DNA. In Panel D, lane M shows a DNA standard ladder, lanes 1 and 2 show PCR reactions using 16S rRNA gene specific primers and the two RNA samples, but with no prior RT step; and lane 3 shows the results with the same primers but using WGK6 genomic DNA as a template.

2.3.6 Orthologs of the dehydrogenase genes from strain WGK6 are also present in other members of the Methanobacteriales.

I next chose to examine the phylogeny of the alcohol and aldehyde dehydrogenases from strain WGK6 using protein coding sequences recovered from the NCBI and JGI databases. In addition to a variety of bacterial sequences used to construct the trees, I also queried the draft genome sequences publically available for all *Methanobrevibacter* spp. (i.e. all 26 *Mbb. smithii* draft genomes, *Mbb. ruminantium* M1, *Mbb. wolinii* SH, *Mbb. olleyae* DSMZ 16632,

Mbb. boviskoreani JH1, *Mbb. millerae* DSMZ 16643, *Mbb. arboriphilus* ANOR1, and *Mbb* sp. AbM4). First, none of the *Mbb. smithii* draft genomes were found to possess orthologues or partial hits to either dehydrogenase coding gene. Additionally, no aldehyde dehydrogenase gene has been identified from the *Mbb. ruminantium* M1 or *Mbb. olleyae* genomes, and there were no strong hits using the WGK6 gene as the query sequence. Although the M1 genome has been annotated to possess no less than 4 putative alcohol dehydrogenase genes (2010) none of these genes produce strong hits with the WGK6 aldehyde dehydrogenase gene. In that context, the phylogenetic tree constructed for the alcohol dehydrogenase genes (Fig. 2.8) clearly reveals a bifurcation of the alcohol dehydrogenases from these gut-derived methanogenic archaea: one branch represented by *Mbb. ruminantium* M1, and the second including *Msp.* WGK6 and the other *Mbb.* spp. Similarly, the phylogenetic tree of the aldehyde dehydrogenase gene retains this clustering of *Mbb.* spp. (Fig. 2.9). Furthermore, there appears to be a strong degree of gene synteny between *Mbb.* AbM4, *Mbb. boviskoreani* JH1 and *Mbb. wolinii* SH (Fig. 2.10), with the genes upstream of the dehydrogenases encoding for the coenzyme F_{420}-reducing hydrogenase complex (*frhADGB*) and downstream genes encoding a putative transposase, F_{420}:NADP oxidoreducatse, asparatate dehydrogenase (AbM4 and *M. boviskoreani* only) and a methionine aminopeptidase.

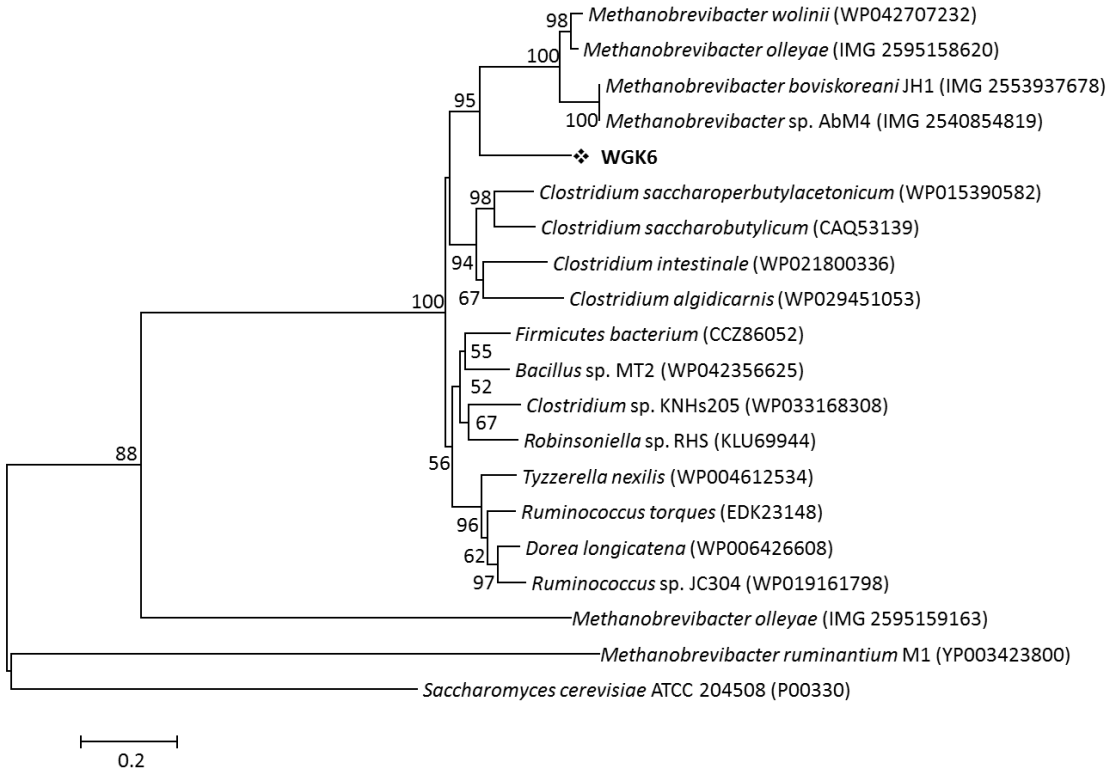

Figure 2.8. The phylogenetic tree constructed with the Jones-Taylor-Thornton (JTT) model, using BLASTp alignments of alcohol dehydrogenase genes sampled from NCBI non redundant BLAST databases. The scale bar represents 20% sequence divergence and the *Saccharomyces cerevisiae* ATCC 204508 alcohol dehydrogenase gene was used as the outgroup. Numbers represent the relative frequency of branch clustering based on 1000 bootstrap runs, bootstrap values less than 50% are removed. Note that the WGK6 gene is closely grouped with similar genes recovered from the draft genomes of 4 different *Mbb.* spp. Notably the putative alcohol dehydrogenase genes from the *Mbb. ruminantium* M1 genome are only distantly related (only a single representative was chosen for display within the phylogenetic tree).

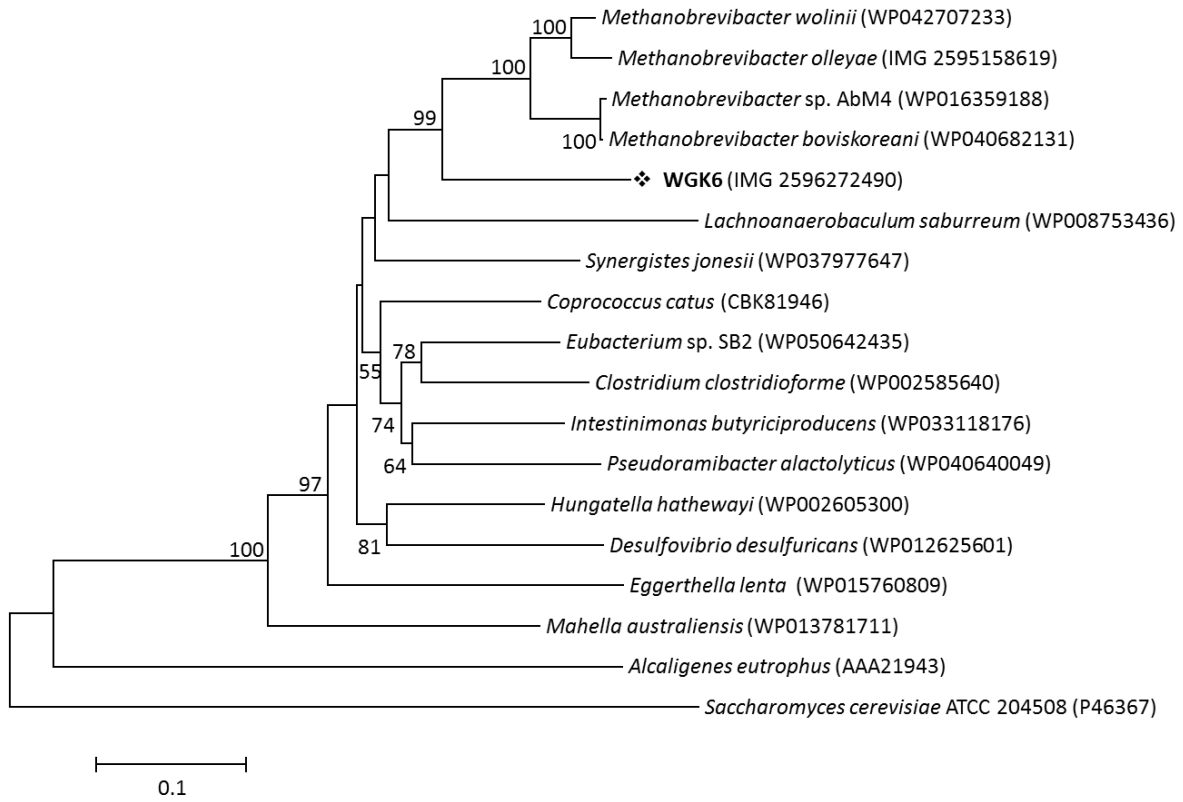

Figure 2.9. The phylogenetic tree constructed with Jones-Taylor-Thornton (JTT) model, using BLASTp alignments of aldehyde dehydrogenase genes sampled from NCBI non redundant BLAST databases. The scale bar represents 10% sequence divergence and the *Saccharomyces cerevisiae* ATCC 204508 aldehyde dehydrogenase gene was used as the outgroup. Numbers represent the relative frequency of branch clustering based on 1000 bootstrap runs, bootstrap values less than 50% are removed. The WGK6 gene is again closely grouped with similar genes recovered from the draft genomes of 4 different *Mbb.* spp., but notably no putative aldehyde dehydrogenase gene(s) have been identified from the *Mbb. ruminantium* M1 genome.

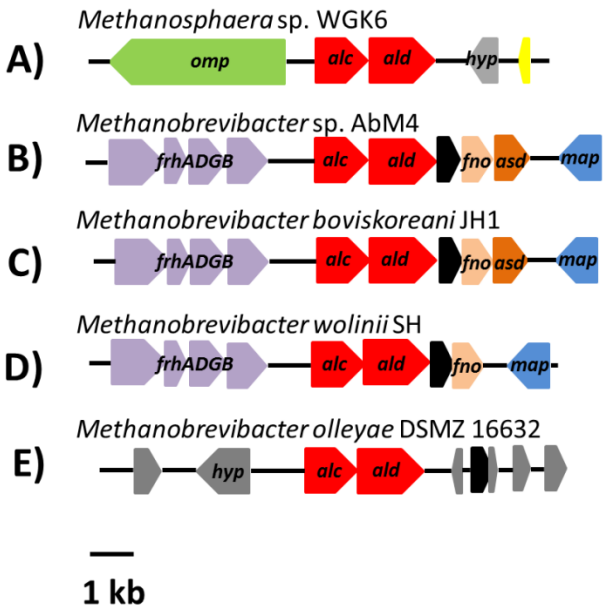

Figure 2.10. Comparison of the genes flanking the alcohol (*alc*) and aldehyde (*ald*) dehydrogenase genes (red) in *Msp.* sp. WGK6, *Mbb.* sp. AbM4, *Mbb. boviskoreani* JH1, *Mbb. wolinii* SH, and *Mbb. olleyae* DSMZ 16632^{T} (A-E, respectively). A high degree of gene conservation is seen between strains AbM4, JH1, and SH, each possessing a coenzyme F_{420}-reducing hydrogenase complex upstream (*frhADGB* - purple); and a transposase (black), F_{420}:NADP oxidoreductase (*fno* - orange), and methionine aminopeptidase (*map* - blue) located downstream; with strains AbM4 and JH1 also possessing an aspartate dehydrogenase (*asd* - brown). *Mbb. olleyae* DSMZ 16632^{T} is surrounded by hypothetical proteins (*hyp* - grey), however there is a transposase (black) downstream of the dehydrogenase genes, while strain WGK6 is flanked by an outer membrane protein (*omp* - green), hypothetical proteins (*hyp* - grey) and a putative histone (yellow).

2.4 Discussion

While *Msp.* spp. have long been recognized to colonize the gastrointestinal tracts of warm-blooded animals, their metabolic niche has remained largely enigmatic, due in large part to the limited number of strains available for culture-based studies. Here, I demonstrate the ability of a new axenic isolate of *Msp.* spp. to use ethanol as a source of reducing power, and also show that biomass yield per mol methane produced is greater when ethanol rather than hydrogen is used as reductant. Furthermore, although previous studies have shown that ethanol can stimulate the growth of hydrogenotrophic methanogens such as *Mbb. smithii* (Samuel et al., 2007) and *Mbb. ruminantium* (Leahy et al., 2010), neither are capable of growth in the absence of hydrogen.

A proposed scheme involving a two-step oxidation of ethanol coupled with methanol reduction and methanogenesis by strain WGK6 is illustrated in Fig. 2.11. Thermodynamically, the 4 protons and electrons released by the oxidation of ethanol to acetate via acetaldehyde could support the reduction of two mols of methanol, compared to one mol when only hydrogen is present. The calculated free energy available (values and equation shown in section 6.12 Table 6.4) is more favourable with ethanol, calculated to be -199.93 kJ/mol (equation i) compared to methanol and hydrogen at -121.16 kJ/mol (equation ii). Additionally, it is possible that the acetate produced from ethanol oxidation can also provide a source of cell carbon, not available via hydrogen-dependent reduction of methanol.

i. $2CH_3OH + CH_3CH_2OH \rightarrow 2CH_4 + H_2O + CH_3COO^-$ ($\Delta G^{o\prime} = -199.93$ kJ/mol)
ii. $CH_3OH + H_2 \rightarrow CH_4 + H_2O$ ($\Delta G^{o\prime} = -121.16$ kJ/mol)

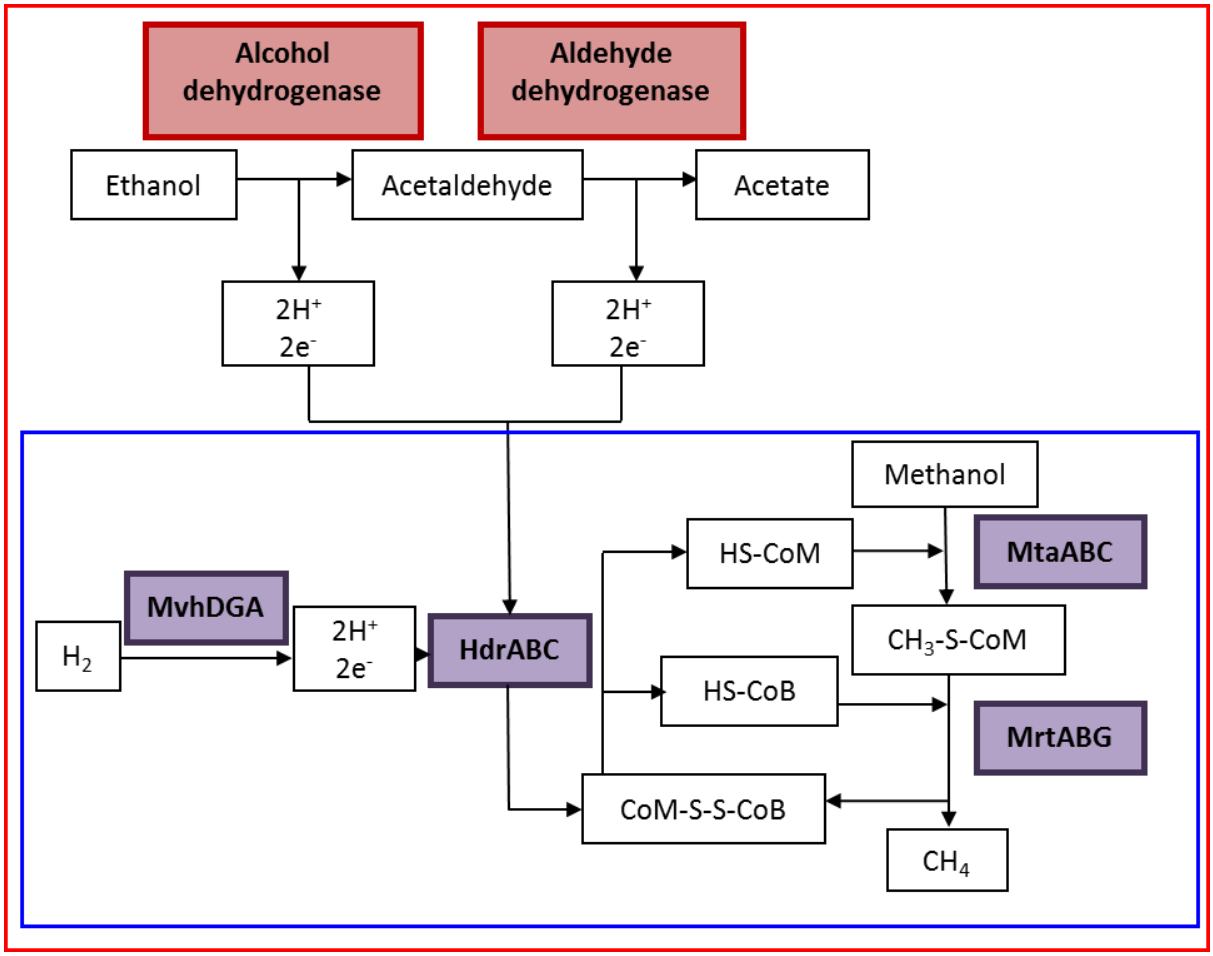

Figure 2.11. A model for methanol reduction via hydrogen (blue box) or ethanol (red box) present in *Msp.* sp. WGK6, based on the results of the genomic and culture-based results presented in this study. The reduction of methanol is initiated by coenzyme M methyltransferase (MtaABC) and coenzyme M (HS-CoM) which produces 2-(methylthio)ethanesulfonic acid (CH_3-S-CoM). Methyl-coenzyme M reductase (MrtABG) reduces the product CH_3-S-CoM with coenzyme B (HS-CoB) to methane and coenzyme M-HTP heterodisulfide (CoM-S-S-CoB). Heterodisulfide reductase (HdrABC) then acts on CoM-S-S-CoB using $2e^-$ and $2H^+$ to reduce the disulfide bond thus regenerating HS-CoM and HS-CoB. The necessary electrons and hydrogen protons are generated by non-F420-reducing hydrogenase (MvhADG) from hydrogen. Alternatively, *Msp.* sp. WGK6 can use a two-step oxidation process with ethanol, performed by the cotranscribed alcohol and aldehyde dehydrogenases, which would result in the provision of 4 protons and electrons used to reduce 2 methanol groups to methane and with acetate as an end product.

The demonstration of an alcohol- rather than hydrogen-fuelled methanogenesis pathway suggests *Msp.* spp. have adapted in order survive in environments with small amounts of free

hydrogen gas, and provides an explanation for their persistence in presumptive "low hydrogen" and/or "low methane" environments. For instance, the nutritional ecology of the macropodids would favour the formation of methanol during pectin hydrolysis, as well as a microbiota capable of the production of some short chain alcohols during fermentation (Hume, 1984, Smith, 2009, Kempton et al., 1976). So even though the relative numbers of methanogenic archaea in these animals are much smaller than found in ruminant livestock, and it has been demonstrated that reductive homoacetogens are effective hydrogen scavengers in the macropodid foregut (Godwin et al., 2014, Gagen et al., 2010) my findings do provide a basis for the persistence of methanogenic archaea in these communities, via alcohol-fuelled methanogenesis.

In ruminant livestock, a combination of metagenomic and metatranscriptomic methods have now showed that total methanogen numbers are similar between the "low" and "high" methane producing sheep, but there are differences in the relative abundances of the methylotrophic *Msp.* spp. (increased in "low methane" sheep) and the hydrogenotrophic *Mbb. gottschalkii* clade (increased in "high methane" sheep) (Shi et al., 2014). The abundance of transcripts encoding most functions coordinating the hydrogenotrophic pathway was also significantly increased in high methane producing sheep. The "high methane" emitting animals have been postulated to possess a longer retention of feed within the rumen as well as alterations in the bacterial "ruminotype" increasing the levels of ruminal hydrogen, with coordinate elevated expression of genes encoding the hydrogenotrophic pathway and greater methane yield (Janssen, 2010, Kittelmann et al., 2014) . So it seems intuitive then to further suggest that the increased relative abundance of methylotrophic methanogens like *Msp.* spp. in "low methane" animals may relate to their capacity for alcohol-fuelled methanogenesis when the bacterial ruminotype favours less hydrogen production during fermentation (Janssen and Kirs, 2008, Attwood et al., 2011).

It is also notable that recent studies of the human large bowel microbiota in patients suffering from non-alcoholic fatty liver disease (NAFLD) and more severe conditions suggest that the microbiota is not only dysbiotic, but fermentation schemes favouring ethanol formation are more active (Zhu et al., 2013). Coincidentally, other studies have remarked that there is also a shift from hydrogenotrophic to methylotrophic methanogens under such conditions, as well as in patients suffering from IBD (Blais Lecours et al., 2014).

In conclusion, the presence of these dehydrogenase genes in multiple members of the Methanobacteriales suggests that the metabolic versatility of these gut-derived methanogens is broader than what has long been accepted, and that alcohol-fuelled methanogenesis may be an important evolutionary adaptation to persist in the gut environment.

2.5 Published journal article detailing work carried out in Chapter 2

The ISME Journal (2016), 1–13

www.nature.com/ismej

ORIGINAL ARTICLE

Differences down-under: alcohol-fueled methanogenesis by archaea present in Australian macropodids

Emily C Hoedt[1], Páraic Ó Cuív[2], Paul N Evans[1], Wendy JM Smith[3], Chris S McSweeney[3], Stuart E Denman[3] and Mark Morrison[2]

[1]*School of Chemistry and Molecular Biosciences, The University of Queensland, St Lucia, Queensland, Australia;* [2]*The University of Queensland Diamantina Institute, Translational Research Institute (TRI), Brisbane, Queensland, Australia and* [3]*Commonwealth Scientific and Industrial Research Organisation, Queensland Bioscience Precinct, St Lucia, Queensland, Australia*

The Australian macropodids (kangaroos and wallabies) possess a distinctive foregut microbiota that contributes to their reduced methane emissions. However, methanogenic archaea are present within the macropodid foregut, although there is scant understanding of these microbes. Here, an isolate taxonomically assigned to the *Methanosphaera* genus (*Methanosphaera* sp. WGK6) was recovered from the anterior sacciform forestomach contents of a Western grey kangaroo (*Macropus fuliginosus*). Like the human gut isolate *Methanosphaera stadtmanae* DSMZ 3091^T, strain WGK6 is a methylotroph with no capacity for autotrophic growth. In contrast, though with the human isolate, strain WGK6 was found to utilize ethanol to support growth, but principally as a source of reducing power. Both the WGK6 and DSMZ 3091^T genomes are very similar in terms of their size, synteny and G:C content. However, the WGK6 genome was found to encode contiguous genes encoding putative alcohol and aldehyde dehydrogenases, which are absent from the DSMZ 3091^T genome. Interestingly, homologs of these genes are present in the genomes for several other members of the Methanobacteriales. In WGK6, these genes are cotranscribed under both growth conditions, and we propose the two genes provide a plausible explanation for the ability of WGK6 to utilize ethanol for methanol reduction to methane. Furthermore, our *in vitro* studies suggest that ethanol supports a greater cell yield per mol of methane formed compared to hydrogen-dependent growth. Taken together, this expansion in metabolic versatility can explain the persistence of these archaea in the kangaroo foregut, and their abundance in these 'low-methane-emitting' herbivores.
The ISME Journal advance online publication, 29 March 2016; doi:10.1038/ismej.2016.41

Introduction

Methane emissions from anthropogenic sources are viewed as a significant contributing factor to climate change and global warming, and ruminant livestock populations are estimated to contribute between 13% and 19% of these emissions (Johnson and Johnson, 1995; Lowe, 2006; IPCC, 2007; Lassey, 2007; Leahy *et al.*, 2010), which is a driving force behind global research efforts to productively alter livestock methane emissions. Recent studies have demonstrated that methane emissions by ruminant livestock is a heritable trait (Lassey *et al.*, 1997; Pinares-Patiño *et al.*, 2011a, b; Pinares-Patino *et al.*, 2013) and that animals selected for a 'low-methane' phenotype do develop and sustain an altered rumen bacterial population (Shi *et al.*, 2014). Interestingly, although the structure of the methanogenic community changes in these animals, metagenomic and other cultivation-independent methods suggest the abundance of methanogens remains largely unchanged. Instead, there appears to be a reduction in the expression of genes that coordinate the hydrogenotrophic (autotrophic) pathway of methanogenesis in the 'low emitters', suggesting that the archaeal populations need to adapt to changing environmental conditions via metabolic niche expansion.

Kangaroos and wallabies are the most numerous members of the Macropodidae and produce substantially less methane per unit of digestible organic matter intake than ruminant livestock when fed the same diet (Engelhardt *et al.*, 1978), and this difference was recently confirmed with captive zoo populations in Europe (Madsen and Bertelsen, 2012). Although both are foregut digesters, the digestive

Correspondence: M Morrison, The University of Queensland Diamantina Institute, Translational Research Institute (TRI), 37 Kent St, Woolloongabba, Queensland 4102, Australia.
E-mail: m.morrison1@uq.edu.au
Received 19 July 2015; revised 10 February 2016; accepted 25 February 2016

Chapter 3 Culture- and metagenomics-based expansion of the genus *Msp.* reveals their evolutionary depth and metabolic versatility

3.1 Introduction

Methanogenic archaea colonise a variety of environments including the animal and human gastrointestinal tract (Brusa et al., 1993, Evans et al., 2009, Mao et al., 2011) and those present in ruminant livestock are widely perceived to contribute as much as 20% of the annual global anthropogenic greenhouse gas emissions (IPCC, 2007, Lowe, 2006, Johnson and Johnson, 1995, Lassey, 2007). Methanogenic archaea typically possess a restricted capacity in terms of the carbon sources and reducing power supporting energy transduction and growth (Liu and Whitman, 2008). The methanogenic archaea resident in the gastrointestinal tracts of warm-blooded animals have long been recognized for their key role in coordinating interspecies hydrogen transfer, promoting more efficient growth of heterotrophic, fermentative bacteria (Bryant and Wolin, 1975). Generally, the principal members of the gut methanogenic communities are *Mbb.*, *Msp.* and *Mms.* spp. (Luo et al., 2013, Poulsen et al., 2013, Eckburg et al., 2005). *Mbb.* spp. are often the numerically predominant members of these taxocenes, and favour hydrogen-dependent reduction of carbon dioxide and/or formate for methanogenesis and growth. There are currently no less than 41 axenic isolates of *Mbb.* spp. described, and for which either draft or complete genome sequences are publically available. In contrast, there are much fewer axenic isolates of *Msp.* and *Mms.* spp., and draft genomes are available for four hydrogen-dependent methylotrophic isolates of *Mms.* spp. from the rumen and human digestive tracts (Rea et al., 2007, Leahy et al., 2013, Leahy et al., 2010, Hansen et al., 2011, Dridi et al., 2012), and only one finished genome available for *Msp.* spp. (*Msp. stadtmanae* DSMZ 3091^{T}, Miller and Wolin, 1985). Interestingly, *Msp.* spp. have recently been reported to be more abundant in "low methane" producing ruminants, as well as in human subjects suffering from IBD. Additionally, these patients (but not the healthy controls) were found to possess high titres for serum IgG reactive to *Msp. stadtmanae* DSMZ 3091^{T}, and the archaeon was shown to be more immunogenic then *Mbb. smithii* in a murine model of respiratory disease, suggesting that *Msp.* may elicit proinflammatory effects in the gut (Blais Lecours et al., 2014, Blais Lecours et al., 2011).

For these reasons, I contend the genus *Msp.* remains underexplored and poorly defined relative to their ubiquity and abundance in the gut of animals and humans, as well as their contributions to gut function, health and disease. In this chapter I describe the isolation and

genomic characteristics of *Msp.* sp. BMS from the bovine rumen, which is the first reported isolate of its type. I have also recovered seven *Msp.*-affiliated population genomes from human, ovine, and bovine metagenomic datasets, and I present the pan-genomic analysis of all these datasets. Collectively, these results show that the genus is comprised of two genomotypes, differentiated by their genome size, with the most recent evolutionary adaptations favouring a "smaller" genome (<2.0 Mbp).

3.2 Materials and Methods

3.2.1 Animal sampling, enrichment and isolation of *Methanosphaera* sp. BMS

Rumen fluid was collected using previously described procedures (Chapter 2) from a fistulated Brahman steer grazing on native grass/legume forage at the Gatton campus of the University of Queensland's School of Agriculture and Food Sciences approved by DEEDI (AEC Proposal Reference Number SA 2011/08/365). A subsample of the strained liquid (~2ml) was mixed with an equal volume of pre-reduced, anaerobic, and sterilized solution of 30% (vol/vol) glycerol, then stored -80^{o}C.

Methanogen enrichment cultures were produced using BRN-RF30 medium (Joblin et al., 1990) supplemented with either a combination of methanol and ethanol (each 1% vol/vol) or the same concentration of methanol, but with H_2 gas added to a final pressure of 150 kPa. These media were inoculated with 0.2 mL of the glycerol stock and incubated at 39 ^{o}C for 36 hours, when the cultures were subsampled and examined for headspace methane gas formation and autofluorescent cells (via UV transillumination of wet mounts). The methanol:H_2 enrichments produced a culture that was positive for both criteria, and it was used to inoculate BRN-RF30 medium supplemented with methanol:H_2, and 50 µg/mL penicillin. The second-round enrichment culture was again examined after 36 hours incubation for autofluorescent cells, and subcultured using the same medium, but with 100 µg/mL penicillin added. This third-round enrichment culture was then serially diluted to extinction in BRN-RF30 medium containing methanol:H_2 with 50 µg/mL tetracycline added. The greatest dilution still producing methane and autofluorescent cells was then used to inoculate BRN-RF30 agar roll tubes to isolate single colonies. Several colonies were picked using a sterile glass pipettes and then aseptically transferred to fresh medium, and incubated at 39 ^{o}C. At this point, the resulting culture was confirmed by microscopy to be comprised of two cell types, and 16S rRNA clone library sequencing confirmed the presence of both *Msp.*

(fluorescent) and *Mms.* (non-fluorescent) affiliated species. The co-culture was again serially diluted to extinction, this time with 100 µg/mL novobiocin added, and the outgrowth of the greatest dilution producing autofluorescent cocci and methane in headspace gases was used to inoculate agar roll tubes. Only one axenic colony pick for *Msp*. sp. was achieved (hereafter referred to as strain BMS), others had a bacterial contaminant when checked and for the sake of time they were not further purified. As described in Chapter 2 of this thesis the BMS culture was presumed to be axenic and used for further study after microscopic examination (the culture appeared to be comprised exclusively of autofluorescent coccoid-shaped cells forming clumps) and no detectable amplicon was produced with Bacteria-domain specific primers. The PCR amplicon produced with Archaeal primers was sequenced and found to share 96% sequence identity with the 16S rRNA gene sequence of *Msp. stadtmanae* DSMZ 3091^T.

3.2.2 *Methanosphaera* sp. BMS substrate utilization and growth kinetics

The substrate utilization profiles of *Msp.* strains BMS, as well as *Msp.* sp. WGK6 and *Msp. stadtmanae* DSMZ 3091^T were determined as previously described in detail in Chapter 2 of the thesis. To determine the substrate affinities and maximal growth rates (Kovarova-Kovar and Egli, 1998) for *Msp. stadtmanae* DSMZ 3091^T, WGK6 and BMS when provided either ethanol or H_2 as a reductant when grown in medium BRN-RF30 (Joblin et al., 1990). The substrate affinities and maximal growth rates were calculated from triplicate cultures grown with varying concentrations (S) of ethanol (0, 3, 10, 30, 50 and 171 mM) or H_2 (0, 1.3, 1.8, 2.6, 3.5 and 4.6 mM). The optical densities of these treatments were monitored longitudinally as described above for substrate utilization profiles. The linear phase of these growth profiles over time was used to calculate the specific growth rate (μ) relative to the concentration of the limiting substrate for growth (S). These data were plotted as double-reciprocal plots, similar to the Lineweaver-Burke using the Michaelis-Menten nonlinear regression type function used for characterising enzymes (Lineweaver and Burk, 1934, Johnson and Goody, 2011), with this an estimation of substrate affinity (K_s) was determined by finding the substrate concentration needed to achieve a half-maximum of the maximal growth rate (μ_{max}).

$$\mu = \mu_{\max}\frac{S}{K_s + S}$$

3.2.3 *Methanosphaera* sp. BMS genome sequencing and closure

For high molecular weight genomic DNA isolation, cultures (40 mL) of BMS were harvested by centrifugation (17,000 x *g*) after 5 days growth, and the cell pellets were subject to 15 freeze-thaw cycles, followed by a phenol:chloroform extraction and ethanol precipitation (see Appendix 6.13), with the resulting DNA resuspended in ultra-pure water. The DNA was quantified using the Quant-iT dsDNA BR Assay Kit according to the manufacturer's instructions (Invitrogen) and its integrity was determined by agarose gel electrophoresis. Aliquots (20 µg) of BMS genomic DNA was then sheared by Hydroshear® Shearing Device (Pacific Biosciences, CA, USA) to produce fragments ~20 Kb in length, which were then used for library construction and SMRT-cell sequencing with the PacBio RS2 "continuous long read" platform and the SMRT portal assembly (Pacific Biosciences). The genome assembly was performed using HGAP2 and a seed cut-off length of 10 Kb. The quality of the genome assemblies for all three strains was assessed using CheckM, which examines lineage-specific marker genes in order to estimate genome completeness and contamination (Parks et al., 2015). In addition, the quality of the BMS genome assembly was assessed using the software program Contiguity used for contig adjacency graph construction and visualisation (Sullivan et al., 2015). Finally, specific primers were designed (see Appendix 6.5, Table 6.2) to sequence "walk" across the determined ends of the single BMS contig and sequenced using an Applied Biosystems 3130xl Genetic Analyser as described in Chapter 2 of this thesis. The closed BMS genome was further examined using JGI IMG/ER (Markowitz et al., 2012) which annotates and assigns genes to Clusters of Orthologous Groups (COG) and KEGG pathways (Kanehisa and Goto, 2000, Kanehisa et al., 2010, Kanehisa et al., 2006). The genome has been deposited at JGI IMG/ER under the accession 2626541600, and DDBJ/EMBL/GenBank whole genome submission portal under the accession CP014213.

3.2.4 Nucleotide pattern analysis and Mauve alignment of *Methanosphaera* genomes

The genome "barcodes" for each *Msp.* sp. isolate was generated using barcodeByMers (https://github.com/minillinim/mikezbioscripts) to determine the tetramer frequency for window sizes of 2 Kb and the resulting heat map was generated in RStudio (www.rstudio.com) using the package ggplot2 (http://ggplot2.org/). Mauve (Darling et al., 2010) was used to examine genome synteny and with *Msp. stadtmanae* DSMZ 3091^T as the reference genome, as described in Chapter 2.

3.2.5 Comparative analyses of *Methanosphaera* spp. genomes

The GenBank annotations and COG gene profiles, mobilome, as well as the fused protein coding genes of each genome were obtained via JGI IMG/ER. The three genomes were also uploaded to the software platform EDGAR (Blom et al., 2009) to determine the core, shared and accessory genome for the isolate genomes, which were visualised using a Venn diagram. The atlas of fused protein coding genes and the mobilome were constructed using Gview (https://server.gview.ca/) by providing Genbank and fasta files of the genes of interest for each respective genome, recovered using BLASTn.

3.2.6 Retrieval of *Methanosphaera* population genomes using MetaBAT

The NCBI Sequence Read Archives (SRA) was queried with the 16S rRNA from *Msp. stadtmanae* DSMZ 3091^{T} to identify datasets most likely to contain sequences associated with *Msp.* spp. (see Appendix 6.14, Table 6.5). Metagenomic datasets identified as possessing *Msp.* spp. associated sequences included; 10 stool samples from the Karlsson et al. (2013) study of elderly European women with glucose control profiles considered either normal, impaired, or diabetic; Shi et al. (2014) analysis of ovines bred for "low" (n=4) or "high" (n=4) methane production; and an unpublished CSIRO study of rumen fluid collections of 10 Brahman steers consuming improved Rhodes grass pasture (*Chloris gayana*) +/- supplementation with Leucaena (*Leucaena leucocephala*), sequence data (Illumina HiSeq 2000; Macrogen Inc., Korea) provided by Chris McSweeney (unpublished work part of project 01200.035/B.CCH.6510). Datasets were quality checked with Trimmomatic v0.32 (Bolger et al., 2014) to remove adapters and trim low-quality bases, and bbmerge v34.49 (http://sourceforge.net/projects/bbmap/) was used to merge overlapping pairs. The quality checked paired-end and merged reads were assembled using CLC Genomics Workbench 8 **(**http://www.clcbio.com**)**. MetaBAT v0.25.4 (Kang et al., 2014) was used to recover population genomes independently from the two metagenomic studies. An estimate of population genome completeness and contamination was performed with CheckM v1.0.3 (Parks et al., 2015). Annotations for the population genomes were generated through the Rapid Annotation using Subsystems Technology (RAST) server (Aziz et al., 2008).

3.2.7 Whole genome phylogeny

Whole genome phylogeny was obtained using GTDBLite (https://github.com/Ecogenomics/GTDBLite), built from the concatenation of 122 universal marker genes identified by PhyloSift (Darling et al., 2014). Tree inference was performed with FastTree v2.1.7 (Price et al., 2010) and included all genomes in IMG v4.510 (Markowitz et al., 2012). The resulting tree was imaged using ARB (Ludwig et al., 2004). In addition the whole genome phylogeny was re-examined once the core genome (307 genes) was identified aligned and concatenated using the software platform EDGAR (Blom et al., 2009). The extrapolated genome size is also listed beside each genome, which was calculated based on draft genome size and CheckM completeness scoring (Parks et al., 2015). Both phylogenetic tress are identical and show a clear separation of smaller genomes (< 2.0 Mbp) which appear to be descendants of larger (> 2.1Mbp) ruminant genomes. However, only the tree resulting from GTDBLite is presented here.

3.2.8 Comparative analysis of select functional gene sets across all *Methanosphaera* spp. isolate and population genomes

The phylogeny of protein coding sequences for methyl-coenzyme M reductase component A2 (*mrtA*) and energy conserving hydrogenase (*ehaRST*) were constructed with sequences recovered from the EDGAR core genome assignment. MEGA6 (Tamura et al., 2011) was used to construct phylogeny for each dehydrogenase gene respectively, ClustalW (Thompson et al., 1994) was used to align the sequences, and the stability of the Jones-Taylor-Thornton modelled neighbour-joining tree was evaluated by 1000 bootstrap replications. EDGAR was also used to recover the gene alignment view for *ehaRST*. The DataBase for automated Carbohydrate-active enzyme Annotation (dbCAN; Yin et al., 2012) was used to provide automated and comprehensive CAZyme annotation for each of the *Msp.* genomes, and genes encoding for enzymes of ammonium assimilation were also identified from the pan-genome collection produced using EDGAR.

3.2.9 Average nucleotide identity (ANI) matrix and pan/core development plot

The Genbank files prepared from RAST annotation system (Aziz et al., 2008) were provided to the software framework EDGAR for genomic comparative analysis including average nucleotide identity (ANI) matrix generation (Blom et al., 2009). The core-genome for the 10 *Msp*. genomes were examined for their average nucleotide identity, which was calculated

from blast hit results between the orthologous genes of the core genome. *The resulting* ANI values are presented as a matrix based on phylogeny with ANI values higher than 95% considered to be the same species (Konstantinidis et al., 2006) and values from 62-100% belong to the same genus (Kim et al., 2014). To determine the development plots for the pan/core genome, the perl script PGap (Zhao et al., 2012) was used on the Bio-Linux Platform v.8.0.5 (http://environmentalomics.org/bio-linux-software-list/). The three files required by this script for each genome included: annotation file (.ptt), nucleotide sequences (.ffn) and protein sequences (.faa). The PGap analysis pipeline provided gene clusters assigned to either the core or pan-genome and was visualised using the software package PanGP (Zhao et al., 2014).

3.3 Results

3.3.1 *Methanosphaera* sp. BMS is a hydrogen-dependent methylotroph

Methanogenesis and growth of BMS was not supported by methylated amines, acetate, formate, propanol or a mixture of H_2:CO_2; nor could strain BMS use ethanol as an alternative to hydrogen to support methanogenesis. Based on these results I conclude that strain BMS is a hydrogen-dependent methylotroph (Fig. 3.1), similar to that shown for *Msp*. *stadtmanae* DSMZ 3091^T rather than for strain WGK6, as presented in Chapter 2.

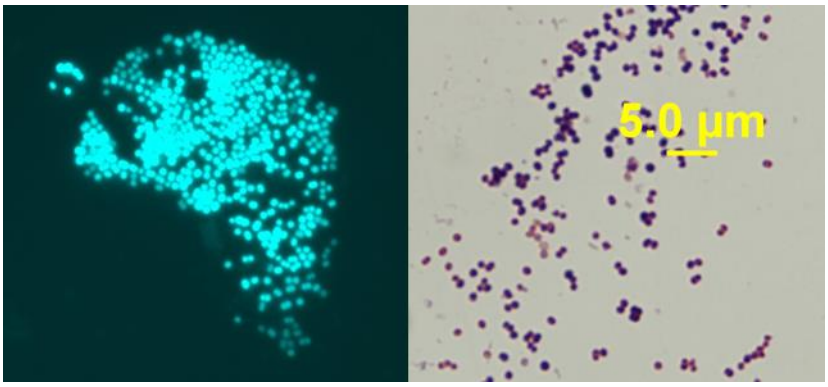

Figure 3.1. Photomicrographs of *Msp.* sp. BMS upon UV-transillumination (left), or following Gram staining (right). Both images were produced from BMS cultures following growth with BRN-RF30 medium containing methanol and hydrogen.

The growth of strains *Msp*. *stadtmanae* DSMZ 3091^T, BMS and WGK6 with different amounts of hydrogen is shown in Fig. 3.2. Interestingly, and unlike the growth of the other

two strains (Fig. 3.2A and B) the growth rate of *Msp.* sp. WGK6 was found to slow with greater amounts of hydrogen added (Fig. 3.2C) and was slower than the growth rates observed for this strains when provided different amounts of ethanol as a reductant (Fig. 3.2D). Based on these results the K_S values calculated for hydrogen (0.09 mM) show that WGK6 has the strongest affinity, in contrast to DSMZ 3091^T (0.11 mM) and BMS (1.58 mM), which of all three *Msp.* spp. examined has the weakest affinity for hydrogen. The affinity for ethanol by WGK6 (8.46 mM) however, is the weaker of the two reducing substrates examined.

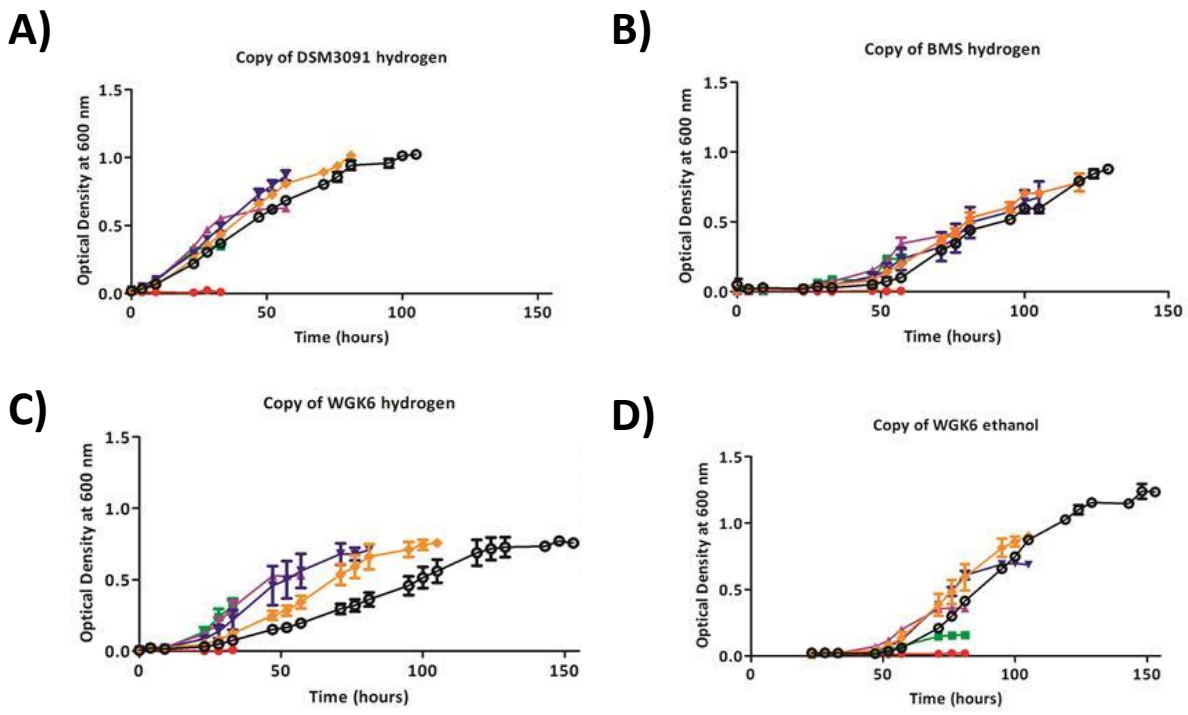

Figure 3.2. Longitudinal monitoring of the growth of *Msp. stadtmanae* DSMZ 3091^T (A), strain BMS (B) and strain WGK6 when provided with either methanol:hydrogen (C) or methanol:ethanol (D). The coloured lines and symbols denote different concentrations of either H_2 (0 ●, 1.3 ■, 1.8 ▲, 2.6 ▼, 3.5 ♦ and 4.6 ○ mM) or in the instance of panel D, ethanol (0 ●, 3 ■, 10 ▲, 30 ▼, 50 ♦ and 171 ○ mM). The growth of the individual cultures is plotted until the time point at which maximal OD_{600} was measured. Individual values represent the mean (± SEM) produced from triplicate cultures.

3.3.2 The *Methanosphaera* sp. BMS genome is larger than the DSMZ 3091^T and WGK6 genomes

The PacBio RS2 sequencing of the *Msp.* sp. BMS genome produced a draft genome comprised of 24,202 reads with an average reference coverage of 59.62, a mean length of 8,411 nucleotides, and mean read score of 0.85 (N50 of 13,284 nt). The HGAP2 assembly resulted in a single contiguous sequence where the terminal ends overlapped each other suggesting a closed genome was produced, this was confirmed by Contiguity (Sullivan et al., 2015) and sequenced amplicons from specific primers designed to target the overlap region validated the genome closure. The BMS genome was confirmed to be comprised of a single chromosome that is ~2.90 Mbp in size. The metrics for the BMS genome and the other two strains are shown in Table 3.1. In summary, the BMS genome (2.9 Mbp) is substantially larger than that of the human and kangaroo isolates of ~1.7 Mbp; and the G+C content is higher at 33%, compared to 28% for both strains DSMZ 3091^T and WGK6. The differences in relative proportions of the genome content from DSMZ 3091T and WGK6 that are readily connected with KEGG and COG pathways are slightly greater then stain BMS. Whereas strain BMS possesses a substantially larger proportion of its genome predicted to encode surface associated and/or exported proteins The CheckM analyses showed that the contamination level was estimated to be only 1.6% for BMS, and 0% for both DSMZ 3091^T and WGK6, suggesting that the BMS genome is not a chimeric assembly and is genuinely larger.

Table 3.1. General genome features for *Msp.* isolate genomes DSMZ 3091^T, WGK6 and BMS recovered using the JGI IMG/ER annotation engine. Both the number of genes and the proportion of the genome dedicated to these different categories are shown. Note the differences in relative proportions of the genome content from DSMZ 3091^T and WGK6 that are readily connected with KEGG and COG pathways, whereas strain BMS possesses a substantially larger proportion of its genome predicted to encode surface associated and/or exported proteins.

	DSMZ 3091^T		**WGK6**		**BMS**	
DNA, total number of bases	1767403	100.00%	1729155	100.00%	2868093	100.00%
DNA coding number of bases	1508136	85.33%	1475054	85.30%	2374599	82.79%
DNA G+C number of bases	488399	27.63%	478894	27.70%	944504	32.93%
Protein coding genes	1536	96.48%	1592	96.90%	2204	97.61%
rRNA genes	12	0.75%	6	0.37%	7	0.31%
5S rRNA	4	0.25%	2	0.12%	3	0.13%
16S rRNA	4	0.25%	1	0.06%	2	0.09%
23S rRNA	4	0.25%	3	0.18%	2	0.09%
tRNA genes	42	2.64%	43	2.62%	40	1.77%
Protein coding genes with function prediction	1004	63.07%	1197	72.85%	1500	66.43%
Protein coding genes connected to KEGG pathways	572	35.93%	564	34.33%	603	26.71%
Protein coding genes connected to KEGG Orthology (KO)	913	57.35%	912	55.51%	1002	44.38%
Protein coding genes connected to MetaCyc pathways	472	29.65%	471	28.67%	508	22.50%
Protein coding genes with COGs	1062	66.71%	1067	64.94%	1282	56.78%
with KOGs	333	20.92%	345	21.00%	377	16.70%
with Pfam	1228	77.14%	1256	76.45%	1590	70.42%
with TIGRfam	556	34.92%	554	33.72%	627	27.77%
with InterPro	1271	79.84%	807	49.12%	1020	45.17%
Protein coding genes with enzymes	520	32.66%	520	31.65%	560	24.80%
Protein coding genes connected to Transporter Classification	106	6.66%	109	6.63%	133	5.89%
Protein coding genes containing signal peptides	39	2.45%	39	2.37%	133	5.89%
Protein coding genes coding transmembrane proteins	216	13.57%	329	20.02%	531	23.52%
Genes in Biosynthetic Clusters	39	2.45%	17	1.03%	143	6.33%
Fused protein coding genes	92	5.78%	34	2.07%	86	3.81%

3.3.3 Genome "barcode" validates fidelity of *Methanosphaera* sp. BMS assembly

I next produced a Mauve alignment between the three sequenced genomes as I described in Chapter 2, and which is illustrated in Fig. 3.3. The results show that there is a large amount of synteny among the three genomes, with the "additional" content present in the BMS genome assembly present in large blocks, concentrated to one end of the assembly, and with only a limited amount of collinear blocks interspersed throughout this region.

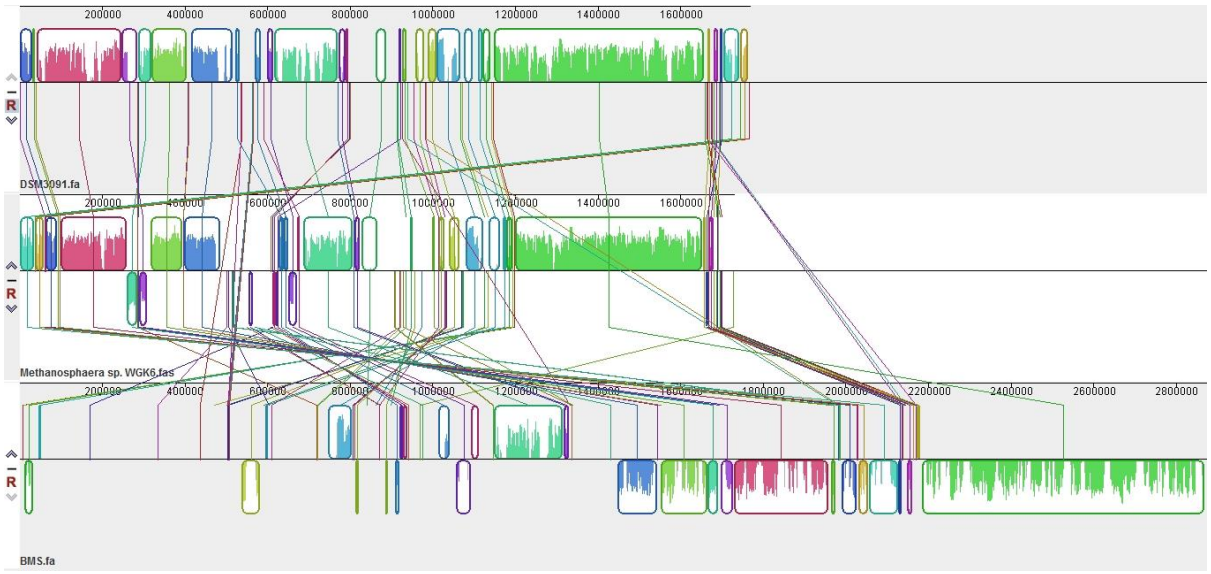

Figure 3.3. The degree of genome synteny evident between the *Msp. stadtmanae* DSMZ 3091^{T}, WGK6 and BMS genomes using Mauve, as described in Chapter 2. The xenologous regions present in the BMS genome are not ubiquitous, as illustrated by the large high degree of synteny between all three genomes.

To further establish whether the additional genome content may represent contaminating and/or chimeric assembly of DNA molecules, I used BarcodeByMers analysis to investigate the tetramer nucleotide frequency distributions across the three genomes. The results of these analyses are shown in Fig. 3.4 and illustrate that the profiles are all highly similar. Last, I selected regions based on the Mauve alignment "unique" to the BMS genome and used BLASTn to query the NCBI databases. I found no significant matches to large blocks of other bacterial or archaeal genomes, which would be expected if the assembly of the BMS genome was comprised of multiple genomes. Taken together, these results suggest that: i) the BMS genome is not a chimeric assembly and originates from an axenic culture and; ii) the extra genome content is not the result of recent gene transfer events.

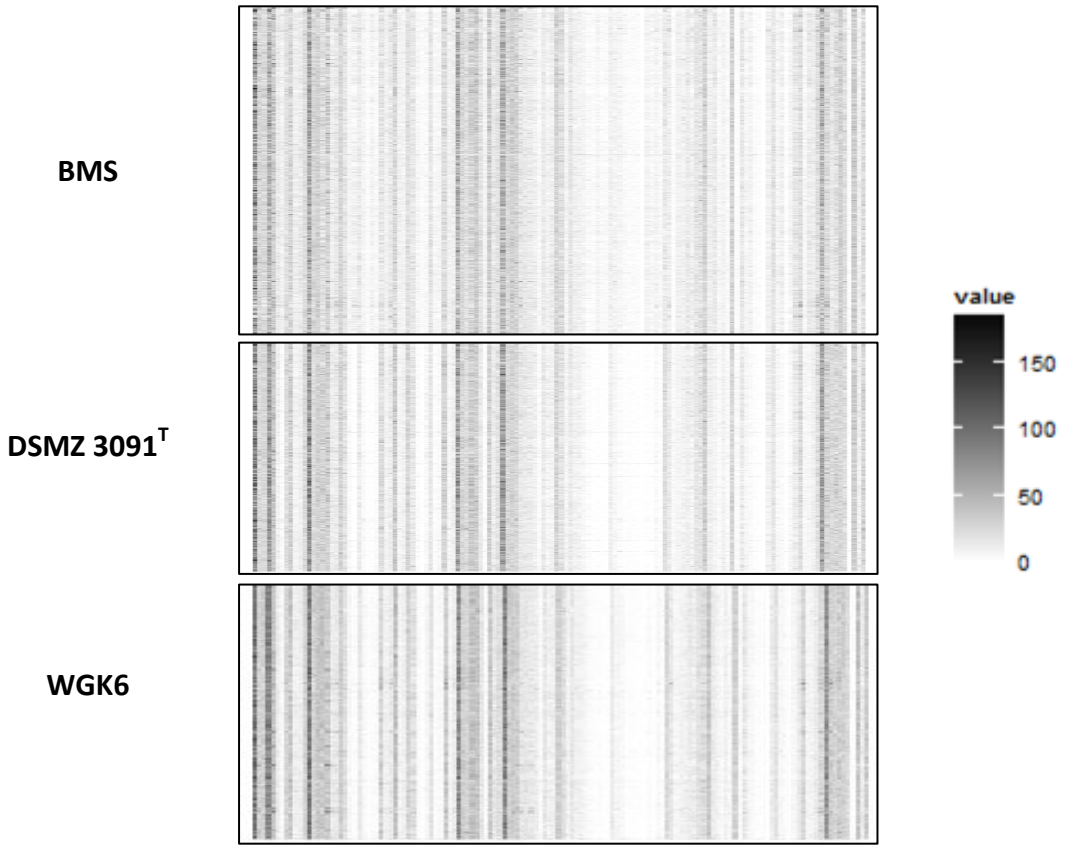

Figure 3.4. The tetramer nucleotide frequency distributions ("barcode") patterns produced by using the BarcodeByMers program with default settings, from the genomes of *Msp.* isolates BMS, DSMZ 3091^T and WGK6. Each column represents a specific tetramer nucleotide sequence, and each row represents windows of 2000 bp, with the occurrence frequency shown by the intensity scale (right). There appears to be no substantial variations in barcoding patterns across the three genomes, further supporting that neither a chimeric assembly, nor substantial amounts level of lateral gene transfer, are responsible for the increased size of the BMS genome.

3.3.4 *Methanosphaera* sp. BMS has a larger mobilome compared to other *Methanosphaera* isolates

Annotations for BMS in comparison to DSMZ 3091^T and WGK6 identified up to 36% of the genes in the BMS are strain specific, shown in Fig. 3.5. These accessory genes appear to be predominately comprised of hypothetical proteins as well as a substantial number of mobile elements (mobilome), including transposases and retroelements (Table 3.2). As shown by Table 3.2, a large portion of these "unique" genes are absent from the COG database (976) this is significantly higher in comparison to unassigned genes observed for DSMZ 3091^T

(525) and WGK6 (576). In addition to this, the BMS genome also contains a larger proportion of genes assigned as "hypothetical/unknown function", while the remainder of the "unique" gene set consists of mediators to resistance to antibiotics/toxic compounds, amino acid transport and metabolism, replication, recombination and repair, transcription, and posttranscriptional modification (Table 3.2). Indeed, the number of transposases and retroelements is dramatically different between DSMZ 3091^{T} (1 transposase in total), WGK6 (0 in total), and BMS (30 transposase and 4 RNA-directed DNA polymerases). The mobilome of BMS shows that the genes are ubiquitous, spread throughout the genome (Fig 3.6). This expanded mobilome may at one point have been responsible for the expansion of the BMS genome and closer BLASTn analysis show that over half of these genes are closely related to *Mbb.* spp., with other matches to genes from *Megasphaera* (16%), *Caldicellulosiruptor* (7%), *Bacillus*, *Methanobacterium* and *Fusobacterium* (<5%). However, the additional 1 Mbp of genomic data does not appear to be a recent acquisition for BMS, as indicated by a stable genomic signature across the genome (Fig. 3.4). Based on these results, I therefore hypothesised that the larger, BMS genome, is representative of the ancestral lineage for *Msp.* spp. and the smaller genomes have evolved as a result of substantial gene loss, possibly upon colonisation of "new" gut environments (i.e. human and kangaroo).

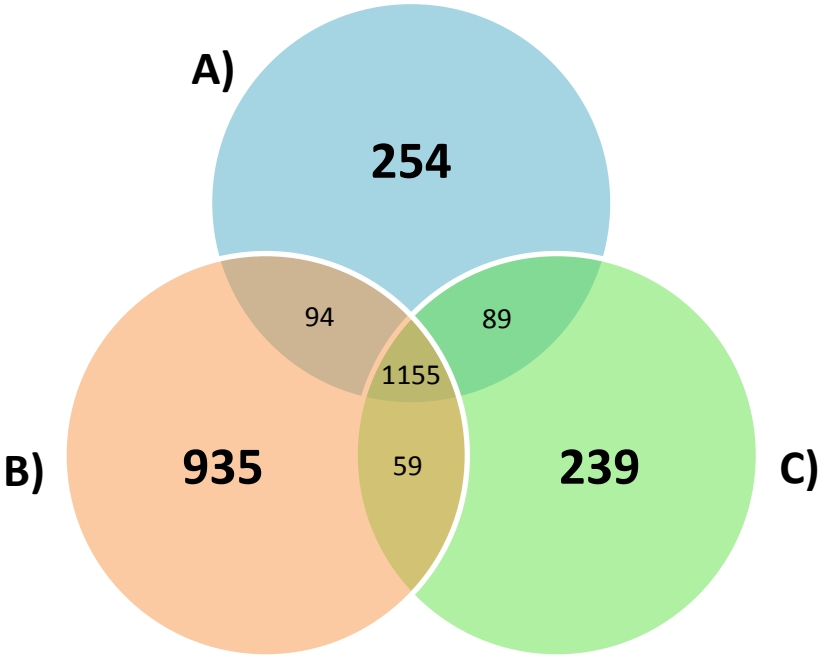

Figure 3.5. Venn diagram depiction of the core, shared and unique genes present in *Msp.* genomes from strain WGK6 (A), BMS (B) and DSMZ 3091^{T} (C). The gene counts are based on reciprocal BLASTp analysis of the EDGAR-based predictions of protein-coding genes from each genome. The *Msp.* core genome consists of 1155 genes with a low count assigned as shared (59-94), while the bulk of the remaining genes are classed as unique. Nearly half of the strain BMS genome is considered to be "unique" (935) in comparison to the other *Msp.* isolates.

Table 3.2. Comparison of the COG categories for *Msp.* isolates DSMZ 3091^T, WGK6 and BMS annotated by JGI IMG/ER. Note that the two main differences (both in gene count and proportion) are the number of genes either lacking a COG assignment, or predicted to possess prophage or transposon-like functions from strain BMS.

COG categories	**DSMZ 3091^T**		**WGK6**		**BMS**	
Not in COG	525	32.65%	576	35.06%	976	43.15%
Translation, ribosomal structure and biogenesis	168	14.53%	173	15.26%	175	12.67%
General function prediction only	110	9.52%	110	9.70%	147	10.64%
Coenzyme transport and metabolism	115	9.95%	111	9.79%	121	8.76%
Amino acid transport and metabolism	105	9.08%	96	8.47%	118	8.54%
Energy production and conversion	100	8.65%	106	9.35%	106	7.68%
Function unknown	83	7.18%	78	6.88%	105	7.60%
Cell wall/membrane/envelope biogenesis	76	6.57%	69	6.08%	79	5.72%
Replication, recombination and repair	55	4.76%	54	4.76%	72	5.21%
Transcription	47	4.07%	48	4.23%	63	4.56%
Inorganic ion transport and metabolism	53	4.58%	44	3.88%	59	4.27%
Posttranslational modification, protein turnover, chaperones	44	3.81%	45	3.97%	58	4.20%
Nucleotide transport and metabolism	53	4.58%	53	4.67%	51	3.69%
Carbohydrate transport and metabolism	43	3.72%	41	3.62%	46	3.33%
Lipid transport and metabolism	25	2.16%	29	2.56%	38	2.75%
Mobilome: prophages, transposons	1	0.09%	0	0.00%	34	2.46%
Defence mechanisms	24	2.08%	22	1.94%	26	1.88%
Signal transduction mechanisms	15	1.30%	13	1.15%	23	1.67%
Secondary metabolites biosynthesis, transport and catabolism	6	0.52%	8	0.71%	18	1.30%
Intracellular trafficking, secretion, and vesicular transport	13	1.12%	14	1.23%	16	1.16%
Chromatin structure and dynamics	8	0.69%	7	0.62%	12	0.87%
Cell cycle control, cell division, chromosome partitioning	8	0.69%	8	0.71%	10	0.72%
Cell motility	3	0.26%	3	0.26%	3	0.22%
Extracellular structures	1	0.09%	2	0.18%	1	0.07%

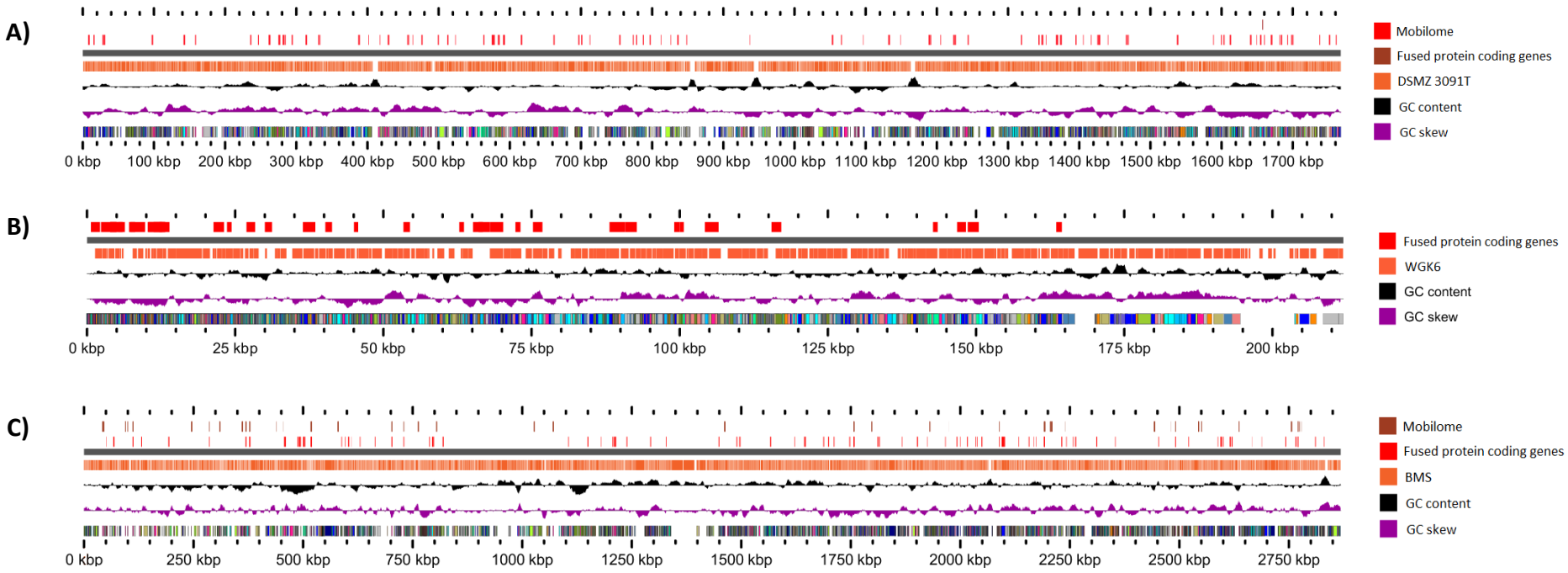

Figure 3.6. Linear representations of the genomes of DSMZ 3091^{T} (A), WGK6 (B) and BMS (C) showing the location of their respective mobilome and fused protein coding genes; as identified by JGI IMG/ER and COG assignment and visualised using Gview, as described in the materials and methods. The genome of strain BMS possesses the greatest number of genes assigned to the mobilome (34) and second highest number of fused protein coding genes (86) which are ubiquitous throughout the genome. The genome of strain DSMZ 3091^{T} is predicted to contain only one gene encoding mobilome function, but the highest number of ubiquitous fused protein coding genes (92) of the three isolate genomes. Finally, WGK6 has no genes assigned to the mobilome and only 34 fused protein coding genes assigned to a 0.75 Mbp region of the genome (1.7 Mbp in total).

3.3.5 The *Methanosphaera* population genomes extracted from other metagenome sequence datasets are comprised of two "genomotypes"

Seven additional *Msp.* spp. population genomes were recovered from two publically available metagenomic datasets and one unpublished CSIRO project, and the statistics for each population genome are presented in Table 3.3. I have estimated the size of the "complete" genomes by using CheckM's completeness score and the size of each population genome, and based on these calculations I was successful in recovering another two "small" (<2.0 Mbp) and five "large" (>2.1Mbp) genomes, further validating that the BMS genome is a true representation of *Msp.* affiliated archaea.

Table 3.3. Summary statistics of the *Msp.* isolate and MetaBAT-recovered population genomes, with respect to population genome size, CheckM completeness and contamination scores, and the predicted complete genome size, based on these metrics.

Genome designation	Source	Location	Population genome size (bp)	GC (%)	CheckM completeness (%)	CheckM contamination (%)	Predicted complete genome size (Mbp)
DSMZ 3091^{T}	Human	US	1767403	28.0	99.0	0	
WGK6	Western Grey kangaroo	AUS	1729155	28.0	98.1	0	
BMS	Bovine	AUS	2868093	33.0	99.1	0.8	
DEW79	Human	Europe	1594581	27.6	97.2	0.8	1.6
SHI613	Ovine	NZ	1859301	33.0	90.4	0	2.1
SHI1033	Ovine	NZ	1496386	29.9	74.3	0	2.0
rholeuAM6	Bovine	AUS	1935828	32.9	92.7	0	2.1
rholeuAM74	Bovine	AUS	2004016	35.5	75.9	0.8	2.6
rholeuAM130	Bovine	AUS	2057527	34.8	77.6	4.7	2.5
rholeuAM270	Bovine	AUS	1763900	35.5	61.8	0	2.9

3.3.6 All *Methanosphaera* isolate and population genomes possess a high degree of synteny

The Mauve alignments of the small genomotypes showed there is high level of synteny between all these genomes, illustrated in Fig. 3.7. Additionally, the Mauve alignments of the large genomotypes revealed a high level of synteny and importantly, the population genomes provide confirmatory evidence of syntenic regions extending across the 1 Mbp "unique" region produced by the sequencing of the BMS genome (Fig. 3.8). Based on these findings, I hypothesised that *Msp.* phylogeny could be reconstructed from a pan-genome approach. To address this hypothesis, I first constructed a phylogenetic tree using 122 universal marker genes identified by PhyloSift. Next the core genome was identified, and these genes were concatenated with EDGAR and also used to construct a phylogenetic tree. Both these analyses produced similar results, as shown in Fig. 3.9; which depicts a clear separation between species with a smaller genome (< 2.0 Mbp: DSMZ 3091^{T}, WGK6, DEW79 and SHI1033) from those with genomes larger than 2.1 Mbp. It would also appear that the smaller genomes have evolved from ancestral strains with a larger genome through gene dispensation, supporting my hypothesis that the human and kangaroo strains evolved through a loss of genomic content as a result of host adaptation.

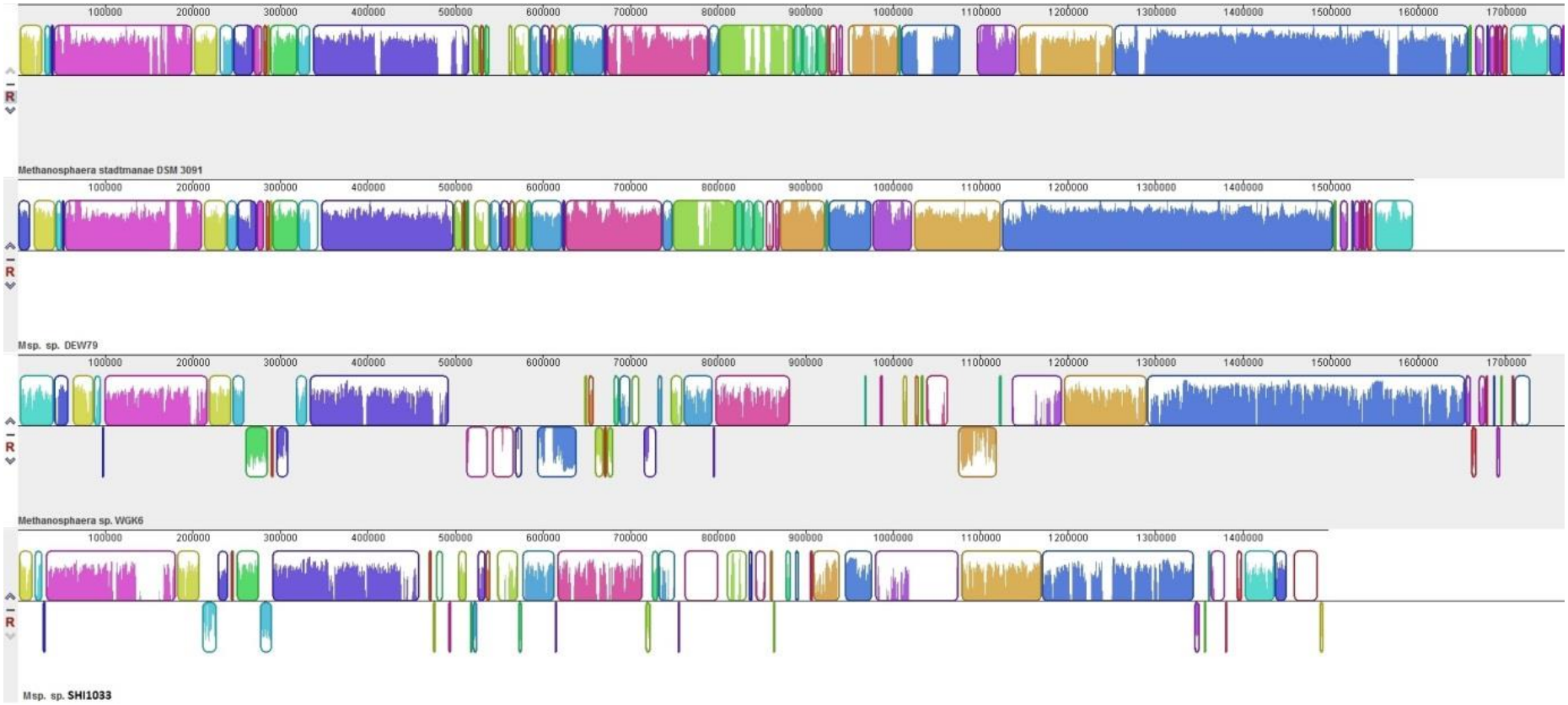

Figure 3.7. Mauve alignments of the "small" (< 2.0 Mbp) genomes *Msp. stadtmanae* DSMZ 3091^{T}, DEW79, WGK6 and SHI1033. The extent of the synteny between all the genomes is striking, and especially so between the *Msp. stadtmanae* DSMZ 3091^{T} and DEW79 population genome, both representing isolates of human origin.

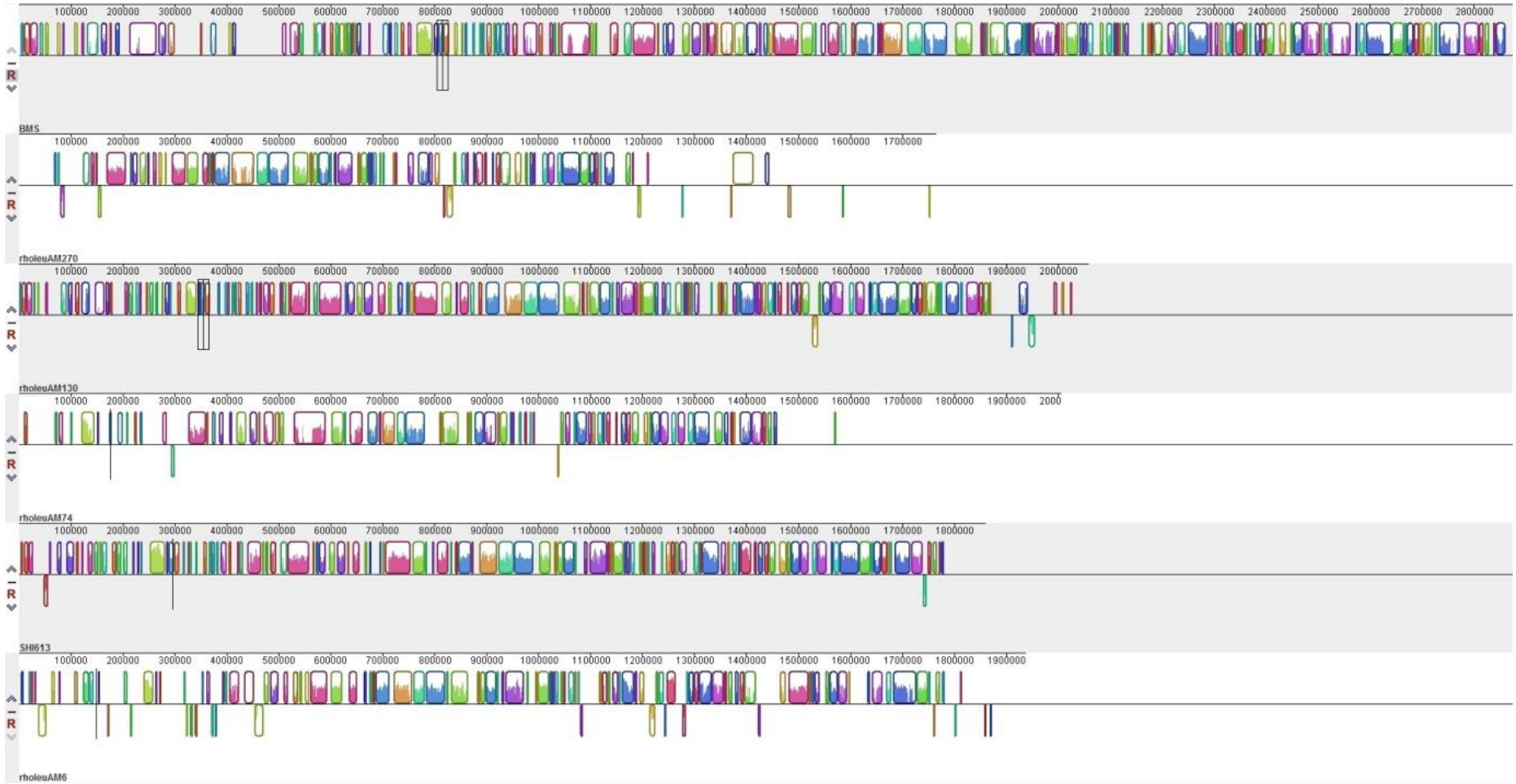

Figure 3.8. Mauve alignments of the "large" (> 2.1 Mbp) *Msp.* spp. population genomes (rholeuAM270, rholeuAM130, rholeuAM74, SHI613 and rholeuAM6) against reference isolate genome BMS. The extent of gene synteny among all ruminant originating species is notable, save for rhoeuAM270 and rholeuAM74, which have noticeable xenologous regions at the end of their sequence lengths.

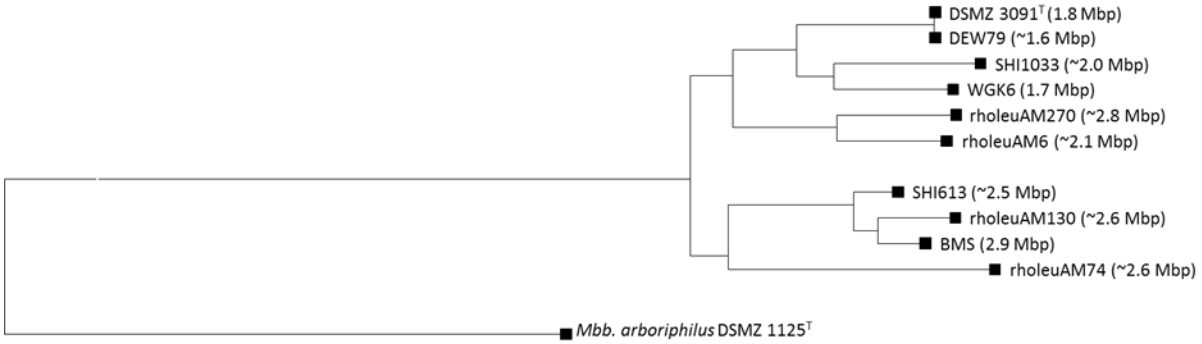

Figure 3.9. The whole genome phylogenetic tree of the isolate and population genomes recovered for *Msp.* spp. The tree was constructed by ARB from concatenation of 122 universal marker genes and genomes available in IMG v4.510 and shows a clear separation of "smaller" genomes (< 2.0 Mbp) which appear to be descendants of "larger" (> 2.1 Mbp) ruminant genomes.

Comparative analyses of the 3 isolate and 7 population genomes core housekeeping genes were examined through phylogenetic placement and are shown in Fig. 3.10 and 3.12. The core methanol-reducing methanogenesis gene methyl-coenzyme M reductase component A2 (*mrtA*) recapitulates the finding of the whole genome phylogeny (Fig. 3.10). In addition to this the comparison of the energy conserving hydrogenase gene (*ehaRST*) demonstrates a high degree of synteny (Fig. 3.11) across all the *Msp.* spp. representatives validating the initial Mauve alignment of whole genomes (Fig. 3.7 and 3.8). Phylogenetic placement for each of the *Eha* genes reveals the same findings as those shown for *mrtA* gene (Fig. 3.12).

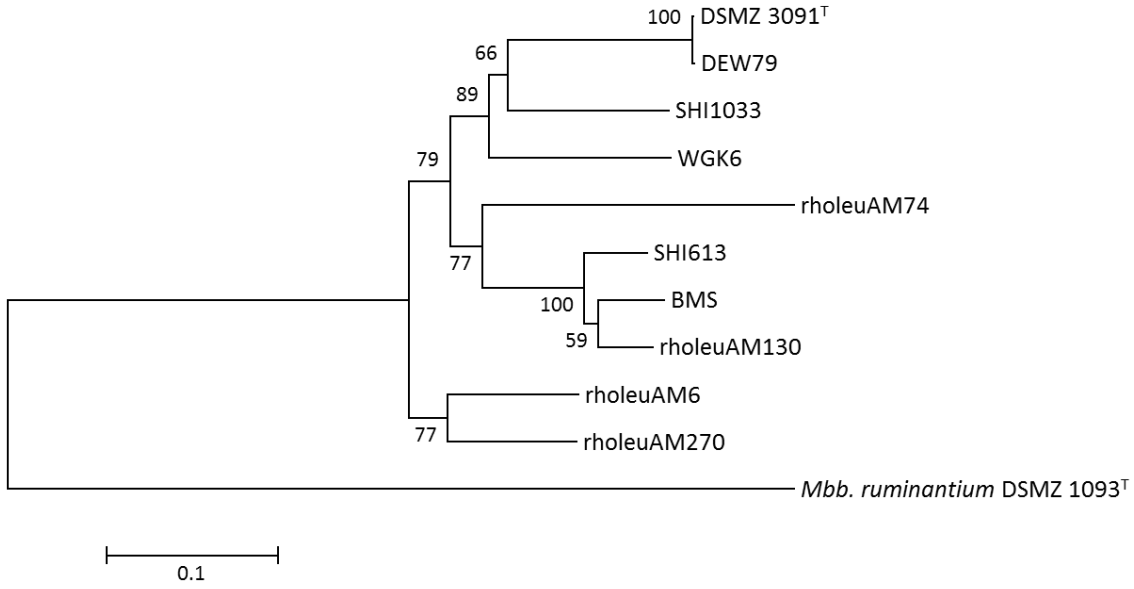

Figure 3.10. The phylogenetic tree constructed with Jones-Taylor-Thornton (JTT) model, using BLASTp alignments of methyl-coenzyme M reductase component A2 (*mrtA*) genes sampled from the core set of the 10 *Msp.* genomes. Recapitulating the findings from the whole genome phylogeny (Fig. 3.8) the *mrtA* phylogeny shows a clear separation of "smaller" genomes (< 2.0 Mbp) which appear to be descendants of "larger" (> 2.1 Mbp) ruminant genomes. The scale bar represents 10% sequence divergence. Numbers represent the relative frequency of branch clustering based on 1000 bootstrap runs, bootstrap values less than 50% are removed, with *Mbb. ruminantium* DSMZ 1093^T used as the outgroup.

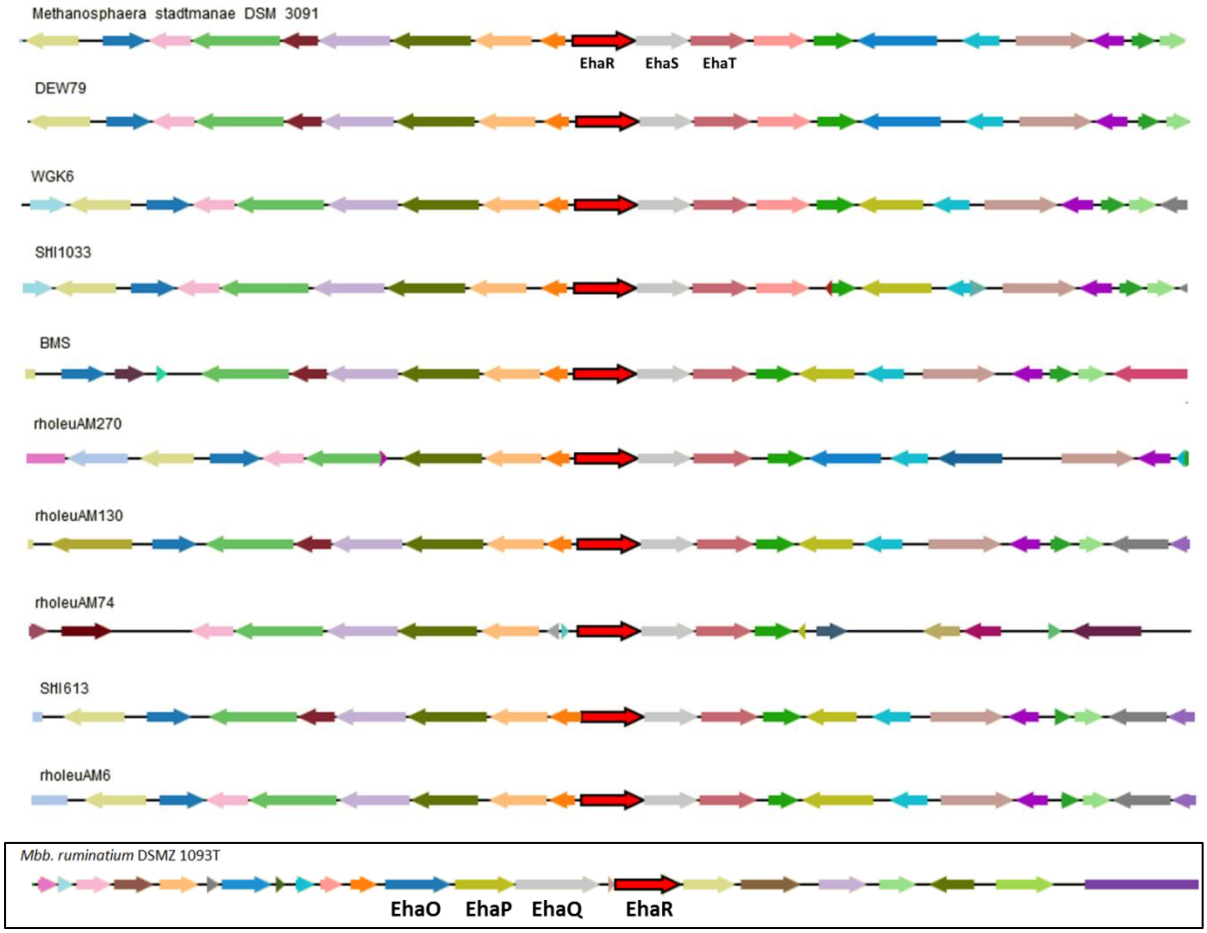

Figure 3.11. EDGAR software alignment of gene regions containing the energy conserving hydrogenase gene (e*haRST*) for the 10 *Msp.* genomes. The extent of gene synteny and conservation supports the contention that all these genomes are representative of the *Msp.* genus; *Mbb. ruminantium* DSMZ 1093^{T} is used as the outgroup.

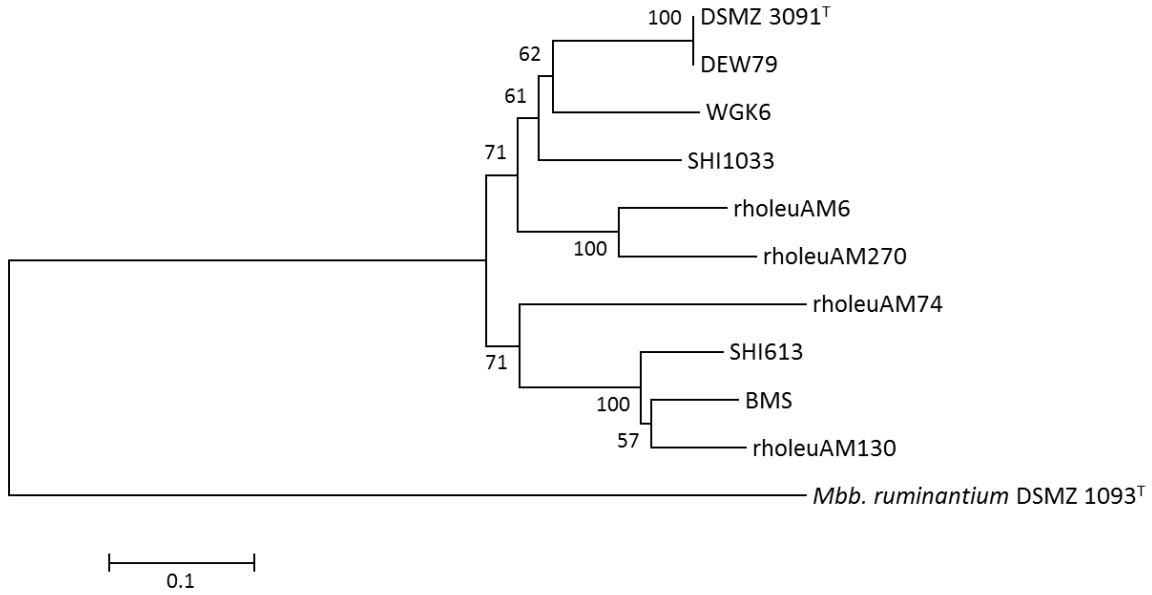

Figure 3.12. The phylogenetic tree constructed with Jones-Taylor-Thornton (JTT) model, using BLASTp alignments of energy conserving hydrogenase gene (*ehaR*) genes sampled from the core set of the 10 *Msp.* genomes. Recapitulating the findings from the whole genome and *mrtA* phylogeny (Fig. 3.8 and 3.9), the *ehaR* phylogeny shows a clear separation of "small" genomes (< 2.0 Mbp) which appear to be descendants of "large" genome (> 2.1 Mbp) ruminant ancestors. The scale bar represents 10% sequence divergence. Numbers represent the relative frequency of branch clustering based on 1000 bootstrap runs, bootstrap values less than 50% are removed, with *Mbb. ruminantium* DSMZ 1093^T used as the outgroup.

KEGG pathways for methane metabolism for each of the population genomes are partially assembled, but it is apparent that methanol and no other methylated derivatives (i.e. methylamines) are the used as substrates for methanogenesis with the presence of coenzyme M methyltransferase subunits A, subunit B and/or subunit C. While hydrogen-dependent reduction of methanol to methane may be a common feature throughout my collection of genomes I have also identified some substantive differences which may support my previous findings that at least some species of *Msp.* are not strictly hydrogen dependent methylotrophs. As shown in Chapter 2 of this thesis, culture-based studies of WGK6 revealed that this archaeon can use ethanol as a sole source of reducing power for methanol reduction and methanogenesis, via genes encoding for alcohol- and aldehyde- dehydrogenases. Interestingly, homologues of these genes are also present in the ovine-derived population

genome SHI1033 (both dehydrogenase genes having 88% identity and 94% coverage compared to WGK6 dehydrogenase genes, see Fig. 3.13) which originates from animals described as “low methane” producers. Homologues of these genes are absent from all the other population genomes, as well as the BMS and DSMZ 3091^{T} genomes, which is consistent with BMS and DSMZ 3091^{T} culture-based studies. Consistent with analysis of the whole genome phylogeny I have also confirmed that WGK6 and SHI1033 are closely related (Fig. 3.9).

A)

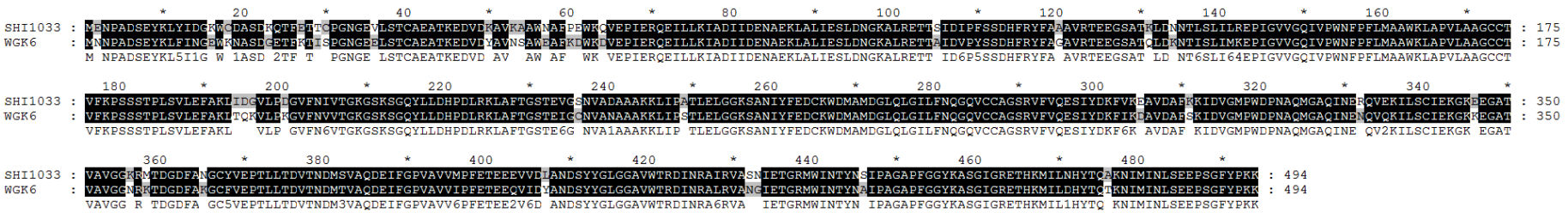

B)

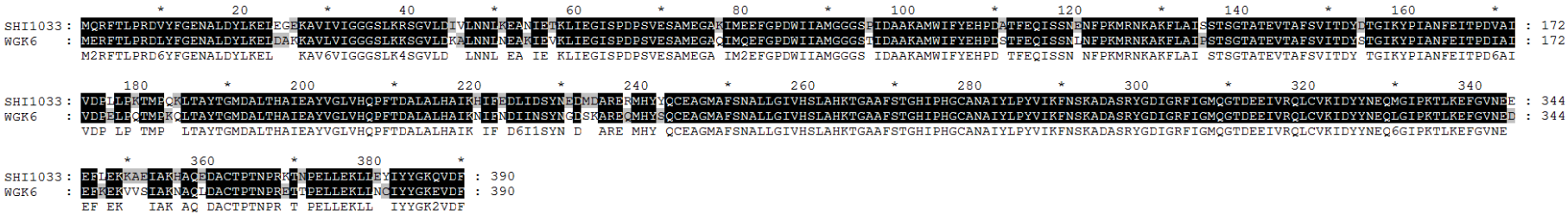

Figure 3.13. The clustalW alignment for the aldehyde (A) and alcohol (B) dehydrogenase genes identified in both *Msp.* sp. SHI1033 and WGK6, which are 88% identical across 94% of the two genes.

The CAZyme annotations from dbCAN for each of the *Msp.* genomes are shown in Table 3.4. There are six CAZyme families identified across the 10 *Msp.* genomes and the general profile appears to be evolutionarily conserved and maintained across all genomes. This serves to validate the veracity of the population genomes recovered, considering the level of completeness of the population genomes the assembly would appear to be accurate and precise. Taking a closer look at the CAZyme families the first is defined as auxiliary activity (AA) classified as 1,4-benzoquinone reductase (KEGG enzyme EC. 1.6.5.6) for the shunting of protons and electrons for the conversion of NADPH, H^+ and p-benzoquinone to $NADP^+$ and hydroquinone, for types AA3 and AA6 the profile is the same across the genomes. In contrast the carbohydrate-binding module (CBM) is poorly represented across the *Msp.* genome representatives. Carbohydrate esterase (CE) family plays a role in the metabolism of methane as S-formylglutathione hydrolase (KEGG enzyme EC 3.1.2.12) converting S-formylglutathione to formate and the profile is again conserved across all genomes. The glycoside hydrolases (GH) have scant representation across the genomes, save for GH109, an α-N-acetylgalactosaminidase which supports the cleavage of peptidoglycan in the cell wall formed from linear chains of two alternating amino sugars, namely N-acetylglucosamine and N-acetylmuramic acid (Ashida et al., 2000, Balch et al., 1979). Of these CAZyme families the most numerically abundant and conserved is glycosyltransferases (GT), namely GT2 and GT4, these genes are involved with glycosylation, attaching glycans to proteins most commonly found in cell surface proteins (Jarrell et al., 2010, Magidovich and Eichler, 2009). These conserved GT modification enzymes decorate the cell wall and may play a role in the variation of immunomodulation between methanogenic archaea. Finally, the CAZyme family polysaccharide lyase (PL) had a low gene count but was still represented by most genomes, in particular was PL9 a pectate lyase (KEGG enzyme EC 4.2.2.2).

Table 3.4. Gene counts for CAZyme families obtained from annotation of the 10 *Msp.* spp. genomes by dbCAN. Overall the profile of CAZyme families and total gene counts represented by each genome are virtually the same, suggesting that these functions have been conserved and maintained across both genomotypes.

CAZyme Family	DSMZ 3091^{T}	WGK6	BMS	DEW79	SHI613	SHI1033	rholeuAM6	rholoeuAM130	rholeuAM74	rholeuAM270
Auxiliary Activity										
AA3	1	1	1	1	1	1	1	1	1	1
AA6	7	10	14	7	13	13	10	10	8	7
AA9			2		1			1		
Carbohydrate-Binding Module										
CBM35					1				5	
CBM54					1					
Carbohydrate Esterase										
CE1	3	3	3	3	2	3	3	2	1	3
CE10			3				1		3	1
CE2								1		2
CE3							1			
Glycoside Hydrolase										
GH10			1							1
GH109	1	1	2	1	1	1	2	1	1	
GH120							1	1	1	
GH2									1	
GH20									1	
GH24						1				
GH46							1			
Glycosyltransferase										
GT2	31	28	26	29	17	25	27	18	11	12
GT27		4	1	1	2	1	1	3	1	1

GT28	5	2	2	5	2	2	3	2		
GT31								1		
GT4	12	15	14	12	14	15	12	14	13	13
GT44			1							
GT45		1	1		2		1	1		
GT5									1	
GT66	3	3	2	3	3	2	2	1	3	3
GT8									1	
GT81	1	1	1	1	1	1	1	1	1	
GT83	3	2	3	3	2	3	2	2	2	2
GT93						1				
Polysaccharide Lyase										
PL14							1			
PL6						1				
PL9	3		2	3			2	1	1	1
Total	70	71	79	69	63	70	72	61	56	47
Total based on completeness	71	72	80	71	69	88	77	76	69	65

Gene counts for the ammonium assimilation pathway were recovered from the pan-genome annotation for all 10 *Msp.* spp. and are shown in Table 3.5. Ammonium assimilation and metabolism is important for its incorporation into cell material, this occurs mainly by the glutamate dehydrogenase (GDH) and/or glutamine synthetase-glutamate synthase pathway (GS-GOGAT; Cabello et al., 2004). The NADP-specific GDH gene is present as a single copy across all of the isolate genomes, with only missing from 3 of the draft population genomes. The GS-GOGAT pathway is represented by conserved glutamine synthetase gene Type 1 (GS1) profile across all of the genomes averaging a single gene count while there is some variation for glutamate synthase. This variation is most notable for WGK6 as the other isolate and population genomes have 2-4 copies of the gene (consisting of the mainly of the 3 glutamate synthase subunits) WGK6 only possesses one copy (GS-GOGAT subunit 2).

Table 3.5. Profile of genes assigned to encode for NADP-specific glutamate dehydrogenase (GDH) or the glutamine synthetase Type 1 (GS1)/glutamate synthase (GS-GOGAT) pathways of ammonia assimilation.

	Glutamate dehydrogenase (GDH)	**Glutamate synthase (GS-GOGAT)**	**Glutamine synthetase (GS1)**
DSMZ 3091^{T}	1	3	1
WGK6	1	1	1
BMS	1	3	2
DEW79	1	3	1
SHI1033		4	2
SHI613	1		1
rholeuAM6	1	3	1
rholeuAM74	2		1
rholeuAM130		2	1
rholeuAM270		3	1

3.4 Discussion

Collectively my results demonstrate an expansion of the genomic representation for *Msp.* spp., which revealed 2 separate genomotypes characteristically identified as either possessing a “large” (>2.1 Mbp) or “small” (<2.0 Mbp) genome with evidence to suggest that the “small” genomotype is a more recent evolutionary event (Fig. 3.9) occurring through the dispensation of genes (Fig. 3.4). While there have obviously been events to drive these species to adapt to their respective host environments the average nucleotide identity (ANI) of the core-genome recovered from complete and draft genome (Fig. 3.14) supports my

identification of 9 new *Msp*. representatives. Of the ten genomes DSMZ 3091^{T} and DEW79 have an ANI value above the generally accepted threshold for species recognition (> 95%) (Konstantinidis et al., 2006) while the others ranged between 77-85%, values which are still considered to occur within a genus (typically 62-100%) (Kim et al., 2014). Collectively these values suggest that of all the genomes recovered during this study 8/10 are novel species to the genus *Msp*. The findings presented in this Chapter are not an exhaustive comparative analysis and only provide preliminary findings which focus on differences in genome size and validation of this observation, for the previously poorly represented *Msp*. spp.

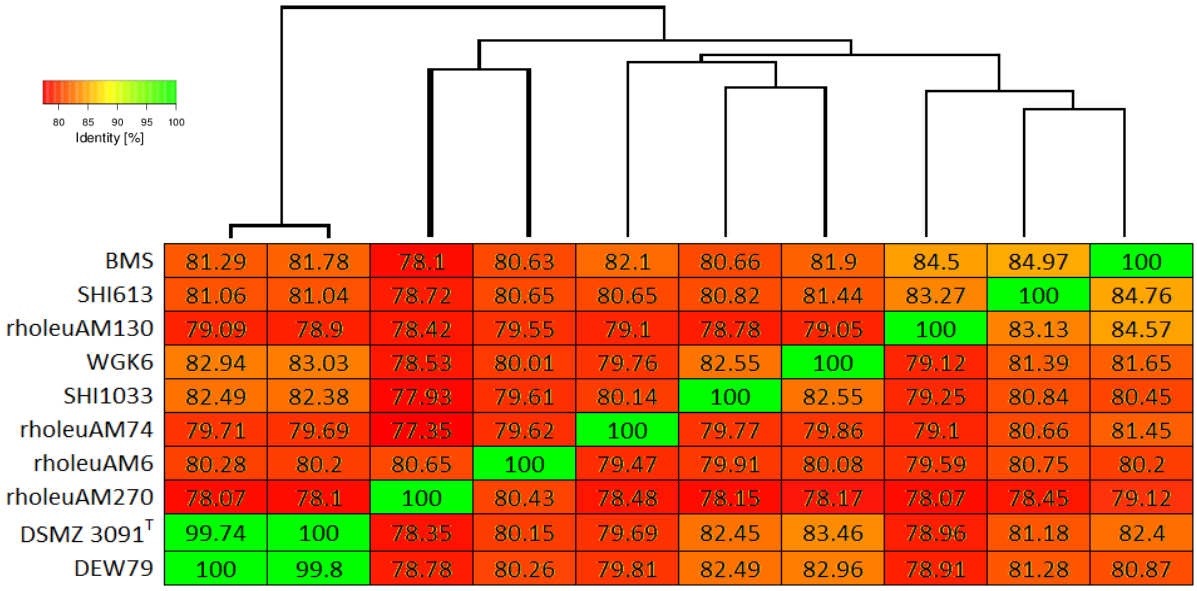

Figure 3.14. The average nucleotide identity (ANI) matrix of both *Msp.* isolate and population genomes, calculated from blast hit results between the orthologous genes of the core-genome using software platform EDGAR. ANI values higher than 95% are considered to be the same species and values from 62-100% belong to the same genus. All ANI values displayed in the matrix are greater than 77% but only two genomes exceed 95%, indicating that they are members of the same species (i.e. DSMZ 3091^{T} and DEW79).

Development plots for the core and pan-genome of these *Msp.* spp. representative genomes are showed in Figure 3.15. The pan-genome consists of 5,321 genes and 305 are assigned to the core-genome, which essentially consists of genes supporting methanogenesis (*hdr* Heterodisulfide reductase, *mtd* F420-dependent methylenetetrahydromethanopterin dehydrogenase, *mcrA* methyl-coenzyme M reductase A2, NADPH-dependent F420 reductase, formylmethanofuran--tetrahydromethanopterin formyltransferase, coenzyme F420

hydrogenase), ABC transporters, glycosyltransferases, transcription/translational initiation factors and hypothetical genes. Growth of the pan-genome continues to trend upwards suggesting that there is still room for the development of this collection (Fig. 3.15). However, the core-genome would appear to be covered upon the addition of the eighth genome, a representation which may be improved if complete genomes were used rather than draft population genomes, as I have shown with the *Msp.* isolate core genome (n= 1155; Fig. 3.4). In addition to this we can see from the dbCAN profile (Table 3.4) that there is a level of conservation of enzymes linked to cell wall biosynthesis across both the isolate and draft population genomes. These findings not only confirm the veracity of the genome recovery and phylogenetic relatedness among the isolate and population genomes, but also provide important information for rumen microbiologists who are interested in developing vaccines for methane abatement strategies, as well as human immunologists who are investigating the role of methanogenic archaea in the onset and/or progression of non-communicable diseases. As demonstrated by Blais Lecours et al. (2014) persons suffering IBD had an increased prevalence of *Msp*. sp. as well as a high specific IgG response. Additionally, the human isolate of *Msp. stadtmanae* DSMZ 3091^{T} can elicit a stronger inflammatory response than *Mbb. smithii* (Blais Lecours et al., 2011, Blais Lecours et al., 2014, Bang et al., 2014).

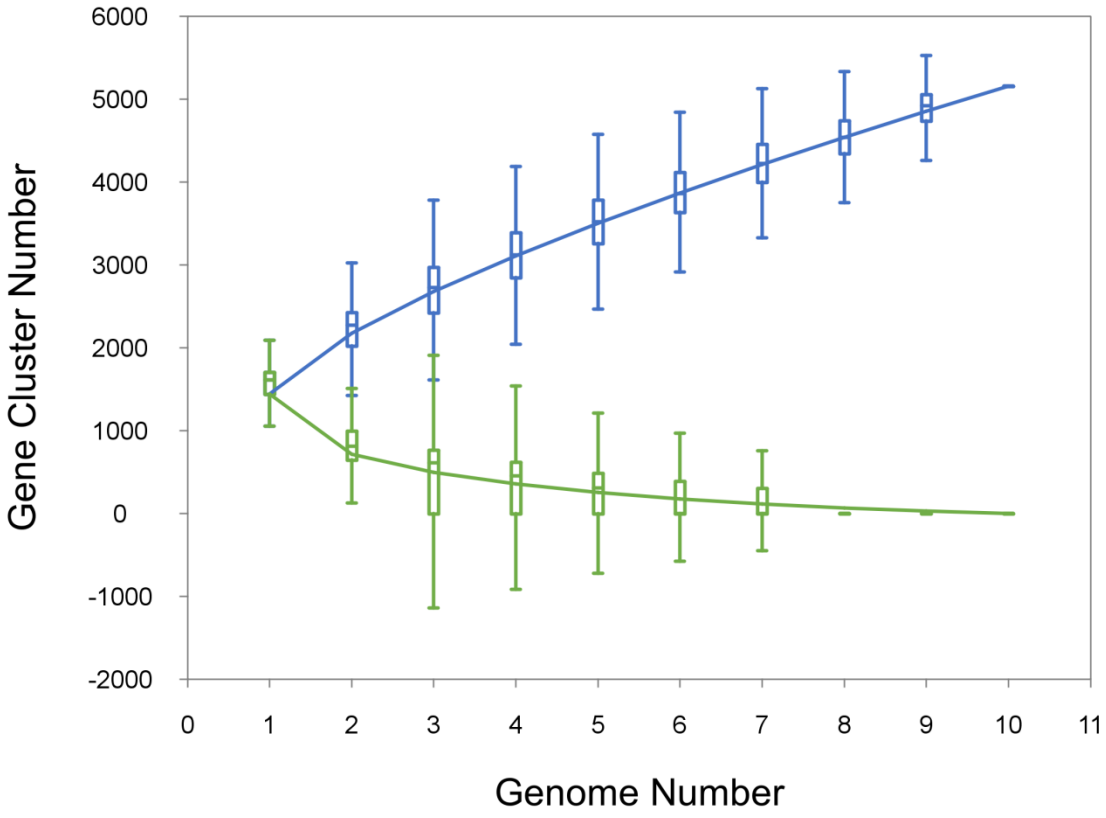

Figure 3.15. Development plots depicting the growth of the core (green, $y = 2349.33e^{-0.55x} + 45.92$) and pan-genome (blue, $y = 14255.55x^{0.55} + 42.25$) for the *Msp.* isolate and population genomes clustered through Biolinux command line PGap, and plotted with software package PanGP. The total pan-genome consists of 5,321 genes, while the core-genome for all 10 *Msp.* representatives has a relatively small gene count (305) in comparison to the isolate genomes (Fig. 3.5) most likely due to the incomplete nature of the population genomes.

In Chapter 2, I showed that the alcohol-fuelled methanogenesis pathway of strain WGK6 involves tandemly located alcohol and aldehyde dehydrogenase genes. Investigation of the isolate and population genomes showed that these dehydrogenase gene orthologs were only present in the ovine-derived population genome SHI1033 (Fig. 3.13). The SHI1033 dehydrogenase genes originate from an ovine phenotypically typed as a low methane producing animal. I believe this is an example of adaptation in response to a "low hydrogen" environment, a pressure which would force *Msp.* spp. to utilise an alternate source of reducing power in order to persist within the microbiome. These findings not only validate the findings of Chapter 2 but I feel they also provide new insights into the nutritional ecology

of gut methanogens, and in particular the ability of methanogenic archaea to adapt to change. The question still remains, to what extent are these metabolically versatile *Msp.* spp. present within a wider variety of gut environments? Are they in fact present in environments which encourage adaption to "low hydrogen" or increased availability of short chain alcohols? Such findings are not only relevant to efforts curbing livestock methane emissions, but also have potential implications in regards to our understanding and monitoring of gut dysbiosis in humans. It has been shown that fermentation schemes favouring ethanol formation are more active in non-alcoholic fatty liver disease where periods of gut "dysbiosis" results in a shift in the microbial community structure (Lau et al., 2015). In fact *Msp.* spp. are receiving more attention as their potential link to gut "dysbiosis" conditions such as IBD become more likely. For instance, a notable shift from the prevalence of hydrogenotrophic to methylotrophic methanogenic archaea such as *Msp.* spp. has been reported for IBD patients (Blais Lecours et al., 2014).

In conclusion, the identification of larger *Msp.* genomes, which appear to be the ancestor of the model representative *Msp. stadtmanae*, and presence of dehydrogenase genes within another "low methane" environment further validate my previous findings that *Msp.* spp. have undergone some important evolutionary adaptions to persist within a variety of gut environments and are more diverse/metabolically versatile than previously thought.

Chapter 4 Variations in *Methanobrevibacter* and *Methanosphaera* spp. populations in clinical studies and assessment of their immunomodulatory properties

4.1 Introduction

As outlined in the preceding Chapters of my thesis, the methanogen communities of livestock and other herbivores are typically dominated by *Mbb.* spp., which is widely recognized to sustain syntrophic metabolism via hydrogen and carbon dioxide utilization for methanogenesis (e.g. Miller et al., 1982, Bryant and Wolin, 1975). The methylotrophic methanogenic archaea such as *Mms.* and *Msp.* spp. are also commonly encountered, usually at lower numbers, but sometimes, they are the predominant members of these archaeal communities (Seedorf et al., 2015, Dridi et al., 2011, St-Pierre and Wright, 2013). Recent studies suggest that the abundance of these methylotrophic archaea may be linked with total methane output. For instance, an increased abundance of *Msp.* spp. were observed in the "low" methane sheep by Shi et al. (2014), in contrast to the typical *Mbb.* spp. domination seen within "high" methane emitting sheep. Parallel studies in Europe with beef cattle produced similar findings with respect to higher numbers of *Mbb.* spp. in the "high" emitters (Wallace et al., 2015). Such findings suggest that gaseous hydrogen formation by the microbiota can affect both the ecology and quantity of methanogenic archaea (Kittelmann et al., 2014).

As outlined in my literature review, much of our understanding about human gut methanogens and methanogenesis is based on studies conducted with subjects from first-world countries. A higher prevalence of methane excretors (and when measured, methanogen abundance in faeces) is seen among persons suffering from gastrointestinal disorders, including IBS-C, colorectal cancer and diverticulosis (Chatterjee et al., 2007, Conway de Macario and Macario, 2009). In a recent case-controlled study of inflammatory bowel disease (IBD), Blais Lecours et al. (2014) found that healthy control subjects had a higher prevalence of *Mbb. smithii* and a paucity of *Msp. stadtmanae*. However, the IBD group not only had a much reduced total number of methanogens, but the community had changed to a greater prevalence of *Msp. stadtmanae.* Although none of these associations establish whether methanogens and/or methanogenesis are the cause or a consequence of these conditions, Conway de Macario and Macario (2009) did propose that the role for methanogenic archaea in gut disorders may be indirect: a reflection of the nutritional ecology and metabolic interactions that "shape" the gut microbiota during the periods of microbial "dysbiosis" seen

with many non-communicable diseases, from periodontitis to obesity. In that context, recent studies of the gut microbiota of patients with non-alcoholic fatty liver disease and more severe conditions (i.e. end-stage renal disease (ESRD)) suggest that the microbiota is not only "dysbiotic", but fermentation schemes favouring short chain alcohol formation are more active (Lee et al., 2012, Zhu et al., 2013).

The interaction between methanogens and the host immune system have been relatively underexplored although Conway de Macario and Macario (2009) hypothesised that it may occur and have relevance to health and well-being. Consistent with this Blais Lecours et al. (2011) reported that *Msp.* spp. are a principal component of bioaerosols in animal houses, and using a mouse model showed that *Msp. stadtmanae* provokes a stronger immune response within the lung tissue (including stimulation of macrophage, lymphocyte, neutrophil, and eosinophil recruitment to lung tissue) than mice exposed to preparations of the *Mbb. smithii*. Blais Lecours et al. (2014) also found that with the increased prevalence of *Msp. stadtmanae* in IBD patients as determined by qPCR methods targeting the *mtaB1* gene, there was a measurable production of anti-*Msp. stadtmanae* IgG antibodies in their serum, which was not seen in healthy controls, or patients found to be *Msp. stadtmanae* "negative". Additionally, *Msp. stadtmanae* cell preparations were found to produce a much stronger release of the proinflammatory cytokine TNF-α from the peripheral blood mononuclear cells (PBMC) of healthy control subjects than similar preparations of *Mbb. smithii*. A separate study confirmed that *Msp. stadtmanae* cells stimulate a greater release of the proinflammatory cytokines IL-1β and TNF-α than *Mbb. smithii* from moDCs. However, there appeared to be no differences in the response of a human intestinal epithelial cell line (Caco-2/BBe) to these methanogens (Bang et al., 2014).

Collectively, these findings suggest that: i) not unlike what is seen in ruminants, a change in the bacterial fermentation and nutritional ecology of the gut, such as reduced hydrogen formation and/or formation of short chain alcohols, can result in changes in both methanogen abundance and profile; ii) that the human isolate of *Msp. stadtmanae* can elicit a stronger inflammatory response than *Mbb. smithii*, and; iii) *Msp. stadtmanae* is also capable of triggering an adaptive immune response (via IgG).

In this Chapter, I report the results from a collection of studies that seek to address some of these aspects of gut methanogen-host interactions. First, I have investigated whether and how

the composition of the methanogenic archaea in patients with CKD is altered in response to synbiotic administration, as an intervention designed to restore a "healthy" gut microbiota and fermentation pattern. I have also assessed the immunogenic properties of the type strains of *Mbb. smithii* DSMZ 861^T, *Mbb. ruminantium* DSMZ 1093^T and *Msp. stadtmanae* DSMZ 3091^T as well as my newly isolated strains WGK6 and BMS using a combination of mouse macrophage and human PBMC. I have conducted these studies because the findings could have important consequences for the diagnosis and treatment of gut diseases and disorders in humans. Furthermore, furthering our knowledge of how gut methanogens interact with the host immune system might prove to be valuable for the development of effective anti-methanogen vaccines for livestock methane abatement.

4.2 Materials and Methods

4.2.1 Samples from the SYNERGY study

Faecal samples from the SYNERGY study (Rossi et al., 2014) were kindly provided by Megan Rossi and the SYNERGY team based at the Princess Alexandra Hospital and Translational Research Institute (Brisbane, Australia). In brief detail, the SYNERGY study aimed to assess the effectiveness of synbiotics (the co-administration of pre- and probiotics) to 37 patients with moderate to severe CKD as a treatment to reduce the serum concentrations of indoxyl sulphate, endotoxemia and trimethylamine-N-oxide (TMAO). The study was designed as a double-blind, placebo-controlled, randomised, cross-over trial, with a 2 week pre-treatment period, a synbiotic therapy or placebo arm for 6 weeks, than a 4 week washout period before cross-over to synbiotic therapy or placebo for 6 weeks. Of the 37 CKD patients, 21 consented to faecal sample collection at entry (week 0) and at the end point of the first treatment period and washout, and then at the end of the study (end of second treatment) as described by (Rossi et al., 2014). The samples were stored at -80 °C prior to DNA extraction.

4.2.2 Clinical samples from healthy subjects

Six "healthy" volunteers were recruited under an ethics application #2015000775 approved by the University of Queensland HREC. This group is comprised of 2 males and 4 females between the ages of 21 and 36 years described as "healthy" (exclusion criteria: any chronic illness; any acute illness in the preceding 2 months; antibiotic use within the last 2 months). Blood (30 ml) was collected by a qualified phlebotomist via venous puncture into vacuum pressurised tubes containing EDTA, and processed immediately for PBMC isolation. Of the 6

volunteers, 3 (HMI0004-6) also consented to provide a stool sample that was stored at -80 °C with 1 hour of collection (collected in Sarstedt Feaces tubes (55x44mm) from Brisbane, Australia donors in September 2015) , prior to DNA extraction and PCR-based tests for the presence of *Msp.* and *Mbb.* spp.

4.2.3 PBMC isolation procedures

The whole blood was diluted 1:1 with PBS-EDTA, and PBMC were isolated using Ficoll-Paque PLUS (GE Healthcare Life Sciences, Parramatta, NSW, Australia) separation, according to manufacturer's specifications. In brief, 35 mL of the diluted blood was carefully layered onto 15 mL of Ficoll-Paque PLUS contained within a 50 mL Falcon tube, using a sterile plastic pipette. The mixture was then centrifuged at 400 x *g* for 30 minutes without braking at ambient temperature. The PBMCs were sedimented at the interface between the serum and Ficoll-Paque layer (Appendix 6.15), and this fraction (~10 mL) was collected by sterile, disposable pipette, and transferred into a new 50 mL Falcon tube. This fraction was then diluted to 50 mL with PBS-EDTA to wash the PBMCs, which was harvested by centrifugation at 400 x *g* for 5 minutes with brake. After the supernatant was removed, the PBMCs were resuspended in 20 mL PBS only, and an aliquot (0.01 ml) was taken for PBMC counting using a hemocytometer. At this point, the PBMCs were harvested again by centrifugation and diluted to a final concentration of 2.7 x 10^6 cells/mL. Cells were diluted with RPMI medium supplemented with foetal bovine serum (heat-inactivated and filter sterilised, 10% vol/vol) and also with penicillin-streptomycin L-glutamine (stock consists of 10,000 units/mL pen-strep and 29.2 mg/mL L-glutamine; 1% vol/vol).

4.2.4 Faecal DNA extraction, PCR and qPCR methods

For each respective stool sample from the SYNERGY study, as well as those from the 3 healthy subjects above, 0.15 g was weighed out and total DNA extracted. The weighed out samples had 0.4 g of sterile zirconia beads added with 600 µL of RBB+C lysis buffer (Yu and Morrison, 2004) which were first homogenized for 3 minutes at 5000 x *g* using the Precellys 24 (Bertin Technologies, France). This was followed by a 15 minutes heating step at 70 °C. The samples were then centrifuged at 17,000 x *g* for 5 minutes, with the supernatants collected and treated with 30 µL of 20 mg/mL Proteinase K (Promega, Madison, WI, USA) at 56 °C for 20 mins. The lysates were then processed with the Maxwell® 16 Research Instrument, and the LEV blood DNA extraction kit (Promega) according to the manufacturer's instructions. All DNA extracts were stored at -30 °C until required.

The PCR primers and conditions used to quantify *Mbb.*, *Msp.*, and *Methanomassiliicoccus* spp. (*Mms.*) groups are listed in Appendix 6.5 Table 6.2. The primers used to quantify *Msp.* and *Mbb.* are the same as those described by Blais Lecours et al. (2014) and Johnston et al. (2010) which target the *mtaB1* gene and *nifH* gene, respectively. For *Mms*, primers specific for the *mttB* gene, as described by Poulsen et al. (2013) were used only for PCR and the conditions used were one cycle of DNA denaturation at 95 °C for 3 min, followed by 40 cycles of denaturation at 95 °C for 30 seconds and subsequent elongation at 60 °C for 30 sec, with positive control consisting of *Mms*. sp. BMP DNA (see thesis Chapter 3). For both PCR and qPCR reactions, 100 ng total microbial DNA was used as a template. For *mtaB1* and *nifH* gene qPCRs, aliquots (1 µl of 100 ng stocks) were added to 12.5 µl of power SYBR green qPCR Master Mix (Applied Biosystems), 0.25 µl each of forward and reverse primer pair, and then made up to a final volume of 25 µl. The qPCR conditions used were one hold at 95 °C for 3 min, followed by 40 cycles at 95 °C for 30 sec, and an elongation step for 30 seconds at either 55.5 °C or 57 °C, for *Msp.*, and *Mbb.*, spp., respectively. Standard template for both the *mtaB1* and *nifH* gene qPCR/PCR consisted of genomic DNA from *Mbb. smithii* and *Msp. stadtmanae* DSMZ 3091^T. The efficiencies (*E*) of the qPCR reactions were calculated from standard curves generated for each template of the type strains, by preparing a ten-fold serial dilution of each template between a range of 10^2 and 10^6 copies (each done in triplicate; as outlined at http://www.thermoscientificbio.com/webtools/copynumber/). The *E* values were then calculated as described by Rasmussen (Rasmussen, 2001) where $E = (10([^{-1/slope}])-1)*100$, and primer set efficiencies were 73% and 96% for the *mtaB1* gene and *nifH* gene, respectively.

4.2.5 Methanogen culture and cell preparations

Initially, *Mbb. smithii* DSMZ 861^T, *Mbb. ruminantium* DSMZ 1093^T and *Msp. stadtmanae* DSMZ 3091^T and *Msp.* sp. WGK6 and BMS were all cultured using 100 ml RF30 and H_2:CO_2 (80:20 vol/vol) pressurized to 150 kPa; and all the *Msp.* spp. cultures were also supplemented with 1% methanol (vol/vol). Subsequently, the culture volumes were reduced to 10 ml. All the cultures were incubated at 39 °C in a shaking incubator cabinet (Multitron Pro, Infors HT, Switzerland) and agitated at 100 rpm until they reached an OD_{600} of ~1 .0 (within 48 hours, as previously described). The cells were harvested by centrifugation at 21,000 x *g* for 5 min. The pelleted cells were resuspended with 0.5 vol of a sterile solution of saline (0.85% wt/vol) prepared with milliQ water, and centrifuged as before. This washing

step was repeated twice more, with the cells finally resuspended in 0.5 vol of the same buffer, then frozen and lyophilized (VirTis Benchtop K Freeze Dryer). The resulting preparations were all stored dry at ambient temperature until used for ELISA and RAW 264.7 assays, described below.

For the later studies conducted with RAW 264.7, and the PBMCs prepared from subjects HMI0004-6 assayed using the Biolegend LEGENDplex multi-analyte flow assay kit, only *Mbb. smithii* DSMZ 861^T and *Msp. stadtmanae* DSMZ 3091^T were cultured using BRN-RF30 medium, as described previously. Duplicate cultures were harvested during exponential phase (OD_{600} of ~0.5) and late exponential phase (OD_{600} of ~1), and the cell biomass was collected by centrifugation (21,000 x *g* 15 mins). The supernatants were removed and the cell pellets were washed twice with 0.85% (wt/vol) saline solution as described previously. The combined cell washes were also collected and the washed cells were finally resuspended in 1 mL of 0.85% saline solution.

Blais Lecours et al. (2014) added 0.05 mg/mL of cell dry weight to their challenge assays, and this protocol was followed for the ELISA-based assays described below. For all other assays I also determined the concentration of cellular protein for each of my preparations, using the Quick Start™ Bradford Protein Assay kit (Bio-Rad, Hercules, CA, USA) and with Bovine Serum Albumin (BSA) used as a standard, according to the manufacturer's instructions. These assays were performed using an added amount of biomass based on their respective protein concentrations to give a final concentration of 0.05 mg protein/mL for each assay (rather than dry weight).

4.2.6 ELISA-based assay of TNF-α release from PBMC following methanogen challenge

Aliquots (180 µL) of the PBMC preparations (2.7 x 10^6 cells/mL) from 3 subjects (i.e. HMI0001-3) were transferred to individual wells of a 96-well microtiter plate and incubated at 37 °C in a 5% CO_2 atmosphere for 30 min. The PBMCs were then challenged with 0.1 vol of one of the different lyophilized methanogen cell preparations, which had been resuspended in sterile saline buffer to a final concentration of 0.05 mg/ml. As a positive control, aliquots of the PBMC preparation from each subject were challenged with 0.1 vol of 1 µg/mL solution of LPS (lyophilized lipopolysaccharide from *E. coli* O55:B5 which was resuspended with PCR grade water, Sigma-Aldrich) solution, and negative controls consisted of adding

0.1 vol sterile saline solution (each done in duplicate). Following incubation for either 4 or 12 hours (at 37 °C and within a 5% CO_2 atmosphere) the cell-free supernatants were harvested by low speed centrifugation (400 x *g* for 5 min) and stored at -80 °C until required. The quantity of TNF-α released into the supernatants was then determined using BioLegend's Human TNF-α ELISA MAX Deluxe kit (Biolegend, San Diego, CA, USA) according to manufacturer's specifications. To determine the optimal dilution for detection of TNF-α release, the supernatant samples from HMI0003 challenged with *Msp. stadtmanae* DSMZ 3091^T cells were diluted with PBS to 1:10, 1:50, 1:100, 1:200, 1:300 and 1:400 of their original concentration prior to TNF-α measurement, and on the basis of these results, the remaining samples were diluted 1:10 before assay.

4.2.7 PBMC cytokine release in response to *Mbb. smithii* DSMZ 861^T and *Msp. stadtmanae* DSMZ 3091^T cell preparations using the Biolegend LEGENDplex bead array

The Biolegend LEGENDplex multi-analyte flow assay kit (#740118) quantifies a panel of cytokines (IFN-α, IFN-γ, IL-10, IL-12p70, IL-17A, IL-18, IL-1β, IL-23, IL-33, IL-6, IL-8 and TNF-α) through flow cytometry rather than ELISA. I chose to use this product because it is offered as a time efficient, high throughput and overall holistic approach to the quantification of a range of (customisable) cytokines. However, because this assay is new and still in development, I first needed to perform a pilot experiment to optimize the conditions of the assay for the accurate and precise detection of the cytokine response. For this purpose I used *Mbb. smithii* DSMZ 861^T and *Msp. stadtmanae* DSMZ 3091^T challenged PBMCs. To perform the pilot study, aliquots (180 µL) of the PBMC preparations (2.7 x 10^6 cells/mL) from 3 subjects (i.e. HMI0004-6) were transferred to individual wells of 3 separate 96-well microtiter plates and incubated at 37 °C in a 5% CO_2 atmosphere for 30 min. The PBMCs were then challenged with 0.1 vol of one of *Mbb. smithii* DSMZ 861^T or *Msp. stadtmanae* DSMZ 3091^T mid-exponential phase cell preparations, which had been resuspended in sterile saline buffer to a final concentration of 0.05 mg protein/mL. As a positive control, aliquots of the PBMC preparation from each subject was challenged with 0.1 vol of 1 µg/mL LPS solution, and negative controls consisted of adding 0.1 vol sterile saline solution (each done in duplicate). The individual 96-well microtiter plates were then incubated for 6, 12 or 24 hours, and the cell-free supernatants were harvested at each time point by low-speed centrifugation (400 x *g* for 5 min), and stored at -80 °C until required. The quantities of the cytokines released from the PBMC after each time period was then determined using the

LEGENDplex multi-analyte flow assay kit according to manufacturer's specifications. To determine the optimal dilution for detection of all the cytokines released, the supernatant samples from HMI0004 challenged with *Msp. stadtmanae* DSMZ 3091^T cells were diluted with the LEGENDplex assay buffer to 1:2, 1:10, 1:50 and 1:100 of their original concentrations prior to cytokine measurement. On the basis of these results, the remaining samples were diluted 1:10 and 1:100 before assay. The cytokine-analyte responses were measured using a BD LSR II fluorescence-assisted cell sorter, and the data were analysed using the software package available from Vigenetech LEGENDplex v7.0 (http://www.vigenetech.com/LEGENDplex7.htm). The standard curves for each of the 13 cytokines (see appendix 6.14) revealed that IFN-γ, IL-12p70, IL-17A and IL-23 were too inconsistent for use and these cytokines have been excluded from further sections.

4.2.8 RAW264.7 cell preparation and NF-κB ELAM luciferase assay

RAW264.7 expressing the ELAM luciferase reporter gene for NF-κB activation (Hume et al., 2001) were cultured in RPMI medium supplemented with foetal bovine serum (heat-inactivated and filter sterilised, 10% vol/vol) and also with penicillin-streptomycin L-glutamine (1% vol/vol). The cells were collected and transferred into a 50ml falcon tube, and then centrifuged at 400 x *g* for 5 minutes at ambient temperature. After the supernatant was removed, the RAW264.7 cells were resuspended with 10 ml of culture medium, and an aliquot (0.01 ml) was taken for cell counting using a hemocytometer. At this point, the RAW264.7 cells were harvested again by centrifugation and diluted to a final concentration of 4 x 10^5 cells/mL.

Aliquots (100 µL) of the RAW264.7 cell preparations were transferred to individual wells of a 96-well microtiter plate and incubated at 37 °C in a 5% CO_2 atmosphere for 30 min, then challenged with 0.1 vol of one of the different lyophilized methanogen cell preparations, which had been resuspended in sterile saline buffer to a final concentration of 0.05 mg protein/mL. In parallel, a series of assays were also set up as described above, but with 0.1 vol of a 20 µg/mL LPS stock preparation added 30 minutes after adding the methanogen cell preparations, to test whether the pro-inflammatory response of RAW264.7 cells to LPS was affected by the five methanogen strains. As a positive control, aliquots of the RAW264.7 preparations were challenged with 0.1 vol of 20 ng/mL LPS solution, and negative controls consisted of adding 0.1 vol sterile saline solution. All assays were performed in triplicate.

Following incubation for 4 hours, the amount of luciferase activity produced was measured after the RAW264.7 cells were lysed with 50 µL of 1.25x Passive lysis buffer (Promega). Aliquots (30 µL) of luciferin substrate (Steady-Glo Luciferase assay system; Promega) were added to each well, and the luciferase activity was quantified using a Fluostar Optima Luminometer reading each well for 1 seconds with an Emission filter Gain of 4095 (BMG Labtech, Mornington, VIC, Australia).

To determine whether the stage of growth stage affects the level of NF-κB response, mid and late exponential phase *Mbb. smithii* DSMZ 861^T and *Msp. stadtmanae* DSMZ 3091^T cell suspensions (0.5 mg protein/mL), culture supernatants, and cell washes were also used to challenge RAW264.7, as described above. As a positive control, aliquots of the RAW264.7 preparations were challenged with 0.1 vol of 20 µg/mL LPS stock preparation, and negative controls consisted of adding 0.1 vol filter sterilised; saline solution; methanol; saline solution with 0.01 vol methanol; blank BRN-RF30 methanogen medium; BRN-RF30 with added 0.01 vol methanol (each done in technical triplicate).

Finally, to examine the NF-κB response elicited by the different *Mbb.* and *Msp.* isolates, cultures of *Mbb. smithii* DSMZ 861^T, *Mbb. ruminantium* DSMZ 1093^T and *Msp. stadtmanae* DSMZ 3091^T and *Msp.* sp. WGK6 and BMS were harvested at late exponential stage of growth and the cells resuspended to give a final concentration of 0.05 mg protein/mL, then used to challenge RAW264.7 cells, with positive and negative controls as described above, each done in biological and technical triplicate. A series of assays with 0.1 vol of 20 µg/mL LPS stock preparation was added 30 minutes after adding the methanogen cell preparations was done as described earlier.

4.2.9 Statistical analyses

Cytokine concentrations and NF-κB luminescence values were plotted, standard error of the mean (SEM) calculated and analysed for statistical significance determined using the software package GraphPad Prism version 5.00, for Windows (GraphPad Software, San Diego California USA, www.graphpad.com). Statistical significance of results were determined through one-way ANOVA analysis with Tukey's post-test performed, significance was assigned to $p < 0.05$, with a 95% confidence interval.

4.3 Results

4.3.1 Synbiotic treatment of CKD patients has no effect on abundance or composition of the methanogen community

Only a small number of the stool samples from the CKD patients in the SYNERGY study were found to contain detectable levels of the methanogenic archaea, and *Mbb.* spp. were the predominant type (Table 4.2). The dataset is limited to 81/84 samples due to failure to collect stool samples from 3 patients (at the end of the washout period). In general terms, the amplicon libraries (Rossi et al., 2016) and my PCR-based assays showed that: i) most of the CKD patients were found to have no detectable archaeal population in their stool samples; ii) for those patients that do possess a detectable abundance of methanogenic archaea, the population is predominantly *Mbb.* spp. and; iii) no amplicons were produced using the *Msp.*-specific primers from any of the stool samples; nor were there sequence reads assigned to the *Msp.* genus from the amplicon libraries. In a small number of instances (9/81 samples) the Arch-specific primers did produce an amplicon, but the *Mbb.* and *Msp.*-specific primers did not. These stool samples were then used in PCR reactions using the *Mms.*-specific primers and a detectable amplicon was produced for 5/9 of these samples (see Table 4.1).

Additionally, those patients with a detectable population of methanogenic archaea in stool at baseline retained a measureable population of archaea throughout the trial period, which was predominantly comprised of *Mbb.*-spp. Although the normalised read counts suggest there was some fluctuation in the population size of the archaea for these patients across the study period, these changes could not be attributed to the interventions (placebo or synbiotic) used in the SYNERGY study. As such, it would appear that the synbiotic intervention has neither a positive or negative affect on either the population size or composition of the methanogenic archaea in stool samples from this cohort of CKD patients.

Table 4.1. The prevalence and composition of the methanogen populations present in stool samples collected from patients enrolled in the SYNERGY study (Rossi et al., 2016). The percentage of Illumina MiSeq reads assigned to the *Methanobacteriales* order are shown (norm-MiSeq), but all reads were further classified to the *Mbb.* genus. Stool samples producing a detectable amplicon by PCR-based screening with either the methanogen-specific primers (Arch), as well as the genus-specific *Mbb.* primers are marked (+). Values annotated in red, represent periods during which the patient was also treated with antibiotics. Notably, none of the stool samples produced an amplicon with the *Msp.*-specific primers, and are therefore not annotated in the Table.

Patient	**Baseline (week 0)**			**Placebo (week 6)**			**Wash-out (week 10)**			**Synbiotic (week 16)**		
	Norm-Miseq	Arch	*Mbb.*	Norm-Miseq	Arch	*Mbb.*	Norm-Miseq	Arch	*Mbb.*	Norm-Miseq	Arch	*Mbb.*
A		+		<0.10%		+		+	+			
B												
C				<0.10%								
D	0.90%	+	+	3.20%	+	+	<0.10%		+			
E	0.70%			4.10%	+		4.00%	+		1.00%	+	+
F	4.60%	+	+	4.90%	+	+	3.50%	+		2.30%	+	+
G			+			+	N/A	N/A	N/A			+
H			+						+			+
I							N/A	N/A	N/A	<0.10%	+	
J												
K							<0.10%			<0.10%		
L								+	+			+
M							<0.10%					
N					+		<0.10%	+	+	<0.10%		
O										<0.10%		
P												
Q			+				<0.10%	+		<0.10%		
R	<0.10%											
S	3.30%	+	+	3.80%	+	+	N/A	N/A	N/A	9.00%	+	
T	<0.10%	+	+	0.20%	+		<0.10%	+	+	0.10%	+	+
U	<0.10%											

4.3.2 The TNF-α release from PBMC varies in response to challenge with the different methanogens

The TNF-α release from PBMC in response to their exposure to the five methanogen strains for either 4 or 12 hours are shown in Figs. 4.1 and 4.2, respectively. Relative to the negative controls, the release of TNF-α by PBMC was induced by all the methanogen strains except *Msp.* BMS. After 4 hours exposure, there was a significantly higher release of TNF-α by HMI0001 PBMC in response to *Msp. stadtmanae* DSMZ 3091^T cells (1495.6 ± 107.9) compared to *Mbb. smithii* DSMZ 861^T cells (1033.9 ± 33.6, $p < 0.05$, see Fig. 4.2). The PBMC from all 3 subjects exhibited an overall increase in the amount of TNF-α released after 12 hours exposure to the 4 methanogens (Fig. 4.1), and again, the amount released from the PBMC of both HMI0001 and HMI0002 was significantly greater in response to *Msp. stadtmanae* DSMZ 3091^T (1991.1 ± 137.3 and 1190.7 ± 135.4, HMI0001 and HMI0002 respectively; see Fig. 4.2) compared to *Mbb. smithii* DSMZ 861^T (710.4 ± 18.1 and 740.4 ± 29.4, HMI0001 and HMI0002 respectively; see Fig. 4.2, $p < 0.05$). Interestingly, *Mbb. ruminantium* DSMZ 1093^T cells induced TNF-α release comparable to that of *Msp. stadtmanae* DSMZ 3091^T at both time points, while *Msp.* sp. WGK6 cells induced a response similar to that measured for *Mbb. smithii* DSMZ 861^T cells. Unfortunately, subjects HMI0001-0003 did not consent to stool sample collection, so I was unable to measure the presence and proportions of methanogen species present within these persons. Subsequently, the LEGENDplex PBMC challenge work was performed with three new subjects willing to provide both a blood and stool sample.

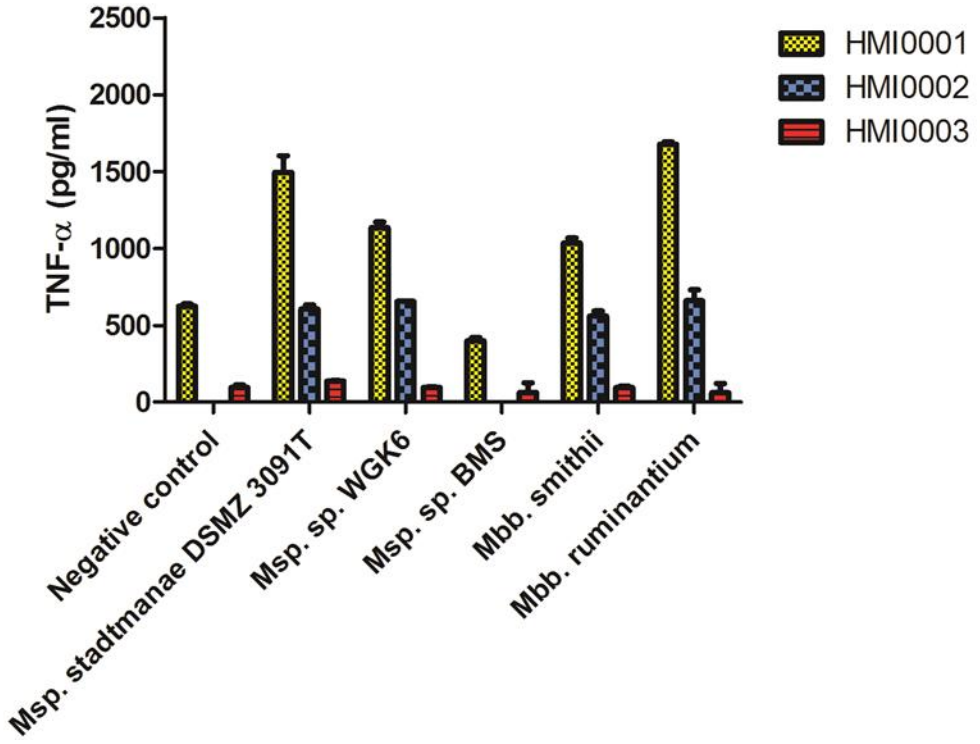

Figure 4.1. ELISA-based measurement of the concentrations of TNF-α released into culture fluids from PBMC (2.7 x 10^6 cells/mL), in response to 4 hours challenge with either whole cell preparations of the five individual methanogen strains, or saline (negative control), as described in materials and methods. For PBMCs recovered from HMI0001 and HMI0003, the maximal response (5000 pg/mL) was observed for LPS (100 ng/mL, positive control), while HMI0002 had a minimal response (540 pg/mL) to the LPS challenge. In addition there was significant variation between each subject in terms of their response to the different methanogen preparations: a greater release of TNF-α was observed in response to the *Msp. stadtmanae* DSMZ 3091^T challenge, when compared to that of *Mbb. smithii* DSMZ 861^T. Of the non-human isolates the greatest responses were observed for *Mbb. ruminantium* DSMZ 1093^T and *Msp.* sp. WGK6, with only a minimal release measured in response to *Msp.* sp. BMS, and the negative control.

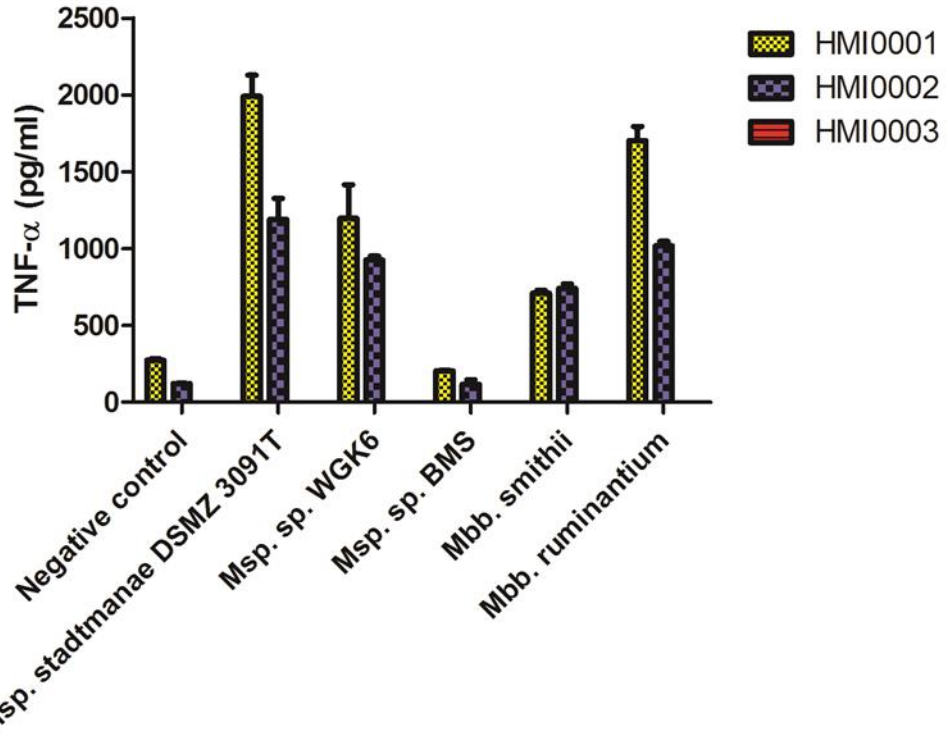

Figure 4.2. ELISA-based measurement of the concentrations of TNF-α released into culture fluids from PBMC (2.7 x 10^6 cells/mL), in response to 12 hours challenge with either whole cell preparations of the five individual methanogen strains, or saline (negative control), as described in materials and methods.

4.3.3 The cytokine profiles released from the PBMC of healthy subjects was similar, in response to *Msp. stadtmanae* DSMZ 3091^T and *Mbb. smithii* DSMZ 861^T cells, and LPS

The cytokine release from the PBMC prepared from HMI0004-0006 in response to their exposure to either LPS, saline, *Mbb. smithii* DSMZ 861^T or *Msp. stadtmanae* DSMZ 3091^T cells for 6, 12 or 24 hours, and measured with the LEGENDplex multi-analyte flow assay, are shown in Figs. 4.3A-F. As expected, LPS resulted in a strong release of the pro-inflammatory cytokines IL-1β, TNF-α, IL-6, IL-8 and MCP-1 (Fig. 4.3A-E). Similar cytokine profiles were also observed for the PBMC challenged with *Msp. stadtmanae* DSMZ 3091^T or *Mbb. smithii* DSMZ 861^T, but in these assays, the *Mbb. smithii* DSMZ 861^T cells appeared to induce a stronger release of pro-inflammatory cytokines compared to *Msp. stadtmanae* DSMZ 3091^T. However, the statistical analyses suggested that only the differences of TNF-α release across all time points (Fig. 4.3B) were statistically significant. While the statistical analyses suggested that *Mbb. smithii* DSMZ 861^T had a significantly higher release of IL-1β (6 hours,

Fig. 4.3A) and TNF-α (all time points, Fig. 4.3B) compared to LPS. Finally, statistical analyses of PBMC challenge with LPS challenge suggested that only the differences of MCP-1 release at 12 and 24 hours (Fig. 4.3E) are statistically significantly when compared to the second highest challenge, *Mbb. smithii* DSMZ 861^T. In addition to the release of these pro-inflammatory cytokines, release of the "anti-inflammatory" IL-10 cytokine was also measureable over the 24 hours incubation period, and not significantly different between PBMC challenged with either LPS or the two methanogen cell preparations (Fig. 4.3F).

The PCR assays of DNA extracted from the stool samples of HMI0004-0006 showed that all 3 subjects were PCR-positive for the *Mbb.*-spp. primers but not for *Msp.*-spp. primers. The *Mbb.*-spp. amplicon from HMI0004 stool DNA was larger than anticipated (~175 bp) and produced a different melt curve in qPCR assays compared to the *Mbb. smithii* DSMZ 861^T DNA used as a standard (Fig. 4.4). The best match (<100% identity and <26% coverage) for the sequenced HMI0004 amplicon included various parasites (i.e. *Toxocara canis* and *Schistosoma mattheei*) and bacteria (i.e. *Staphylococcus agnetis* and *Treponema putidum*). Based on these results it was concluded that the amplicon produced from subject HMI0004 stool DNA is unlikely to be derived from *Mbb.* spp. The qPCR analysis estimated that per gram of stool sample HMI0005 and HMI0006 possess 8.7×10^5 and 3.3×10^5 copies of the *Mbb.*-specific 16S rRNA gene, respectively.

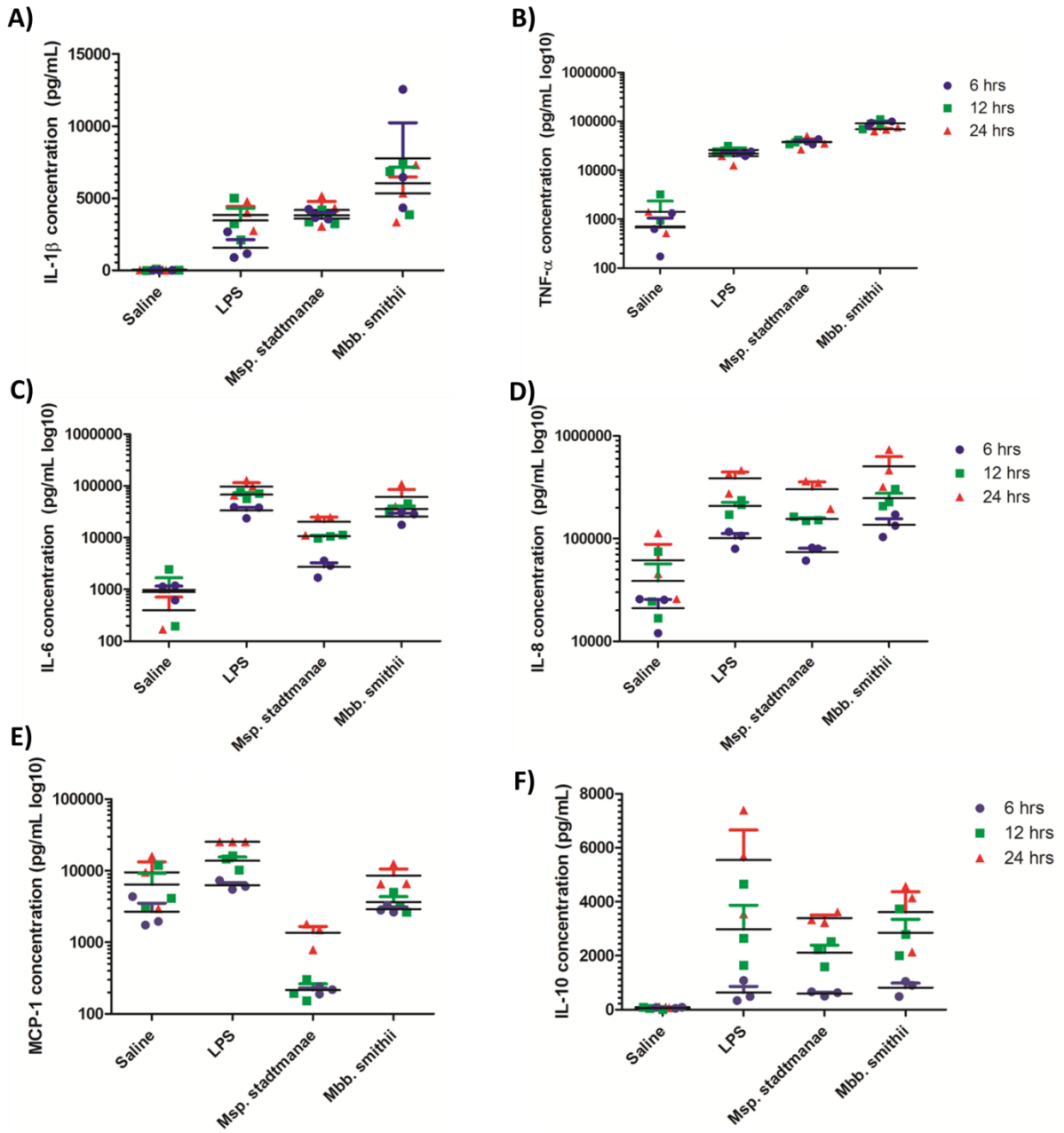

Figure 4.3. Cytokines concentration profiles produced from the PBMC harvested from three donors (HMI004-006) as determined using the LEGENDplex assay, after 6 (●), 12 (■) and 24 (▲) hours challenge with either saline (negative control), LPS (100 ng/mL, positive control), *Msp. stadtmanae* DSMZ 3091^T or *Mbb. smithii* DSMZ 861^T. Each datum point represents the mean value for triplicate samples from each respective donor. In summation, the LPS, *Msp. stadtmanae* DSMZ 3091^T and *Mbb. smithii* DSMZ 861^T challenges resulted in the same cytokine profiles with respect to the release of IL-1β (A), TNF-α (B), IL-6 (C), IL-8 (D), MCP-1 (E) and IL-10 (F). The cytokine profile of saline challenged cells differed slightly

with only an induction of TNF-α, Il-6, IL-8 and MCP-1 observed. The data were analysed by one-way ANOVA and significant differences are denoted by * (Table 6.4).

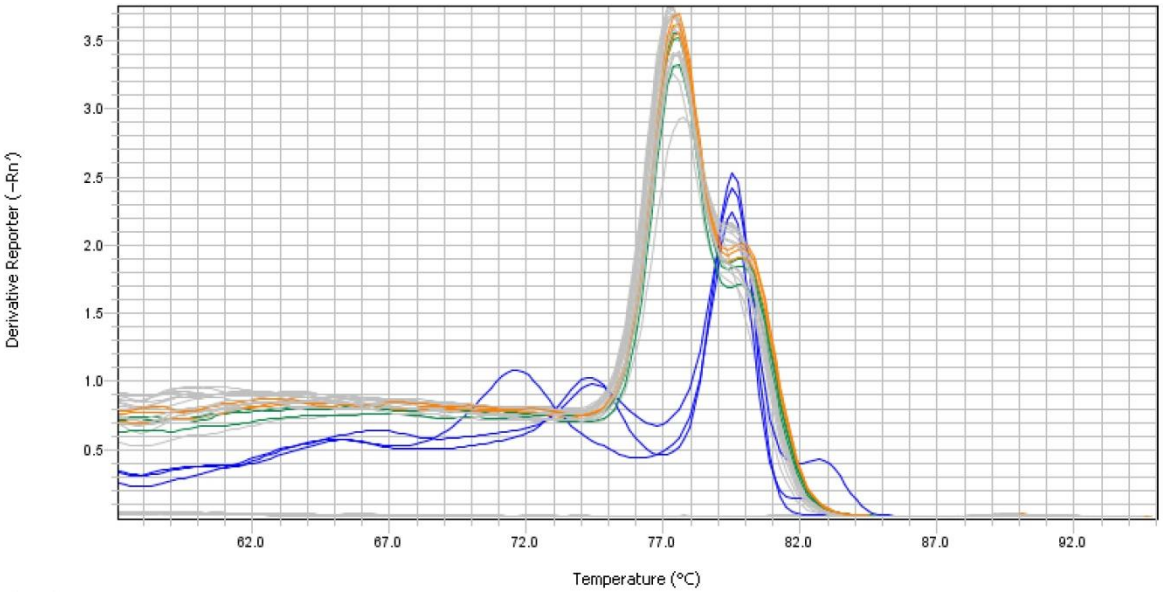

Figure 4.4. The qPCR Melt curve for positive control *Mbb. smithii* (white), HMI0004 (blue), HMI0005 (green) and HMI0006 (orange) using *Mbb*.-specific primers designed by Johnston et al. (2010). Subject HMI0004 produced a larger PCR product with these primers as well as a different melt curve compared to the other subjects and positive control *Mbb. smithii* DSMZ 861^{T} as a result it was concluded that the product for HMI0004 was not a *Mbb*. spp.

4.3.4 The five methanogen cell preparations induce similar NF-κB activated responses from RAW264.7 macrophage cells

The variations in the immunomodulatory capacity of RAW264.7 macrophage cells in response to whole cell preparations from the five methanogen strains, in the presence or absence of LPS stimulation, are shown in Fig. 4.5A-B. For both types of assays, all of the methanogen strain challenges resulted in a significantly higher activation of NF-κB reporter activity compared to the positive control (LPS 10 ng, $p < 0.05$). None of the *Mbb.* or *Msp.* strains tested result in a suppression of NF-κβ activation when the macrophage cells were first challenged with LPS (Fig. 4.5A); nor did the methanogen cell preparations result in any additive effect of NF-κB activated reporter gene activity when co-cultured with LPS (Fig. 4.5B).

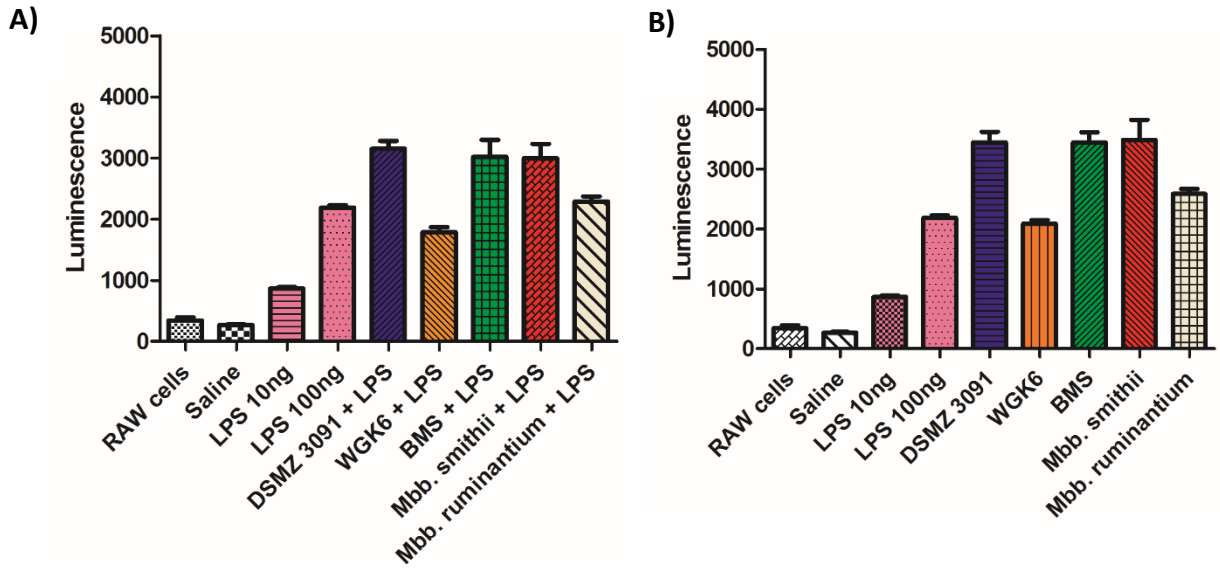

Figure 4.5. The immunomodulatory response of RAW264.7 mouse macrophage cells in response to whole cell preparations of the 5 methanogen strains, normalised with respect to total cell protein added, and the response measured by NF-κB directed transcription of the luciferase reporter gene. The results obtained when the cells were also challenged with LPS (10 ng/ml), or not, are shown in panels A and B, respectively. The presence of LPS did not have an additive affect to that of any of the methanogen challenges. Individual values represent the mean (± SEM) produced from three technical triplicates.

4.3.5 The NF-κB response of RAW264.7 cells to *Msp. stadtmanae* DSMZ 3091^T and *Mbb. smithii* DSMZ 861^T is limited to whole cell preparations

The reporter gene responses to the spent culture fluids, cell wash fractions, and whole cells of *Msp. stadtmanae* DSMZ 3091^T or *Mbb. smithii* DSMZ 861^T, and harvested at either mid- and late-exponential phase are shown in Fig 4.6. Both the mid- and late-exponential phase spent culture fluids produce a smaller NF-κB reporter gene response compared to sterile, un-inoculated BRN-RF30 medium. When the sterile fluids from mid or late exponential growth phase cultures were compared, no significant differences were seen for *Msp. stadtmanae* DSMZ 3091^T or *Mbb. smithii* DSMZ 861^T. For the cell wash collections there was no difference between mid- and late-phase NF-κB inductions for both methanogen strains. The most significant level NF-κB activation is that seen for mid- *Msp. stadtmanae* DSMZ 3091^T whole cell harvest with approximately half the NF-κB observed for late- whole cell harvest, even though all whole cell stimulants were standardised based on the total protein

concentration (0.05 mg protein/mL). A similar profile is observed for *Mbb. smithii* DSMZ 861^T (Fig. 4.6B) whole cell harvest with the exception that the level of NF-κB activation was reduced across all components in comparison to *Msp. stadtmanae* DSMZ 3091^T (Fig. 4.6A).

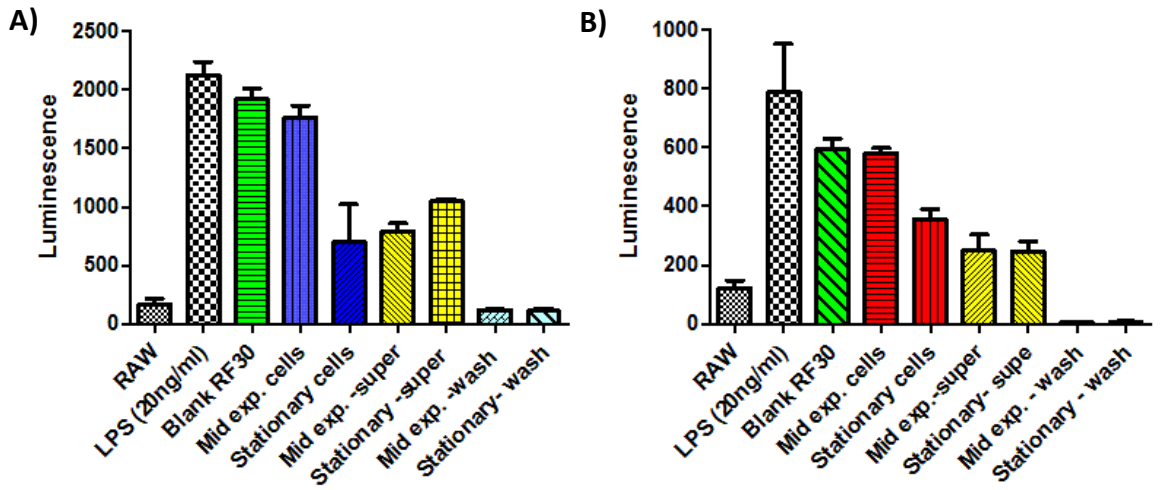

Figure 4.6. The immunomodulatory response of RAW264.7 mouse macrophage cells in response to either whole cells, cell washes, or the residual medium fluids from *Msp. stadtmanae* DSMZ 3091^T (panel A) or *Mbb. smithii* DSMZ 861^T cultures (panel B); as measured by NF-κB directed transcription of the luciferase reporter gene. Individual values represent the mean (± SEM) produced from technical triplicates.

4.4 Discussion

Based on our current knowledge of the pathways and substrates that are required for methanogen growth, it is plausible that changes in bacterial fermentation coincident with "dysbiosis" may result in alterations in the total and/or specific abundances of gut methanogens. In addition the growing evidence that gut methanogens can modulate an immune response suggests that instances of "dysbiosis" with gastrointestinal inflammation may be due to methanogenic archaea. Persons suffering CKD experience intestinal inflammation, constipation, accumulation of nitrogenous waste products and most notably increased levels of TMAO and methanol (Kang, 1993, Murtagh et al., 2007, Lee et al., 2012, Tang et al., 2014, Nallu et al.). As described earlier in this chapter's introduction elevated levels of breath methane have been correlated to the severity of constipation for individuals diagnosed with IBS, while prevalence of *Msp*. spp. is increased in IBD patients (Chatterjee et al., 2007, Blais Lecours et al., 2014). With all these factors considered it led me to hypothesise that the abundance and profile of the methanogenic community within CKD

patients could favour methylotrophic methanogens such as *Msp*. and *Mms*. spp., a theory which has not been investigated by previous CKD microbiota profiling studies.

The primary outcome measures of the CKD SYNERGY study were serum para-cresyl sulfate (PCS) and indoxyl sulfate (IS) concentrations. Both these uremic toxins were reduced in CKD patients during the synbiotic administration period, and significantly so for PCS in all patients, and for IS in patients not receiving antibiotic treatment (Rossi et al. 2016). These changes were coincident with measureable, statistically significant changes in gut bacterial composition, specifically in terms of an increased relative abundance of *Bifidobacterium* and *Faecalibacterium* spp. However, it appears that neither the abundance nor profile of methanogenic archaea in the stool samples were affected over the course of the SYNERGY trial, with both the PCR assays and MiSeq 16S rRNA profiling data suggesting *Mbb.* spp. dominated when present (Table 4.2). There were 5/81 samples that did appear to be PCR positive when the *Mms.*-specific primers were used, and TMAO was measureable in the serum of these patients (Rossi et al., unpublished data). However, there were no significant changes in serum TMAO during the course of the study, which is consistent with my results identifying only a few amplicons for the methylamine utilising *Mms.* spp., suggesting a low abundance. Notably, none of the stool samples proved to be PCR positive for *Msp.* spp. suggesting the nutrient and/or environmental milieu in these CKD patients was not sufficient to support its growth.

Up to 28% of the CKD patients recruited as part of the SYNERGY study were found to be PCR positive for Archaea, which increased to 38% based on the recovery of MiSeq reads assigned to the Domain Archaea. In comparison, Scanlan et al. (2008) reported the prevalence and diversity of methanogenic archaea from the stool samples of 207 individuals considered to be either healthy (HC), or assigned to one of five non-communicable gastrointestinal disease groups: colorectal cancer (CRC), polypectomised (PPx), IBS, ulcerative colitis (UC), or Crohn's disease (CD) patients. The PCR positivity was 48% for HC, 45% for CRC, 50% for PPx, 48% for IBS, 24% for UC, and 30% for CD patients. Protein and amino acid fermentation is elevated in CKD patients and in addition to uremic toxins there is also a high ammonia concentration, which raises the pH levels above neutral (Carrero et al., 2013, Nallu et al., 2016). Such conditions along with my PCR assay results would indicate that even though methylated compounds are increased in CKD patients the shift in fermentation schemes and shift in pH may result in a hostile environment for methyl-

group utilising methanogens such as *Msp*. and *Mms*. spp. The examination of methanogen diversity for CKD patients was limited as I only had access to stool samples and preferential colonization of the colonic mucosa by methylotrophic methanogens could be an alternative explanation for relative low detection of this archaeal group in stool. This is an area of investigation that has not been rigorously pursued but would be of interest, considering how my results and those of Blais Lecours et al. suggest a role for some archaea to interact with and stimulate the immune system.

The remaining discussion will be broken into two parts; first I will discuss the immunomodulation of human derived methanogenic strains, and; second the comparison of TNF-α and NF-κB activation after challenge with each of the five methanogenic strains respectively. Both Blais Lecours et al. (2014) and Bang et al. (2014) reported that cell preparations of the human type strain *Msp. stadtmanae* DSMZ 3091^T elicited a stronger release of TNF-α from PBMC and dendritic cells than similar preparations of *Mbb. smithii*. My findings using the same archaea and PBMC preparations from 3 healthy subjects are consistent with these results, as shown in Figs 4.1 and 4.2.

The amount of TNF-α release from PBMCs in my assays ranged between 0.08 ng to 2 ng, which is approximately 4-fold less than that reported by Blais Lecours et al. (2014). At least part of this difference could be attributed to the cryptic description of the methanogen cell preparation methods used by Blais Lecours et al. (2011) and Blais Lecours et al. (2014) which precluded my replication of their approach. First, the specific strain of *Mbb. smithii* used in their studies is not described and there is no mention at which stage of growth the methanogen cultures were harvested. These are details which are highly relevant as demonstrated by the Conway de Macario et al. (1985) study where variation in immunogenicity was identified between strains *Mbb. smithii* DSMZ 861^T and *Mbb. smithii* DSMZ 2375^T. Blais Lecours et al. (2011) also mention a "sonication step" for 1 minute before their pulmonary challenge assay, although no mention of this is made in their 2014 paper. A sonication step, described as being performed to break up cell clumps, is also highly likely to cause cell lysis, releasing cytoplasmic elements and breaking up cell components which may increase the rate of recognition by PBMC receptors.

In subsequent experiments, I chose to use the LEGENDplex multi-analyte flow assay kit with the goal of making a more holistic assessment of cytokine release from the PBMC

preparations; initially in a pilot study with the *Msp. stadtmanae* DSMZ 3091^T and *Mbb. smithii* DSMZ 861^T cell preparations and subsequently with all 5 methanogens. Using the LEGENDplex method, I compared the PBMC responses from a further 3 donors. In contrast to the results of ELISA and the RAW264.7 cell reporter system, *Mbb. smithii* DSMZ 861^T appeared to generate an increased response. This may highlight the variations in immune responses across genetically diverse humans. However, it is worth noting that while the initial 3 PBMC donors were stimulated using methanogen preparations based on total cell mass, the later subjects were stimulated with preparations based on total protein (discussed in further details below).

Unfortunately, my pilot studies using this relatively new kit were affected by technical issues, specifically in terms of producing the reliable and consistent readouts needed to produce the standard curves for quantifying IFN-γ, IL-12p70, IL-17A and IL-23 release. I worked closely with technical representatives of the kit's manufacturer over a period of weeks to improve the precision and accuracy of their "Human Inflammation Panel Standard Cocktail", including their provision of a new batch of the "standard cocktail" free of charge, because of the variations in readouts measured and the use of polypropylene plates, to try to minimise cytokine "sticking". Despite these efforts, I was not able to improve the standard curve generation for the abovementioned cytokines (see Appendix 6.15), and given the pending deadlines associated with my thesis completion date, I repeated the studies with PBMCs prepared from subjects HMI0004-6, and excluded the readouts produced for these cytokines from my comparisons. Overall, the profiles of the remaining cytokines quantified by this kit indicate that both methanogen cell preparations induce a profile much the same as that following the LPS challenge, with measureable amounts of IL-1β, TNF-α, IL-6, IL-8, MCP-1 and IL-10 observed. Based on these results, I conclude that there is potential for these methanogens to modulate a strong immune response and the induction of TNF-α and IL-6 suggests that there is a potential link to IBD (Mudter and Neurath, 2007). It is unfortunate that the full cytokine LEGENDplex profile failed as IL-23 has been associated with IBD as well as IL-17A being associated with UC (Geremia and Jewell, 2012, Cătană et al., 2015). Also, IFN-γ and IL-17A are produced by T cells and measuring these would have allowed me to start to investigate adaptive immune responses to the methanogens (reviewed by Weyand et al., 2011).

Using the RAW264.7 cell assay, I demonstrated that the stage of growth affects the immunomodulatory capacity of the human originating methanogen cell preparations (Fig. 4.6). Previous studies have demonstrated that there is a correlation between the stage of growth of methanogen cell and the composition of tetraether lipids and fatty acid methyl esters, which decreases during later stages of growth (Kramer and Sauer, 1991). It was hypothesised that the increased composition of tetraether lipids could provide a more rigid membrane for younger cells. In addition the ratio change of diether and tetraether lipids demonstrated that there is a decrease in the level of biosynthesis as the cell ages. Since this assay demonstrates that it is indeed whole methanogen cells which mediate the immune response it seems reasonable to conclude that "late" growth harvest cultures have a reduced capacity to express and synthesis the MAMPs on their cell surface which is responsible for activating an immune response. These are considerations not previously examined by other researchers and demonstrate how big the knowledge gap surrounding methanogen and human health interaction actually is.

The final section of this discussion will address the five methanogen strains and their immunomodulatory variation. In the PBMC stimulation with lyophilized strain preparations (Fig. 4.1-2), using ELISA to assay TNF-a production, the methanogen isolates of animal origin produced contrasting results. *Mbb. ruminantium* DSMZ 1093^{T} induced the strongest release, while the preparations from *Msp.* sp. WGK6 ("small" genome) and BMS ("large" genome) appeared to produce the weakest release of TNF-α. When comparing the animal and human isolates for the *Msp*. spp. the human type-strain *Msp. stadtmanae* DSMZ 3091^{T} had the strongest TNF-α production, followed by WGK6 and then BMS. However, for *Mbb*. spp. the reverse was true with the ruminant representative *Mbb. ruminantium* DSMZ 1093^{T} producing a stronger TNF-α signal compared to the human type strain *Mbb. smithii* DSMZ 861^{T}. The variation in TNF-α production may be a result of a variable element between each genus and/or specific host adaption. A vaccine trial conducted by Subharat et al. (2015) in cattle investigated the induction of the immune response to a methanogen protein, recombinant glycosyltransferase protein (GT2). They showed a strong antigen-specific IgG and moderate IgA response was possible from both serum, saliva and rumen samples of the vaccinated animals. All *Msp.* spp. genomes generated and described in Chapter 3 where processed using the automated carbohydrate-active enzyme annotation web resource dbCAN (Yin et al., 2012) to determine the number of GT2 genes (see Table 4.3). In comparison to *Msp. stadtmanae* DSMZ 3091^{T} both WGK6 and BMS have fewer GT2 genes, as do both

Mbb. spp. So while the GT2 protein may induce a strong antigen-specific response in a vaccine trial of livestock it may not be completely responsible for the production of TNF-α from healthy PBMC.

Table 4.2. Glycosyltransferase protein (GT2) gene counts for all *Msp.* and *Mbb.* strain challenges used in this Chapter. The GT2 counts were determined using the automated carbohydrate-active enzyme annotation web resource dbCAN. While *Msp.* spp. had a higher GT2 gene count in comparison to *Mbb.* spp. the similar NF-κB luminescence profile for *Msp.* and *Mbb.* strains whole cell challenge (Fig. 4.5B) would suggest that there is potentially a conserved gene between the *Msp.* and *Mbb.* strains.

Strain	**GT2**
Msp. stadtmanae DSMZ 3091^T	31
Msp. sp. WGK6	28
Msp. sp. BMS	26
Mbb. ruminantium DSMZ 1093^T	20
Mbb. smithii DSMZ 861^T	20

In addition to variations in response to the different methanogens, I also observed a variation in the level of TNF-α release from donors HMI0001-3 in response to LPS. This is similar to findings reported by Liebregts et al. (2007) where PBMC isolated from 36 healthy subjects were challenged with LPS for 24 hours and showed a variation in TNF-α release that ranged between 80 and 550 pg/mL. Such inter-individual variations have been attributed to the amount of Toll-like Receptor 4 (TLR4) expression (Jaekal et al., 2007). An alternative explanation for the variation in response to both TNF-α and methanogen preparations could be a reflection of the different PBMC cell populations among the human donors. PBMC are not a homogenous cell population but are constituted by several immune cell types including, among others, T cells (~60 %), B cells (~15 %), natural killer (NK) cells (~15 %), and monocytes (~10%; Autissier et al., 2010). Future experiments should account for this and the cell populations of PBMC donations should first be quantified to endeavour to account for the variability observed in Figures 4.1, 4.2, and 4.3. Interestingly, while the PBMC prepared from HMI0003 showed a minimal response to all five methanogen strains, these PBMC produced the greatest response to LPS challenge, suggesting that triggering TNF-α release in response to the methanogen cell preparations is mediated via cell receptor(s) other than TLR4. Once such class of receptors are the nucleotide-binding oligomerization domain-like receptors (NOD-LRs), which can activate NF-κB and thus trigger TNF-α release (Inohara and Nunez, 2001, Franchi et al., 2009, Shakhov et al., 1990, Yao et al., 1997, Shames et al., 1999). These NOD-LRs are intracellular sensors, which recognise microbe-associated

molecular patterns (MAMPs) entering the cell via phagocytosis. Archaea are structurally very different to that of bacteria lacking peptidoglycan in their cell wall with some methanogens instead containing pseudopeptidoglycan (also known as pseudomurein) which would provide a different profile of MAMPs recognised by the immune system (Balch et al., 1979). There is currently no literature on the mechanism of interaction between TLRs or NOD-LR and methanogens highlighting how poorly explored this area is.

I next decided to pursue the use of the RAW264.7 NF-κB ELAM reporter macrophage cell line to assess immunomodulatory variation between the five methanogen cell preparations (Fig. 4.5). Interestingly, and in contrast to the results using human PBMCs and specific measurement of TNF-α, the results with the RAW cells shows that all 5 methanogen cell preparations result in similar levels of NF-κB mediated ELAM activation, and more so than that induced by LPS alone (Fig. 4.5B). This highlights the ability of all strains to induce a response, as suggested by the results of HMI0004-6. A key difference between these experiments was the amount of methanogen cell biomass added to the respective assays. In these initial studies, I followed as closely as possible the methods outlined by Blais-Lecours et al. (2011, 2014) by adding equal amounts of total cell biomass. However, as shown in Table 4.4, the protein content of the five lyophilized methanogen cell preparations was quite variable and as such, a standard addition of biomass to those assays resulted in different amounts of total protein being added. By adding an amount of each methanogen cell preparation that was standardised with respect to the amount of protein added, the degree of NF-κB activated ELAM activity was similar in response to all five strains; which is also similar to the observations made by the quantitative cytokine profiling results for *Msp. stadtmanae* DSMZ 3091^{T} and *Mbb. smithii* DSMZ 861^{T} challenges. Thus, perhaps the previously reported results are confounded by the method of methanogen preparation and my results show the important influence that sample preparation has on determining the immunomodulatory capacity of methanogens. Finally, the use of the RAW264.7 reporter gene assay is a rapid and high throughput method which can be utilised to screen a variety of methanogen cell components to determine their immunomodulatory capacity, criteria which would be highly beneficial in the development of anti-methanogen vaccine development.

Table 4.3. Total protein concentrations for 0.5 mg/mL of dry weight *Msp.* and *Mbb.* spp. demonstrates that the dry weight method does not ensure a standardised amount of total cellular protein is achieved and this varies even between genus members.

Strain	**Total protein concentration (mg protein/mL)**
Msp. stadtmanae	0.26
Msp. sp. WGK6	1.07
Msp. sp. BMS	0.15
Mbb. smithii	0.096
Mbb. ruminantium	0.41

In conclusion, the consistent immune response to representative isolates of both *Msp*. and *Mbb*. spp. could be a result of a shared cell surface protein, which has important implications for the development of anti-methanogen vaccines for livestock methane abatement. My results have also demonstrated that the potential of methanogens to elicit an immune response within humans is similar to that of LPS. The future for gastrointestinal inflammatory disorder research should include the profiling and quantification of methanogens as it is apparent that these archaea are important in the area of human health and are commonly over-looked.

Chapter 5 General discussion

Unlike their bacterial counterparts, the methanogenic archaea are comprised of a small number of taxa, with just 7 orders currently identified. The order Methanobacteriales are numerically the most predominant in the gut environments of warm blooded animals, and accordingly, are the most intensively studied. However and as outlined in my literature review, the advent of metagenomics techniques and the recent interest in both reducing livestock methane emissions, and the impacts of human gut microbiome on our health and well-being, have revealed that the methylotrophic archaea warrant greater attention. I believe the results presented in my thesis have substantially advanced our knowledge and understanding of this taxocene of methanogenic archaea, which can be summarised as follows:

1. The results presented in Chapter 2 show that *Msp.* sp. WGK6 is metabolically more versatile than other cultured *Msp.* spp., and employs a novel pathway of alcohol-fuelled methanogenesis that supports growth.
2. Chapter 3 presents the first isolate of a novel lineage of *Msp.* sp. (BMS) which possesses a substantially larger genome compared to the other known *Msp.* isolates.
3. The results in Chapter 3 used metagenomics datasets to recover additional *Msp.* spp. population genomes that not only validate the existence of the large genomotype, but show a monophyletic origin for the genus, and with gene loss driving the evolution of *Msp.* spp. smaller genomes.
4. Chapter 4 shows the methanogen profiles in stool samples from chronic kidney disease patients are unremarkable in terms of their composition and prevalence, and synbiotic intervention had little or no impact on their abundance and/or profile.
5. Chapter 4 also shows the immunomodulatory properties of whole cell preparations of my *Msp*. isolates, and the human *Mbb.* and *Msp.* type strains, were similar when tested using PBMCs from healthy human subjects and a murine macrophage cell line.

The macropodids (kangaroos and wallabies) are reliant on the microbiota colonising their foregut for the breakdown and fermentation of plant biomass. The relatively small methane emissions from these animals was first proposed in the late 1970's and was later reconfirmed by studies using a colony of kangaroos and wallabies from a Denmark zoo (Madsen and Bertelsen, 2012, Engelhardt et al., 1978). Macropodids have been shown to harbour

methanogenic archaea in their foregut that are taxonomically similar to those found in livestock and humans, albeit at densities considerably similar to those found in humans rather than livestock (Evans et al., 2009). Although prior research with *Mbb. ruminantium* strain M1 has shown that ethanol can stimulate its growth, I believe my results presented in Chapter 2 are the first demonstration of a gut methanogen that can exclusively employ an alcohol-fuelled, hydrogen-independent, pathway for methanol reduction, methanogenesis and growth. As such, I believe that these enzymes support the adaptation of methanogenic archaea like WGK6 to survive and persist in environments where gaseous hydrogen levels are limited. Such conditions are known to occur in the macropodids (Kempton et al., 1976) but recent studies have also shown that ruminant livestock can also be stratified according to their hydrogen release (and methane emissions) predicted from their rumen bacterial profiles (e.g. Shi et al., 2014, Wallace et al., 2015). Interestingly, both these studies also remarked on an increase in the relative abundance of *Msp.* in animals classed as being "low methane emitters". Therefore, the pathway I have discovered provides a plausible explanation as to how these changes might be supported, via a shift in the nutritional ecology afforded to those archaea, like strain WGK6, bearing this alternative pathway. In that context, my results in Chapter 2 also show that homologs of the dehydrogenases specific for alcohol-fuelled methanogenesis can be identified within the genomes of other members of the rumen Methanobacteriales, including a number of *Mbb.* spp. Taken together, I contend that this pathway of methanogenesis is not uncommon in ruminant livestock and not just a specific adaptation of WGK6 to the macropodid foregut. In the future, it would be interesting to first attempt to culture some of the rumen strains available that also possess these dehydrogenases in the presence of ethanol, to ascertain their abilities to produce methane and grow with ethanol as the sole reductant. These findings also raise new questions in terms of the metabolic versatility of methanogenic archaea and how effective strategies designed to specifically reduce hydrogen availability in the rumen environment might be, in terms of reducing methanogen numbers and methane output. If such strategies result in the formation of short chain alcohols, rather than hydrogen gas, I would anticipate the niche occupied by methanogenic archaea like WGK6 would be expanded and their numbers increased. Based on my results in Chapter 2, I would also expect the methane output to be reduced, because of the improved growth efficiency per mol of methane produced with ethanol rather than hydrogen. For these reasons, I think it would be possible and interesting to use PCR primers specific for these dehydrogenase genes as "biomarkers" for low methane emitting livestock**.**

While my results and findings presented in Chapter 2 provide new evidence for metabolic versatility of *Methanosphaera* and other rumen-derived methanogens having been enhanced by the acquisition of just several genes, my isolation of strain BMS also shows that the evolutionary depth of the *Methanosphaera* genus may be much deeper and richer than the previously considered. While my culture-based studies confirmed strain BMS is a hydrogen-dependent methylotroph, incapable of methane formation and growth via the hydrogenotrophic or methylated amines dependent pathways; the genome content is almost 50% larger than that reported for the human isolate of *Msp. stadtmanae* DSMZ 3091^{T} and WGK6. At this time, much of the additional genome content is not annotated to known functional COG categories, which does raise the possibility these "unknown" gene products support metabolic pathways other than methanogenesis; and that permit the growth and persistence of BMS-like strains within the rumen environment. However, and with only three isolate genomes to compare, any hypotheses or conclusions drawn are potentially fraught. For these reasons, I pursued the extraction of *Msp.*-affiliated population genomes from independently produced ruminant and one human metagenomic datasets. These efforts proved to be very useful and helpful, with the recovery of seven new population genomes, of which 5 are also predicted to be "large". Importantly, all these population genomes were found to possess a large degree of synteny with the regions "unique" to strain BMS, as well as the smaller genomes of *Msp.* strains WGK6 and DSMZ 3091^{T}. Such findings support the contention that the *Methanosphaera* genus may possess members that are indeed facultative methanogens: capable of growth either independent of methane production or that is augmented by metabolic and/or nutrient acquisition pathways in addition to methanogenesis. One effective way of examining these concepts would be to undertake RNA-seq analysis of the three *Msp.* isolates following growth with methanol and hydrogen. Such studies would be expected to reveal the extent to which the "unique" genes of strain BMS are (or are not) expressed under these conditions, providing new insights into their physiology, metabolic capacity, and versatility. It might also be possible then to select genes of interest from strain BMS, for example, those hypothesized to support/augment their metabolic capacity for using different substrates for methanogenesis and/or growth; and perform gene "knock-in" studies in other methanogens to alter their phenotype (Buan et al., 2011).

While I was able to recover seven new *Msp.* affiliated population genomes there is one limitation encountered by the MetaBAT method with its inability to effectively assign a 16S rRNA to any of the population genomes. However, I was able to build a 16S rRNA

phylogenetic comparison of both isolate and clone sequences from NCBI deposits for *Msp.* spp. of a variety of host gut environments, illustrated in Fig. 5.1. On the basis of the phylogenetic placement of the isolate strains it is apparent that the larger genomotype strain BMS is distantly related and deep branching in comparison to the smaller genomes of DSMZ 3091^T and WGK6. These results again clearly validate my findings of whole genome phylogeny presented in Chapter 3 and are supported by the widely accepted view that the most common form of evolutionary drift is non-adaptive adaption involving gene loss (Ochman and Moran, 2001). Although more research needs to done, I would propose that the "small" genomotype observed for DSMZ 3091^T, WGK6, DEW79 and SHI1033 is a result of such events and that they are the most recent evolutionary descendants from the "large" genomotype, due to their dispensation of genes. The tetramer nucleotide frequency distributions ("genome barcode") comparisons between *Msp.* isolates BMS, DSMZ 3091^T and WGK6 further supports this theory. Although a significant portion of the genome has been lost by the smaller genomotype, there is evidence of gene conservation, supported by the CAZyme family profile, which exhibits a similar profile for auxiliary activity enzymes, carbohydrate esterase and glycosyltransferases. Of particular note the glycosyltransferases are numerically the most predominant conserved profile across all isolate and population genome sequences. I believe this highlights their importance to *Msp.* spp. and potentially provides an opportunity to locate a conserved member responsible for cell wall decoration which could be used as a universal vaccine target against *Msp*. spp. to curb methane emissions in livestock.

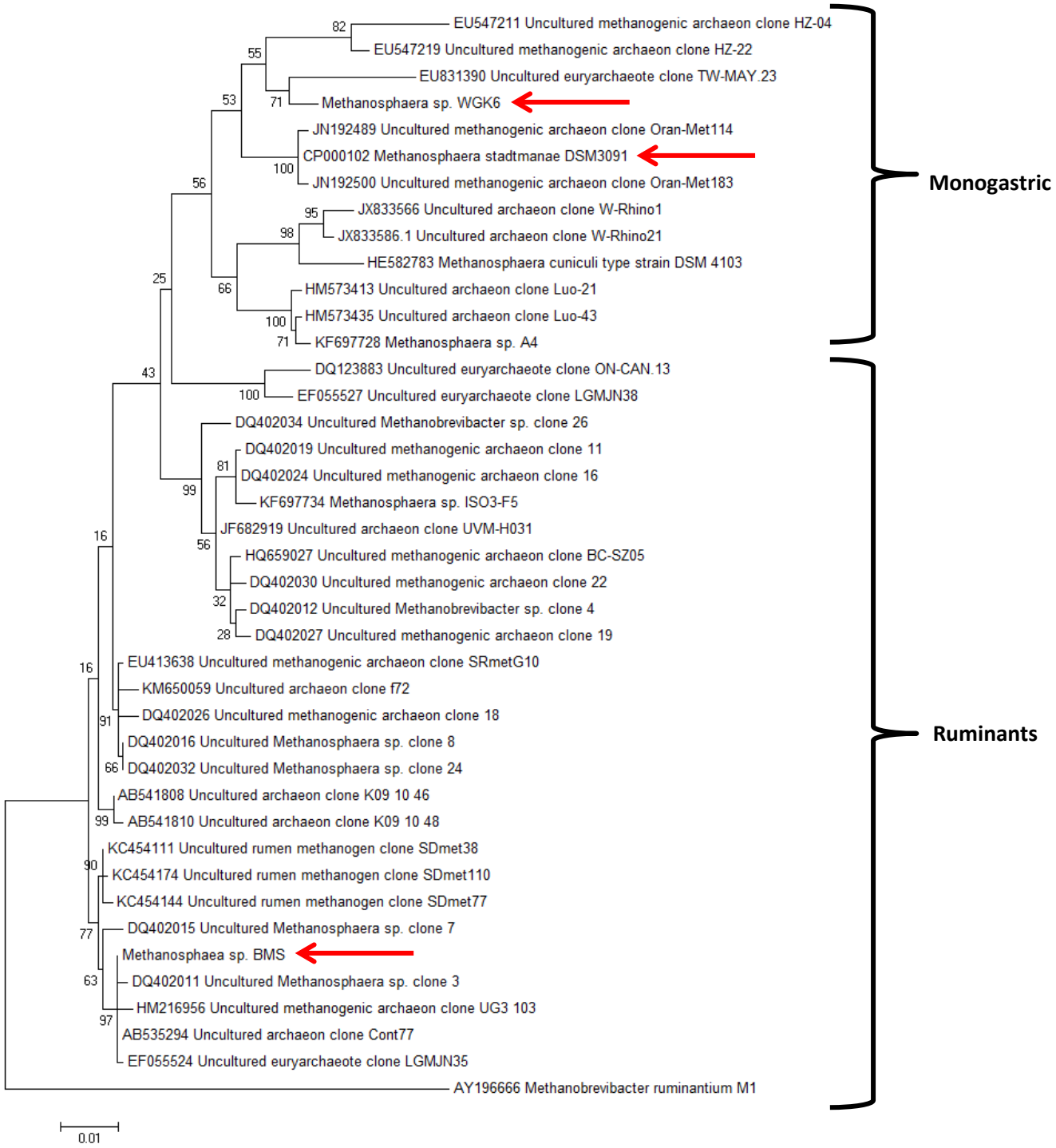

Figure 5.1. Phylogenetic analysis of *Msp.* spp. isolate and clone 16S rRNA gene sequence recovered from NCBI BLASTn when queried with DSMZ 3091^{T}, WGK6 and BMS. WGK6 shows it most similar to clone sequences representing uncultured gut methanogens from the monogastric host the Tammar wallaby (*Macropus eugenii*, TW), *hoatzin* bird (*Opisthocomus hoazin*, HZ) and *Msp. stadtmanae* DSMZ 3091^{T}. In comparison BMS is placed at some distance from these two isolates amongst ruminant uncultured clone sequences. Bootstrap

values are shown and the scale bar represents 1% sequence divergence, with *Mbb. ruminantium* M1 used as the outgroup.

The final research Chapter of my thesis shifted in emphasis from my previous Chapters since during the latter stages of my program my primary supervisor, Professor Mark Morrison, changed his position from CSIRO and relocated to UQ Diamantina Institute. I took this opportunity to redirect my RHD studies, expanding my interests and incorporating some research of human-derived methanogenic archaea and their associated impacts on health and disease. I found this to be an exciting opportunity because it allowed me to expand my knowledge from the animal microbiome to include human microbiology host interaction. Although my knowledge and experience in the field of immunology was limited I felt that the change of focus provided me with an advantage; firstly to my project, secondly by giving me additional learning opportunities and finally expanding on future career opportunities. Even though there was a time cost by making this commitment, I thought it would be worthwhile as recent literature suggested that the methanogen profile can i) respond to diet/nutritional ecology and; ii) appeared to have systemic effects via both arms of the immune system (Conway de Macario and Macario, 2009, Blais Lecours et al., 2014, Bang et al., 2014). The SYNERGY study gave me an opportunity to address the first point while my efforts to work with PBMC and macrophage murine RAW264.7 cell line addressed the second point. In addition the findings from Chapter 3 raised questions as to whether the metabolic versatility and evolutionary diversity of *Msp*. spp. had an effect on their ability to thrive in a human "dysbiotic" gut environment; as well as their capacity to stimulate both arms of the immune system in mammals. I hypothesised that the "dysbiotic" gut microbiota of persons suffering chronic kidney disease (CKD) would be an ideal environment for methylotrophic methanogenic archaea *Msp.* and *Mms.* spp. with particular clinical significance. Interestingly, findings for *Mms*. sp. as demonstrated by Poulsen et al. (2013), Dridi et al. (2012), and Borrel et al. (2012) show these archaea are capable of using methylated amines arising from phosphatidylcholine metabolism to support growth. In that context, establishment of the *Mms.* in the human large bowel might be of clinical relevance for persons known to possess relatively high levels of trimethylamine-oxide in blood as a result of non-communicable diseases (ie: CKD), because of its association with cardiovascular disease pathogenesis (Tang et al., 2014, Brugere et al., 2014). In contrast *Msp.* could be used as a diagnostic tool indicating shifts in fermentation which favour the production of short chain alcohols in diseases such as CKD and non-alcoholic fatty liver disease (Lee et al., 2012, Zhu et al.,

2013). However, my results presented in Chapter 4 would suggest that the SYNERGY trail utilising synbiotic intervention for patients suffering CKD had no effect on the structure or abundance of the methanogenic archaeal community. In fact, my analysis of the MiSeq data produced from these same samples that was assigned to the Methanobacteriales order showed that all reads were classified to the *Mbb.* genus. The stool sample PCR-based screening confirmed that the predominant archaeon was *Mbb. smithii*, in addition to identifying an infrequent occurrence of *Mms*. spp., but there were no detectable populations of *Msp*. spp. from any of these samples. Perhaps the changes in protein and amino acid fermentation schemes resulting in an increased gastrointestinal pH observed for CKD patients (Carrero et al., 2013, Nallu et al., 2016) causes conditions too hostile for the methylotrophic methanogenic archaea to thrive. I believe that this is the first experiment of its kind to investigate a link between CKD and methylotrophic methanogenic archaea and while it is limited to one case study I feel the clinical significance that these methanogens could provide is not something to be overlooked when profiling "dysbiotic" gut microbial communities.

Although I was not able to demonstrate a "dysbiotic" methylotrophic methanogenic community within CKD patients', previous studies have shown that both *Msp. stadtmanae* DSMZ 3091^{T} and *Mbb. smithii* are capable of eliciting a strong immune response. I have demonstrated in Chapter 4 that the immunomodulatory properties of whole cell preparations of human, kangaroo and bovine *Msp*. and *Mbb.* representative isolates were similar, when whole cell preparations were used to challenge PBMCs prepared from healthy human subjects, and a murine macrophage cell line. The similar level of response was achieved when methanogen challenges were standardised based on their total cellular protein concentration suggests a common immunostimulatory element. As demonstrated in Chapter 3 the glycosyltransferases CAZyme family profile (Table 3.4) is conserved across all *Msp.* spp. and this may explain why the challenge assays yielded similar levels of immune activation. Perhaps a conserved glycosyltransferase is responsible for a glycosylated cell surface protein causing similar immunomodulation profiles when the challenge is standardised relative to protein concentration. This theory could be tested through the use of previously validated methods involving cell fractionation and selectively recovering methanogenic surface-exposed proteins through the use of affinity tagging (Francoleon et al., 2009, Rohlin et al., 2012). Alternatively, the level of immune activation for individual conserved genes can be examined by utilising the sequenced *Msp.* genomes and expressing genes of interest in a model system which can then be screened for its immunomodulatory capability. In fact each

process could take advantage of the high-throughput analysis method used within Chapter 4 to rapidly screen genes of interest using the macrophage murine RAW264.7 cell reporter system. While macrophages make up the phagocytic branch of the innate immune system they also play an important role in the activation of the adaptive immune response through the presentation of antigens to T-lymphocytes (Alberts et al., 2003). With the activation of T-lymphocytes recruitment of the major histocompatibility complex (MHC) complex supports the production of a new population of T-lymphocytes that provides immune memory (adaptive immunity). As demonstrated by Blais Lecours et al. (2014) a strong *Msp.* species-specific IgG (adaptive) immune response is produced in persons suffering IBD suggesting that a specific antigen is sampled by macrophage and presented to T-lymphocytes. I propose that activation/training of the host immune response to methanogens occurs though the sampling of the archaeal cell wall components through the lumen by dendritic and macrophage cells. Dendritic and macrophage cells are spread throughout the lamina propria, which forms the core of the mucosa underlying the surface epithelium of the gut (Maric et al., 1996, Cruickshank et al., 2009, Mowat and Bain, 2011). These leucocytes have been proven to sample the microbiota through pores connecting the basement membrane of intestinal villi and through the tight junctions of the gut epithelium (Takahashi-Iwanaga et al., 1999, Rescigno et al., 2001, Farache et al., 2013). With all this taken into account it advocates the idea that knowledge of what this specific "antigen" is could provide a long-term protection against *Msp*. at least. Therefore, the RAW264.7 reporter system would benefit both human immunological studies of methanogen immune interaction and the development of anti-methane vaccines for livestock. Additionally I have evaluated the cytokine profile of peripheral blood mononuclear cells (PBMC) collected from healthy subjects after challenge with whole cell preparations of either *Msp. stadtmanae* DSMZ 3091^{T} or *Mbb. smithii* DSMZ 861^{T} over a 24 hour period I would also find it interesting to examine the response of subjects suffering gut "dysbiosis" such as IBD or IBS. Blais Lecours et al. (2014) being the first to demonstrate that persons suffering IBD have a higher prevalence of *Msp.* as well as higher titres of *Msp.*-specific IgG antibodies. To examine the variation in immune response to *Msp. stadtmanae* DSMZ 3091^{T} challenge between subjects defined as healthy or diseased as well as subjects with and without a *Msp.* population would be enlightening in terms of the differences in activation of the innate and adaptive immune response. This could be evaluated through the use of the cytokine profiling systems developed by LEGENDplex as well as Indirect ELISAs to measure *Mbb*.- and *Msp*.-specific antigen responses. Unfortunately due to time constraints I was unable to address these studies directly, in large part due to the

technical difficulties encountered while using the LEGENDplex system. As described in Chapter 4 there were difficulties in reproducing consistent and reliable standard curves for 4/13 cytokines assayed using the LEGENDplex system and a large portion of my time was dedicated to correspondents with the manufacture to trial new standard cocktails, consumables and improved processing techniques all with little success. With more time I think the LEGENDplex system can be improved to allow the rapid screening of a wide selection of cytokines from a range of donors and challenge scenarios.

In conclusion, despite the intensification of research into the gut methanogens over the last decade, much still needs to be learned. Perhaps the most salient findings of my studies have been the metabolic versatility of gut methanogens, and that the crosstalk between methanogenic archaea and the host are more diverse and intimate than what was once widely accepted. In this thesis, I have focused on methylotrophic methanogens, *Msp.* spp., from two perspectives: the discovery of their expanded range in metabolic/genomic versatility, and the emerging evidence of their direct role in provoking an inflammatory and humoral response. In that context, I contend that the fields of ruminant microbiology and human "microbiome" research have something to learn from each other. Those interested in modulating the human gut microbiota could benefit from the experiences of rumen microbiologists, who have evaluated a variety of dietary interventions over many years to productively manage methane emissions from livestock. In a complementary manner, rumen microbiologists and animal scientists may benefit greatly from the growing interest in the immunomodulatory properties of the human methanogenic archaea, in consideration of their attempts to improve the efficacy and use of vaccine-based approaches to control livestock methane emissions.

Chapter 6 Appendix

6.1 Western Grey kangaroo digesta sample descriptions

Table 6.1. Description of Western Grey kangaroos sampled during a culling exercise in 2008 by licensed hunters, as part of the state's control procedures, on a CSIRO managed farm in Yallenbee (Western Australia).

Sample	Age (years)	Sex	Site of sample collection
1	1	Female	Sacciform
2	2-3	Female	Caecum
3	2-3	Female	Intestine
4	3-4	Male	Sacciform
5	1-2	Female	Sacciform
6	3-4	Female	Sacciform
7	1-2	Female	Sacciform
8	2-3	Female	Caecum
9	2-3	Female	Sacciform
10	4-5	Male	Tubiform
11	4-5	Male	Sacciform
12	2-3	Female	Intestine
13	2-3	Female	Tubiform
14	2-3	Female	Sacciform
15	2-3	Female	Sacciform
16	2-3	Female	Tubiform
17	3-4	Male	Tubiform

6.2 Glycerol 30% stock solution

Measure the liquids into a flask and microwave to bring to a boil. Transfer to a magnetic stirrer and allow the solution to cool while bubbling with N_2. Add dry ingredients in order, which should have a resulting pH of ~6.5. Add the L-cysteine and transfer solution to an anaerobic hood for dispensing. Seal the serum bottles containing dispensed solution with a rubber stopper and crimp seal. Autoclave bottles at 121ºC for 20 minutes under 172 kPa pressure.

- 38 mL mineral 2 solution
    - K_2HPO_4 6g/L
- 38 mL mineral 3 solution
    - K_2HPO_4 6g/L
    - $(NH_4)_2SO_4$ 6g/L
    - NaCl 12g/L
    - $MgSO4_4.7H_2O$ 2.5g/L
    - $CaCl_2.2H_2O$ 1.6g/L
- 1 mL resazurin solution (0.1%)
- 300mL glycerol “AR” grade
- Make up to 1 L with dH_2O
- 1 g L-cysteine HCl

6.3 Dissociation of cells from plant material

1. Resuspend in 0.1 vol of dissociation buffer by vortexing for 30 sec.
2. Spin at 100 g for 20 seconds and remove supernatant to a new tube
3. Repeat dissociation buffer step two more times placing each supernatant in the same tube (or until supernatant becomes clearer- ~5-6 times).
4. Spin the collected supernatant at 100 g for 20 seconds and remove supernatant to a new tube and spin at 12,000 g for 5 min. remove supernatant.
5. Resuspend in 0.1 vol of cell wash buffer and d then spin 12,000g 5 minutes remove supernatant.
6. Store pellet alone in -20ºC or perform direct DNA extraction protocol.

Buffers used

Dissociation buffer saline (pH 2)

- 0.1% tween 80
- 1% methanol
- 1% tertiary butanol

Cell wash buffer (pH 8.0)

- 10 mM Tris-HC1
- 1 M NaCI
- sterilized by autoclaving

6.4 RBB+C DNA extraction method

7. Resuspend in 0.1 vol of dissociation buffer by vortexing for 30 seconds.
8. Spin at 100 g for 20 seconds and remove supernatant to a new tube
9. Repeat dissociation buffer step two more times placing each supernatant in the same tube (or until supernatant becomes clearer- ~5-6 times).
10. Spin the collected supernatant at 100 g for 20 seconds and remove supernatant to a new tube and spin at 12,000 g for 5 min. remove supernatant.
11. Resuspend in 0.1 vol of cell wash buffer and d then spin 12,000g 5 minutes to remove supernatant.
12. Store pellet alone in -20ºC or perform direct DNA extraction protocol.

Buffers used

Dissociation buffer saline (pH 2)

- 0.1% tween 80
- 1% methanol
- 1% tertiary butanol

Cell wash buffer (pH 8.0)

- 10 mM Tris-HC1
- 1 M NaCI
- sterilized by autoclaving

6.5 Primers used for during thesis

Table 6.2. Primers used during this thesis.

Gene target	Primer	Nucleotide sequence (5'-3')	Amplicon (bp)	Annealing temp. (°C)	Reference
16S rRNA gene archaea specific	86-F	GCTCAGTAACACGTGG	1254	60	(Wright and Pimm, 2003)
	1340-R	CGGTGTGTGCAAGGAG			
16S rRNA gene bacteria specific	27-F	AGAGTTTGATCMTGGCTCAG	1465	60	(DeLong, 1992)
	1492-R	TACGGYTACCTTGTTACGACTT			
DGGE designed primers (inc. GC-clamp)	344-F 38nt GC-clamp	TCGCGCCTGCTGCICCCCGT	213	60	(Raskin et al., 1994)
	519R	GWATTACCGCGGCKGCTG			(Lane et al., 1985)
Alcohol dehydrogenase (WGK6)	WALC-F	TTCCACAAACAATGCCAAAA	219	60	This study
	WALC-R	ATGCCATTCCTGCTTCACAT			This study
Aldehyde dehydrogenase (WGK6)	WALD-F	TTGTAAATGGGACATGGCAA	197	60	This study
	WALD-R	TGATTTGTGCACCCATTTGT			This study
BMS closing	BMS B2-R	ACCGTTCTGATTGTAGCCTGGT	364	60	This study
	BMS E5-F	GCATGGTGAACAATGTGGTGT			This study
Universal methanogen (Arch)	*mcrA*-F	TTCGGTGGATCDCARAGRGC	140	60	(Denman et al., 2007)
	mcrA-R	GBARGTCGWAWCCGTAGAATCC			
Msp. stadtmanae (*mtaB*)	122-F	CTAACATCAAAGTAGCTCC	292	55.5	(Blais Lecours et al., 2014)
	414-R	TCCTCTAAGACCGTTT			
Mbb. smithii (*nifH*)	202-F	GAAAGCGGAGGTCCTGAA	151	57	(Johnston et al., 2010)
	353-R	ACTGAAAAACCTCCGCAAAC			
Mms. spp. (*mttB*)	*mtt*B-F	GYRCTTCMACCACATCGACC	160	60	(Poulsen et al., 2013)
	mttB-R	CRGCCATBGCCATGGACAG			

6.6 DGGE denaturing solutions

DGGE was completed using the Bio-Rad D-code System, as described by (Ouwerkerk et al., 2008). The electrophoresis was performed within a buffer of 1x TAE for 12 hours at 75 volts and a constant temperature of 60^{o}C. After electrophoresis the gel was stained for 20 minutes with SYBR safe (Invitrogen) according to the manufacturer's instructions, and the gel images were captured using a Typhoon scanner and Typhoon TRIO Variable Mode Imager (GE Healthcare Life Sciences).

- 30% denaturing solution
  - 20 mL acrylamide/bis
  - 2 mL 50x TAE buffer
  - 12 mL formamide
  - 12.6 g urea
  - 20 mL 10% glycerol
  - Make up to 100 mL with dH_2O
  - 60% denaturing solution

- 20mL acrylamide/bis
  - 2 mL 50x TAE buffer
  - 24 mL formamide
  - 25.2 g urea
  - 20 mL 10% glycerol
  - Make up to 100 mL with dH_2O

6.7 BRN-RF30 media recipe

This recipe makes 1 litre of BRN-RF30 (Joblin et al., 1990). Centrifuge the rumen fluid twice at 23,500 x *g* for 10 min. Transfer the supernatant to a heat proof 1L bottle and add the remaining ingredients, except for L-cysteine hydrochloride·H_2O. The solution was microwaved for 3 minutes with a loose lid to remove oxygen. The solution was then placed onto a heated (75°C) magnetic stirrer, gassing with CO_2 for 45 min; seal the bottle with foil during this step. After 45 minutes the bottle (while continuing CO_2 gassing) was transferred to an ice bucket for 15 minutes to chill the solution to room temperature. After cooling add L-cysteine, quickly remove the CO_2 gas line and cap the bottle, mix well. Transfer solution to an anaerobic chamber, dispense 9 mL into Balch tubes and seal using butyl rubber stoppers. Remove sealed tubes from the anaerobic chamber and crimp seal with appropriate tin caps. Autoclave sealed tubes for 15 minutes at 121°C under 172 kPa pressure to serialise and allow cooling to room temperature.

- 300mL of rumen fluid
- 42.5mL mineral 2 solution
    - K_2HPO_4 6g/L
- 42.5mL mineral 3 solution
    - KH_2PO_4 6g/L
    - $(NH_4)_2SO_4$ 6g/L
    - NaCl 12g/L
    - $MgSO4_4.7H_2O$ 2.5g/L
    - $CaCl_2.2H_2O$ 1.6g/L
- 2g yeast extract
- 5g $NaHCO_3$
- 100µl resazurin
- 615mL distilled water
- 0.5g L-cysteine hydrochloride·H_2O

6.8 Antibiotic stock solution benzyl penicillin and streptomycin sulfate

Benzyl penicillin and streptomycin sulfate 0.1 L^{-1} stock solution (Jarvis et al., 2000) begins with the mixture of salts solution A and B, sodium hydrogen carbonate, resazurin and distilled water. This solution was boiled for 3 minutes in the microwave and then cooled on ice while bubbling with CO_2 for 15 min. After cooling benzyl penicillin, streptomycin sulfate and L-cysteine hydrochloride·H_2O were added to the solution and mixed on a magnetic stirrer. The solution was then transferred to an anaerobic chamber and aliquots of 10 mL were removed and dispensed into autoclaved sterilised capped anaerobic Hungate tubes. To each 10 mL tube of solution 0.1 mL of previously sterilised sodium sulfide solution (reducing agent) was added anaerobically and aseptically. Excess tubes were stored frozen at -20 °C until required.

- 6 g benzyl penicillin
- 2 g streptomycin sulfate
- 17 mL salt solution A
    - KH_2PO_4 3 g/L
    - $(NH_4)_2SO_4$ 3 g/L
    - NaCl 6 g/L
    - $MgSO4_4.7H_2O$ 1.25 g/L
    - $CaCl_2.2H_2O$ 0.8 g/L
- 17 mL salt solution B
    - $K_2HPO_4·3H_2O$ 3 g/L
- 10µL resazurin (0.1% solution)
- 0.5 g sodium hydrogen carbonate
- 50 mg L-cysteine hydrochloride·H_2O
- 66 mL dH_2O

6.9 Sequence cleaning protocol

Agencourt CleanSeq (www.beckmangenomics.com)

1. Shake CleanSeq bottle (stored at 4ºC) to resuspend magnetic particles
2. Add 7 µ to each sequence reaction.
3. For 20 µl sequence reaction, add 62 µl of 85% ethanol. Either pipette mix 7 times or seal and vortex for 30 seconds.
4. Place reaction plate onto magnetic plate for 10 minutes to separate beads from solution.
5. While leaving reaction on plate aspirate supernatant and discard. Be careful not to disturb the beads. It is important to remove all the supernatant at this stage.
6. Dispense 100 µl of 85% ethanol to each well and incubate at room temperature for at least 30 seconds. Aspirate out supernatant and discard.
7. Let the reaction air-dry at room temperature for 10 minutes.
8. Take samples off plate and add 40µl of distilled water to each reaction and incubate for 5 minutes at room temperature to elute DNA.
9. Place back onto magnetic plate for 5 minutes to separate.
10. Transfer 20 µl to a new ABI plate ready to load into sequencer.

6.10 BRN-RF10 medium recipe

This recipe makes 1 L of modified BRN-RF10 media (Balch et al., 1979). Centrifuge rumen fluid twice at 23,500 x *g* for 10 minutes. Transfer supernatant in to a heat proof 1 L bottle. Add remaining ingredients, except for L-cysteine hydrochloride·H_2O and trace vitamins. Microwave the solution for 3 minutes with a loose lid to remove oxygen. Place heated mixture onto a heated (75 °C) magnetic stirrer, gassing with CO_2 for 45 min. Seal the bottle with foil during this step. After 45 minutes the bottle (while continuing CO_2 gassing) was transferred to an ice bucket for 15 minutes to chill the solution to room temperature. After cooling add L-cysteine, quickly remove the CO_2 gas line and cap the bottle, mix well. Transfer solution to an anaerobic chamber, dispense 9 mL into Balch tubes and seal using butyl rubber stoppers. Remove sealed tubes from the anaerobic chamber and crimp seal with appropriate tin caps. Autoclave sealed tubes for 15 minutes at 121°C under 172 kPa pressure to serialise and allow cooling to room temperature. Once cooled add ~0.1 mL of anaerobic trace vitamins solution to each anaerobic tube aseptically with sterile needle and syringe.

- 100 mL of rumen fluid
- 50 mL mineral 2 solution
    - K_2HPO_4 6 g/L
- 50 mL mineral 3 solution
    - KH_2PO_4 6 g/L
    - $(NH_4)_2SO_4$ 6 g/L
    - NaCl 12 g/L
    - $MgSO_4.7H_2O$ 2.5 g/L
    - $CaCl_2.2H_2O$ 1.6 g/L
- 10 mL trace minerals
    - Nitrilotriacetic acid 1.5 g/L
    - $MgSO_4·7H_2O$ 3 g/L
    - NaCl 1 g/L
    - $MnS0_4· H_2O$ 0.5 g/L
    - $FeSO_4·7H_2O$ 0.1 g/L
    - $CoCl_2·6H_2O$ 0.1 g/L
    - $ZnSO_4·7H_2O$ 0.1 g/L
    - $CuSO_4·5H_2O$ 10 mg/L
    - $AlK(SO_4)_2·12H_2O$ 10 mg/L

    - H_3BO_3 10 mg/L
    - $Na_2MoO_4 \cdot 2H_2O$ 10 mg/L
    - $NiSO_4 \cdot 6H_2O$ 30 mg/L
    - Na_2SeO_3 20 mg/L
    - $Na_2WO \cdot 2H_2O$ 20 mg/L
    - Distilled H_2O 1000 mL
- 10 mL trace vitamins
    - Pyridoxine HCl (Vitamin B_6) 10 mg/L
    - L-ascorbic acid (Vitamin C) 5 mg/L
    - Calcium pantothenate (pantothenic acid) 5 mg/L
    - Choline chloride 5 mg/L
    - Lipoic acid (D,L-6,8-thictic acid) 5 mg/L
    - i-Inositol (myo-inositol) 5 mg/L
    - Nicotinamide 5 mg/L
    - Nicotinic acid 5 mg/L
    - *p*-Aminobenzoic acid 5 mg/L
    - Pyridoxal- HCl 5 mg/L
    - Riboflavin (Vitamin B_2) 5 mg/L
    - Thiamine-HCl (Vitamin B_1) 5 mg/L
    - D-biotin (Vitamin H) 2 mg/L
    - Folic acid 2 mg/L
    - Vitamin B_{12} (cyanocobolamin) 0.1 mg/L
    - Distilled H_2O 100 mL
- 5 g $NaHCO_3$
- 2.5 g sodium acetate
- 2.5 g sodium formate
- 2 g yeast extract
- 2 g trypticase
- 100 µl resazurin
- 0.5g L-cysteine hydrochloride$\cdot H_2O$
- Distilled H_2O 780 mL

6.11 The basic annotations for both WGK6 and DSMZ 3091^T

Table 6.3. Basic genome annotations of isolate *Msp.* strains WGK6 and DSMZ 3091^T according to JGI IMG/ER. In brief summary, with the exception of the number of 16S rRNA genes found (1 copy in strain WGK6 c.f. 4 copies in DSMZ 3091^T) the relative proportions of protein coding sequences with (and without) function predictions and/or KEGG pathway designations, are virtually identical.

	WGK6		**DSMZ 3091^T**	
	Number	**% of Total**	**Number**	**% of Total**
DNA, total number of bases	1729155	100.00%	1767403	100.00%
DNA coding number of bases	1475054	85.30%	1512642	85.59%
DNA G+C number of bases	478894	27.70%	488399	27.63%
DNA scaffolds	37	100.00%	1	100.00%
CRISPR Count	3		3	
Genes total number	1643	100.00%	1608	100.00%
Protein coding genes	1592	96.90%	1552	96.52%
RNA genes	51	3.10%	56	3.48%
rRNA genes	6	0.37%	12	0.75%
5S rRNA	2	0.12%	4	0.25%
16S rRNA	1	0.06%	4	0.25%
23S rRNA	3	0.18%	4	0.25%
tRNA genes	43	2.62%	42	2.61%
Other RNA genes	2	0.12%	2	0.12%
Protein coding genes with function prediction	1197	72.85%	1167	72.57%
without function prediction	395	24.04%	385	23.94%
Protein coding genes with enzymes	499	30.37%	508	31.59%
w/o enzymes but with candidate KO based enzymes	73	4.44%	20	1.24%
Protein coding genes connected to Transporter Classification	109	6.63%	105	6.53%
Protein coding genes connected to KEGG pathways	547	33.29%	563	35.01%

not connected to KEGG pathways	1045	63.60%	989	61.50%
Protein coding genes connected to KEGG Orthology (KO)	895	54.47%	902	56.09%
not connected to KEGG Orthology (KO)	697	42.42%	650	40.42%
Protein coding genes connected to MetaCyc pathways	451	27.45%	461	28.67%
not connected to MetaCyc pathways	1141	69.45%	1091	67.85%
Protein coding genes with COGs	1067	64.94%	1083	67.35%
with KOGs	345	21.00%	332	20.65%
with Pfam	1256	76.45%	1234	76.74%
with TIGRfam	554	33.72%	556	34.58%
with InterPro	807	49.12%	796	49.50%
with IMG Terms	265	16.13%	452	28.11%
with IMG Pathways	106	6.45%	172	10.70%
with IMG Parts List	96	5.84%	154	9.58%
in internal clusters	147	8.95%	141	8.77%
in Chromosomal Cassette	1587	96.59%	1560	97.01%
Chromosomal Cassettes	205	-	214	-
Biosynthetic Clusters	2	-	4	-
Genes in Biosynthetic Clusters	17	1.03%	62	3.86%
Fused Protein coding genes	34	2.07%	41	2.55%
Protein coding genes coding signal peptides	39	2.37%	38	2.36%
Protein coding genes coding transmembrane proteins	329	20.02%	321	19.96%
COG clusters	878	82.29%	885	81.72%
KOG clusters	295	27.65%	284	26.22%
Pfam clusters	1042	82.96%	1035	83.87%
TIGRfam clusters	539	97.29%	548	98.56%
Internal clusters	66		62	

6.12 Values and equations used to calculate Gibbs free energy

Table 6.4. Gibbs free energy (ΔG°') equation was calculated under standard culture conditions; all reactants and products are at an initial concentration of 1M, pressure of 1 ATM and temperature of 25°C (298 Kelvin) and using standard enthalpy of formation (ΔH°) and standard entropy of formation (ΔS°) values (1978, 2003). ΔG°' was calculated using the following equation: $\Delta G^{\circ\prime} = (ProductMolarity^{1} * (Product\Delta H^{\circ 1} - (298K * Product\Delta S^{\circ 1})/1000) + ProductMolarity^{2} * (Product\Delta H^{\circ 2} - (298K * Product\Delta S^{\circ 2})/1000)) - (ReactantMolarity^{1} * (Reactant\Delta H^{\circ 1} - (298K * RreactantΔS^{\circ 1})/1000) + ReactantMolarity^{2} * (Reactant\Delta H^{\circ 2} - (298K * Reactant\Delta S^{\circ 2})/1000)$.

	Reactants			**Products**		
	Methanol	**Ethanol**	**Hydrogen**	**Methane**	**Water**	**Acetate**
Standard Enthalpy of formation (ΔH_f° kJ/mol)	-239.03	-276.98	0	-74.85	-285.83	-486
Standard Entropy of formation (ΔS_f° J/(mol.K)	127.24	161.04	130.59	186.27	69.91	85.3
Standard GIBS formation @25°C (ΔG_f° kJ/mol)	-166.82	-174.18	0	-50.75	-237.18	-369
Stoichiometry Meoh:Etoh	2	1		2	1	1
Stoichiometry Meoh:H_2	1		1	1	1	

6.13 High molecular weight DNA extraction for *Msp*. sp. BMS

1. Cells were removed from the spent media by centrifugation at 17,000 x *g* for 4 mins. Repeated if necessary to increase cell pellet collection (~10 mL total 0.8 OD_{600})
2. The cells were washed in 1ml of cell lysis buffer and centrifuged as previously described.
3. The cell pellet was resuspended in 400 µL of RBB+C lysis buffer and incubated at 75 °C for 10 mins to inactivate nucleases.
4. The sample was subjected to 15 rounds of 4 mins freezing on dry ice and 2 mins thawing at 55 °C. The sample was then left subsequently placed at room temperature to cool.
5. When cooled 10 µL of lysozyme (200 mg/mL stock), 1 µL of mutanolysin (20 U/µl) and 5 µL of achromopeptidase (200 U/µL) was added to the cell suspension and mixed gently.
6. The sample was then incubated at 37 °C for 1 hour.
7. Following incubation 20 µL of 10% sodium laurylsarcosine (SLS) and 5 µL of proteinase K (20 mg/mL) were added and the sample was incubated at 55 °C for 30 mins.
8. The sample was extracted by gentle inversion with 400 µL of phenol:chloroform and then centrifuged at 17,000 x *g* for 5 mins.
9. The aqueous phase was carefully removed to a clean microfuge tube while taking care not to disturb the interface.
10. The sample was then further extracted repeating steps 8-9.
11. A 0.1 volume of 3M sodium acetate (pH 5.2) was added and mixed by gentle inversion.
12. Then one volume of isopropanol was added, gently mixed and left to incubate on ice for 30 mins. The DNA is visible as a coiled thread in the solution at high concentrations of extracted DNA.
13. The sample was centrifuged at 17,000 x *g* for 5 mins and the supernatant carefully removed.
14. The DNA pellet was washed twice by the addition of 500 µL 70% ethanol followed by centrifugation at 17,000 x *g* for 5 mins.
15. The DNA was then allowed to air dry and the sample was resuspended in [50-100 µL] of TE buffer.
16. The sample was RNase treated with 5 µL (10 mg/mL) and incubated at 37 °C.

17. Check quality of extraction on a 0.7% agarose gel at 80 volts for 90 mins.

- Cell lysis buffer: Sterilise solution by autoclaving.
    - 6mM Tris-HCl (pH 8.0)
    - 100mM EDTA
    - 1M NaCl
- RBB+C buffer: Sterilise solution by autoclaving.
    - 500 mM NaCl
    - 50 mM Tris-HCl, pH 8.0
    - 50 mM EDTA
    - 4% sodium dodecyl sulfate (SDS)
- TE buffer: Sterilise solution by autoclaving.
    - 10mM Tris-HCl, 1mM EDTA.

Ethanol Precipitate of DNA for PacBio sequencing

1. Measure the volume of the DNA sample.
2. Add 0.1 volume of sodium acetate, pH 5.2, (final concentration of 0.3 M)

- These amounts assume that the DNA is in TE only; if DNA is in a solution containing salt, adjust salt accordingly to achieve the correct final concentration.

3. Mix well.
4. Add 2 to 2.5 volumes of ice cold 100% ethanol (calculated after salt addition).
5. Mix well.
6. Place on ice or at -20 °C for >20 mins.
7. Centrifuge at maximal speed for 10-15 min.
8. Carefully decant supernatant.
9. Add 1 mL 70% ethanol. Mix. Spin briefly. Carefully decant supernatant.
10. Air dry or briefly vacuum dry pellet.
11. Resuspend pellet in the appropriate volume of water.

- 3 M sodium acetate pH 5.2: Sterilise solution by autoclaving.

6.14 NCBI SRA chosen for MetaBAT

Table 6.5. The NCBI SRA projects identified as containing amplicons specific for *Msp. stadtmanae* DSMZ 3091^{T} 16S rRNA and as a result were chosen for MetaBAT population genome binning.

SRA dataset	Sample source	Study
ERR260147	Gut metagenome in European women with normal, impaired and diabetic glucose control	(Karlsson et al., 2013)
ERR260158	Gut metagenome in European women with normal, impaired and diabetic glucose control	(Karlsson et al., 2013)
ERR260183	Gut metagenome in European women with normal, impaired and diabetic glucose control	(Karlsson et al., 2013)
ERR260195	Gut metagenome in European women with normal, impaired and diabetic glucose control	(Karlsson et al., 2013)
ERR260200	Gut metagenome in European women with normal, impaired and diabetic glucose control	(Karlsson et al., 2013)
ERR260216	Gut metagenome in European women with normal, impaired and diabetic glucose control	(Karlsson et al., 2013)
ERR260228	Gut metagenome in European women with normal, impaired and diabetic glucose control	(Karlsson et al., 2013)
ERR260234	Gut metagenome in European women with normal, impaired and diabetic glucose control	(Karlsson et al., 2013)
ERR260236	Gut metagenome in European women with normal, impaired and diabetic glucose control	(Karlsson et al., 2013)
ERR275251	Gut metagenome in European women with normal, impaired and diabetic glucose control	(Karlsson et al., 2013)
SRR094926	Metagenome isolated from cow gut	(Hess et al., 2011)
SRR1206671	NZ high methane producing ovine- time point 1	(Shi et al., 2014)
SRR873595	NZ low methane producing ovine- time point 1	(Shi et al., 2014)
SRR873596	NZ low methane producing ovine- time point 1	(Shi et al., 2014)
SRR873597	NZ low methane producing ovine- time point 1	(Shi et al., 2014)

SRR873599	NZ low methane producing ovine- time point 1	(Shi et al., 2014)
SRR873604	NZ high methane producing ovine- time point 1	(Shi et al., 2014)
SRR873606	NZ high methane producing ovine- time point 1	(Shi et al., 2014)
SRR873608	NZ high methane producing ovine- time point 1	(Shi et al., 2014)

6.15 PBMC extraction from whole blood diagram

1. Pipette 15mL Ficoll-Paque into a 50 mL falcon tube.
2. Dilute blood sample 1:1 with PBS-EDTA (2mM).
3. Gently layer 35 mL of diluted cell suspension over the Ficoll, being careful not to mix the two layers.
4. Spin tubes at 400 x *g* at 21 ºC without brake (Ficoll can burst cells if slowed abruptly or shaken) for 30 minutes.
5. Aspirate top ~15 mL of plasma from each tube.
6. Collect interface containing PBMC using a 10 mL pipette into fresh tubes, be careful to avoid the Ficoll.
7. Top up (to 50 mL) freshly isolated PBMCs with PBS-EDTA.
8. Wash at 400 x *g* for 5 minutes (brake on).
9. Discard supernatant and resuspend cells by gently tapping tube.
10. Add 50mL PBS, and wash; 400 x *g* for 5 minutes (brake on). Discard supernatant.
11. Gently resuspend cells in 20 mL PBS.
12. Take a 10µL aliquot out for cell counts using a hemocytometer.
13. Centrifuge at 400 x *g* for 5 minutes (brake on).
14. Resuspend in appropriate volume of media for culture.

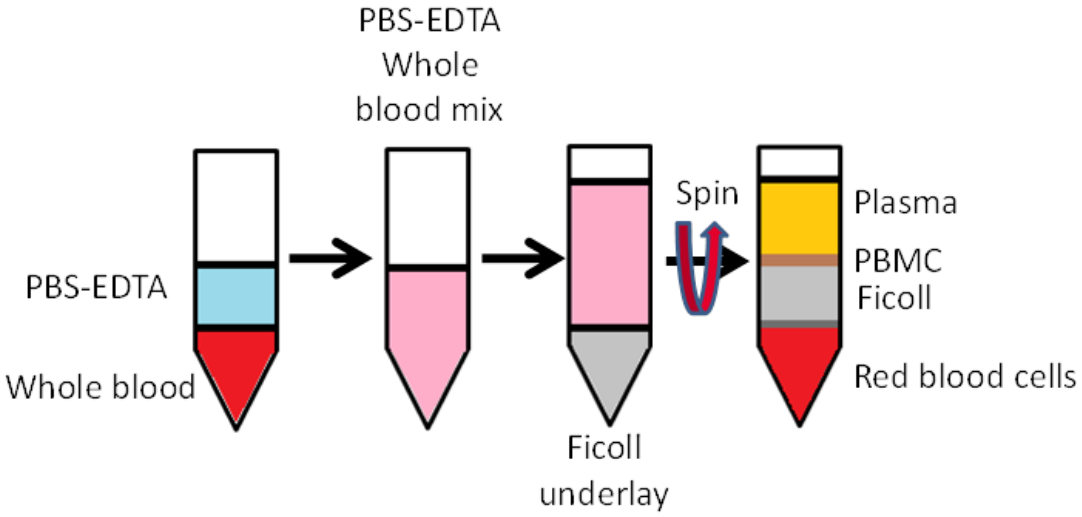

- **Culture medium:**
    - RPMI medium
    - foetal bovine serum (heat-inactivated and filter sterilised, 10% vol/vol)
    - penicillin-streptomycin L-glutamine (1% vol/vol)

6.16 Standard curves for LEGENDplex cytokine

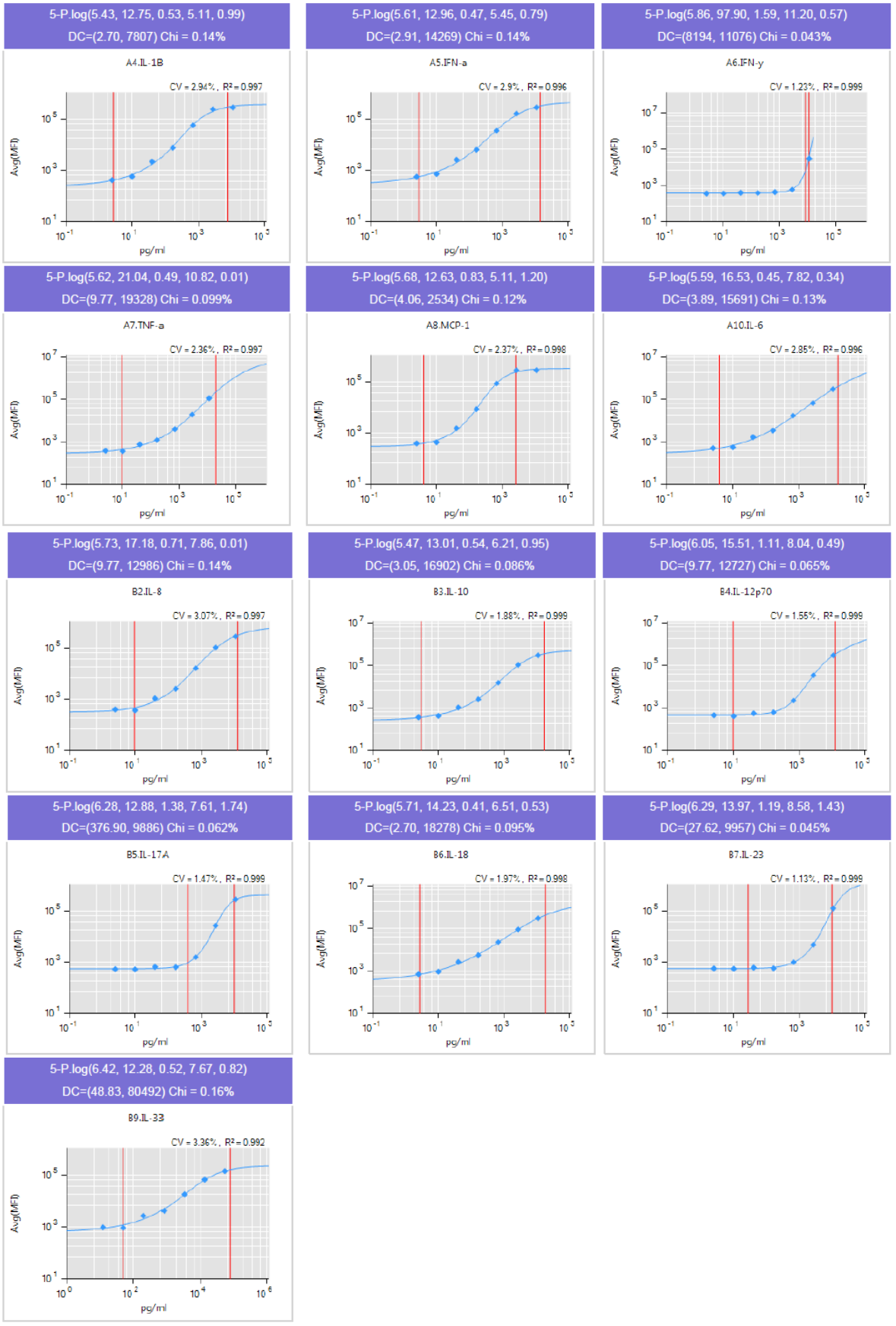

Figure 6.1. The standard curves for each of the 13 cytokines assayed with the LEGENDplex kit. Due to an technical error within the kit which was unable to be resolved during correspondents with the manufacturer 4/13 cytokines (IFN-γ, IL-12p70, IL-17A and IL-23) produced standard curves which were too inconsistent for use and as a result were excluded from results section of Chapter 4.

6.17 LEGENDplex statistics

Table 6.6. Statistics for cytokines (IL-1β, TNF-α, IL-6, IL-8, MCP-1 and IL-10) produced from the PBMC harvested from three donors (HMI004-006) as determined using the LEGENDplex assay, after 6, 12 and 24 hours challenge with either saline (negative control), LPS (100 ng/mL, positive control), *Msp. stadtmanae* DSMZ 3091^{T} or *Mbb. smithii* DSMZ 861^{T}. The data were analysed by one-way ANOVA and degree of significant differences are denoted by *.

IL-1β	**Saline 6hrs**	**LPS 6 hrs**	***Msp. stadtmanae* 6hrs**	***Mbb. smithii* 6hrs**	**Saline 12hrs**	**LPS 12 hrs**	***Msp. stadtmanae* 12 hrs**	***Mbb. smithii* 12 hrs**	**Saline 24 hrs**	**LPS 24 hrs**	***Msp. stadtmanae* 24 hrs**	***Mbb. smithii* 24 hrs**
Saline 6hrs		ns	ns	***	ns	ns	ns	**	ns	ns	ns	*
LPS 6 hrs	ns		ns	**	ns	ns	ns	ns	ns	ns	ns	ns
***Msp. stadtmanae* 6hrs**	ns	ns		ns	ns	ns	ns	ns	ns	ns	ns	ns
***Mbb. smithii* 6hrs**	***	**	ns		***	ns	ns	ns	***	ns	ns	ns
Saline 12hrs	ns	ns	ns	***		ns	ns	**	ns	ns	ns	*
LPS 12 hrs	ns	ns	ns	ns	ns		ns	ns	ns	ns	ns	ns
***Msp. stadtmanae* 12 hrs**	ns	ns	ns	ns	ns	ns		ns	ns	ns	ns	ns
***Mbb. smithii* 12 hrs**	**	ns	ns	ns	**	ns	ns		**	ns	ns	ns
Saline 24 hrs	ns	ns	ns	***	ns	ns	ns	**		ns	ns	*
LPS 24 hrs	ns	ns	ns	ns	ns	ns	ns	ns	ns		ns	ns
***Msp. stadtmanae* 24 hrs**	ns	ns	ns	ns	ns	ns	ns	ns	ns	ns		ns
***Mbb. smithii* 24 hrs**	*	ns	ns	ns	*	ns	ns	ns	*	ns	ns	

TNF-α	**Saline 6hrs**	**LPS 6 hrs**	***Msp. stadtmanae* 6hrs**	***Mbb. smithii* 6hrs**	**Saline 12hrs**	**LPS 12 hrs**	***Msp. stadtmanae* 12 hrs**	***Mbb. smithii* 12 hrs**	**Saline 24 hrs**	**LPS 24 hrs**	***Msp. stadtmanae* 24 hrs**	***Mbb. smithii* 24 hrs**
Saline 6hrs		ns	***	***	ns	*	***	***	ns	ns	***	***
LPS 6 hrs	ns		ns	***	ns	ns	ns	***	ns	ns	ns	***
***Msp. stadtmanae* 6hrs**	***	ns		***	***	ns	ns	***	***	ns	ns	**
***Mbb. smithii* 6hrs**	***	***	***		***	***	***	ns	***	***	***	ns
Saline 12hrs	ns	ns	***	***		*	***	***	ns	ns	***	***

LPS 12 hrs	*	ns	ns	***	*		ns	***	*	ns	ns	***
***Msp. stadtmanae* 12 hrs**	***	ns	ns	***	***	ns		***	***	ns	ns	**
***Mbb. smithii* 12 hrs**	***	***	***	ns	***	***	***		***	***	***	ns
Saline 24 hrs	ns	ns	***	***	ns	*	***	***		ns	***	***
LPS 24 hrs	ns	ns	ns	***	ns	ns	ns	***	ns		ns	***
***Msp. stadtmanae* 24 hrs**	***	ns	ns	***	***	ns	ns	***	***	ns		**
***Mbb. smithii* 24 hrs**	***	***	**	ns	***	***	**	ns	***	***	**	

IL-6	**Saline 6hrs**	**LPS 6 hrs**	***Msp. stadtmanae* 6hrs**	***Mbb. smithii* 6hrs**	**Saline 12hrs**	**LPS 12 hrs**	***Msp. stadtmanae* 12 hrs**	***Mbb. smithii* 12 hrs**	**Saline 24 hrs**	**LPS 24 hrs**	***Msp. stadtmanae* 24 hrs**	***Mbb. smithii* 24 hrs**
Saline 6hrs		ns	ns	ns	ns	**	ns	ns	ns	***	ns	**
LPS 6 hrs	ns		ns	ns	ns	ns	ns	ns	ns	**	ns	ns
***Msp. stadtmanae* 6hrs**	ns	ns		ns	ns	**	ns	ns	ns	***	ns	**
***Mbb. smithii* 6hrs**	ns	ns	ns		ns	ns	ns	ns	ns	***	ns	ns
Saline 12hrs	ns	ns	ns	ns		**	ns	ns	ns	***	ns	**
LPS 12 hrs	**	ns	**	ns	**		**	ns	**	ns	*	ns
***Msp. stadtmanae* 12 hrs**	ns	ns	ns	ns	ns	**		ns	ns	***	ns	*
***Mbb. smithii* 12 hrs**	ns	ns	ns	ns	ns	ns	ns		ns	**	ns	ns
Saline 24 hrs	ns	ns	ns	ns	ns	**	ns	ns		***	ns	**
LPS 24 hrs	***	**	***	***	***	ns	***	**	***		***	ns
***Msp. stadtmanae* 24 hrs**	ns	ns	ns	ns	ns	*	ns	ns	ns	***		ns
***Mbb. smithii* 24 hrs**	**	ns	**	ns	**	ns	*	ns	**	ns	ns	

IL-8	**Saline 6hrs**	**LPS 6 hrs**	***Msp. stadtmanae* 6hrs**	***Mbb. smithii* 6hrs**	**Saline 12hrs**	**LPS 12 hrs**	***Msp. stadtmanae* 12 hrs**	***Mbb. smithii* 12 hrs**	**Saline 24 hrs**	**LPS 24 hrs**	***Msp. stadtmanae* 24 hrs**	***Mbb. smithii* 24 hrs**
Saline 6hrs		ns	ns	ns	ns	ns	ns	ns	ns	***	**	***
LPS 6 hrs	ns		ns	ns	ns	ns	ns	ns	ns	**	ns	***
***Msp. stadtmanae* 6hrs**	ns	ns		ns	ns	ns	ns	ns	ns	**	*	***
***Mbb. smithii* 6hrs**	ns	ns	ns		ns	ns	ns	ns	ns	*	ns	***

Saline 12hrs	ns	ns	ns	ns		ns	ns	ns	ns	***	*	***
LPS 12 hrs	ns	ns	ns	ns	ns		ns	ns	ns	ns	ns	**
***Msp. stadtmanae* 12 hrs**	ns	ns	ns	ns	ns	ns		ns	ns	*	ns	***
***Mbb. smithii* 12 hrs**	ns	ns	ns	ns	ns	ns	ns		ns	ns	ns	*
Saline 24 hrs	ns	ns	ns	ns	ns	ns	ns	ns		**	*	***
LPS 24 hrs	***	**	**	*	***	ns	*	ns	**		ns	ns
***Msp. stadtmanae* 24 hrs**	**	ns	*	ns	*	ns	ns	ns	*	ns		ns
***Mbb. smithii* 24 hrs**	***	***	***	***	***	**	***	*	***	ns	ns	

MCP-1	**Saline 6hrs**	**LPS 6 hrs**	***Msp. stadtmanae* 6hrs**	***Mbb. smithii* 6hrs**	**Saline 12hrs**	**LPS 12 hrs**	***Msp. stadtmanae* 12 hrs**	***Mbb. smithii* 12 hrs**	**Saline 24 hrs**	**LPS 24 hrs**	***Msp. stadtmanae* 24 hrs**	***Mbb. smithii* 24 hrs**
Saline 6hrs		ns	ns	ns	ns	**	ns	ns	ns	***	ns	ns
LPS 6 hrs	ns		ns	ns	ns	ns	ns	ns	ns	***	ns	ns
***Msp. stadtmanae* 6hrs**	ns	ns		ns	ns	***	ns	ns	*	***	ns	*
***Mbb. smithii* 6hrs**	ns	ns	ns		ns	**	ns	ns	ns	***	ns	ns
Saline 12hrs	ns	ns	ns	ns		ns	ns	ns	ns	***	ns	ns
LPS 12 hrs	**	ns	***	**	ns		***	**	ns	**	***	ns
***Msp. stadtmanae* 12 hrs**	ns	ns	ns	ns	ns	***		ns	*	***	ns	*
***Mbb. smithii* 12 hrs**	ns	ns	ns	ns	ns	**	ns		ns	***	ns	ns
Saline 24 hrs	ns	ns	*	ns	ns	ns	*	ns		***	ns	ns
LPS 24 hrs	***	***	***	***	***	**	***	***	***		***	***
***Msp. stadtmanae* 24 hrs**	ns	ns	ns	ns	ns	***	ns	ns	ns	***		ns
***Mbb. smithii* 24 hrs**	ns	ns	*	ns	ns	ns	*	ns	ns	***	ns	

IL-10	**Saline 6hrs**	**LPS 6 hrs**	***Msp. stadtmanae* 6hrs**	***Mbb. smithii* 6hrs**	**Saline 12hrs**	**LPS 12 hrs**	***Msp. stadtmanae* 12 hrs**	***Mbb. smithii* 12 hrs**	**Saline 24 hrs**	**LPS 24 hrs**	***Msp. stadtmanae* 24 hrs**	***Mbb. smithii* 24 hrs**
Saline 6hrs		ns	ns	ns	ns	*	ns	*	ns	***	**	**
LPS 6 hrs	ns		ns	ns	ns	ns	ns	ns	ns	***	*	*
***Msp. stadtmanae* 6hrs**	ns	ns		ns	ns	ns	ns	ns	ns	***	*	*

***Mbb. smithii* 6hrs**	ns	ns	ns		ns	ns	ns	ns	ns	***	*	*
Saline 12hrs	ns	ns	ns	ns		*	ns	*	ns	***	**	**
LPS 12 hrs	*	ns	ns	ns	*		ns	ns	*	*	ns	ns
***Msp. stadtmanae* 12 hrs**	ns	ns	ns	ns	ns	ns		ns	ns	**	ns	ns
***Mbb. smithii* 12 hrs**	*	ns	ns	ns	*	ns	ns		*	*	ns	ns
Saline 24 hrs	ns	ns	ns	ns	ns	*	ns	*		***	**	**
LPS 24 hrs	***	***	***	***	***	*	**	*	***		ns	ns
***Msp. stadtmanae* 24 hrs**	**	*	*	*	**	ns	ns	ns	**	ns		ns
***Mbb. smithii* 24 hrs**	**	*	*	*	**	ns	ns	ns	**	ns	ns	

Chapter 7 References

ALBERTS, B., JOHNSON, A., LEWIS, J., RAFF, M., ROBERTS, K. & WALTER, P. 2003. *Molecular biology of the cell. 4th edn*, Oxford University Press.

ANDERSON, I., ULRICH, L. E., LUPA, B., SUSANTI, D., PORAT, I., HOOPER, S. D., LYKIDIS, A., SIEPRAWSKA-LUPA, M., DHARMARAJAN, L., GOLTSMAN, E., LAPIDUS, A., SAUNDERS, E., HAN, C., LAND, M., LUCAS, S., MUKHOPADHYAY, B., WHITMAN, W. B., WOESE, C., BRISTOW, J. & KYRPIDES, N. 2009. Genomic Characterization of Methanomicrobiales Reveals Three Classes of Methanogens. *PLoS ONE,* 4**,** e5797.

ASHIDA, H., TAMAKI, H., FUJIMOTO, T., YAMAMOTO, K. & KUMAGAI, H. 2000. Molecular cloning of cDNA encoding alpha-N-acetylgalactosaminidase from Acremonium sp. and its expression in yeast. *Arch Biochem Biophys,* 384**,** 305-10.

ATTWOOD, G. T., ALTERMANN, E., KELLY, W. J., LEAHY, S. C., ZHANG, L. & MORRISON, M. 2011. Exploring rumen methanogen genomes to identify targets for methane mitigation strategies. *Animal Feed Science and Technology,* 166–167**,** 65-75.

AUTISSIER, P., SOULAS, C., BURDO, T. H. & WILLIAMS, K. C. 2010. Evaluation of a 12-color flow cytometry panel to study lymphocyte, monocyte, and dendritic cell subsets in humans. *Cytometry A,* 77**,** 410-9.

AZIZ, R. K., BARTELS, D., BEST, A. A., DEJONGH, M., DISZ, T., EDWARDS, R. A., FORMSMA, K., GERDES, S., GLASS, E. M., KUBAL, M., MEYER, F., OLSEN, G. J., OLSON, R., OSTERMAN, A. L., OVERBEEK, R. A., MCNEIL, L. K., PAARMANN, D., PACZIAN, T., PARRELLO, B., PUSCH, G. D., REICH, C., STEVENS, R., VASSIEVA, O., VONSTEIN, V., WILKE, A. & ZAGNITKO, O. 2008. The RAST Server: rapid annotations using subsystems technology. *BMC Genomics,* 9**,** 75.

BALCH, W. E., FOX, G. E., MAGRUM, L. J., WOESE, C. R. & WOLFE, R. S. 1979. Methanogens: reevaluation of a unique biological group. *Microbiological reviews,* 43**,** 260-96.

BANG, C., WEIDENBACH, K., GUTSMANN, T., HEINE, H. & SCHMITZ, R. A. 2014. The Intestinal Archaea *Methanosphaera stadtmanae* and *Methanobrevibacter smithii* Activate Human Dendritic Cells. *PLoS ONE,* 9**,** e99411.

BAPTESTE, E., BROCHIER, C. & BOUCHER, Y. 2005. Higher-level classification of the Archaea: evolution of methanogenesis and methanogens. *Archaea,* 1**,** 353-63.

BLAIS LECOURS, P., DUCHAINE, C., TAILLEFER, M., TREMBLAY, C., VEILLETTE, M., CORMIER, Y. & MARSOLAIS, D. 2011. Immunogenic Properties of Archaeal Species Found in Bioaerosols. *PLoS ONE,* 6**,** e23326.

BLAIS LECOURS, P., MARSOLAIS, D., CORMIER, Y., BERBERI, M., HACHÉ, C., BOURDAGES, R. & DUCHAINE, C. 2014. Increased Prevalence of *Methanosphaera stadtmanae* in Inflammatory Bowel Diseases. *PLoS ONE,* 9**,** e87734.

BLOM, J., ALBAUM, S. P., DOPPMEIER, D., PUHLER, A., VORHOLTER, F. J., ZAKRZEWSKI, M. & GOESMANN, A. 2009. EDGAR: a software framework for the comparative analysis of prokaryotic genomes. *BMC Bioinformatics,* 10**,** 154.

BOLGER, A. M., LOHSE, M. & USADEL, B. 2014. Trimmomatic: A flexible trimmer for Illumina Sequence Data. *Bioinformatics*.

BOND, J. H., JR., ENGEL, R. R. & LEVITT, M. D. 1971. Factors influencing pulmonary methane excretion in man. An indirect method of studying the in situ metabolism of the methane-producing colonic bacteria. *J Exp Med,* 133**,** 572-88.

BORREL, G., HARRIS, H. M., TOTTEY, W., MIHAJLOVSKI, A., PARISOT, N., PEYRETAILLADE, E., PEYRET, P., GRIBALDO, S., O'TOOLE, P. W. & BRUGERE, J. F. 2012. Genome sequence of "Candidatus Methanomethylophilus alvus" Mx1201, a methanogenic archaeon from the human gut belonging to a seventh order of methanogens. *J Bacteriol,* 194**,** 6944-5.

BORREL, G., O'TOOLE, P. W., HARRIS, H. M., PEYRET, P., BRUGERE, J. F. & GRIBALDO, S. 2013. Phylogenomic data support a seventh order of Methylotrophic methanogens and provide insights into the evolution of Methanogenesis. *Genome Biology and Evolution,* 5**,** 1769-80.

BORREL, G., PARISOT, N., HARRIS, H., PEYRETAILLADE, E., GACI, N., TOTTEY, W., BARDOT, O., RAYMANN, K., GRIBALDO, S., PEYRET, P., O'TOOLE, P. & BRUGERE, J.-F. 2014. Comparative genomics highlights the unique biology of Methanomassiliicoccales, a Thermoplasmatales-related seventh order of methanogenic archaea that encodes pyrrolysine. *BMC Genomics,* 15**,** 679.

BREZNAK, J. A. & SWITZER, J. M. 1986. Acetate Synthesis from H2 plus CO2 by Termite Gut Microbes. *Applied and Environmental Microbiology,* 52**,** 623-630.

BRUGERE, J. F., BORREL, G., GACI, N., TOTTEY, W., O'TOOLE, P. W. & MALPUECH-BRUGERE, C. 2014. Archaebiotics: proposed therapeutic use of

archaea to prevent trimethylaminuria and cardiovascular disease. *Gut Microbes,* 5**,** 5-10.

BRUSA, T., CANZI, E., ALLIEVI, L., PUPPO, E. & FERRARI, A. 1993. Methanogens in the human intestinal tract and oral cavity. *Current Microbiology,* 27**,** 261-265.

BRYANT, M. P. 1979. Microbial methane production- theoretical aspects. *Journal of Animal Science,* 48**,** 193-201.

BRYANT, M. P. & WOLIN, M. J. Rumen bacteria and their metabolic interactions. *In:* HASEGAWA, T., ed. Proceedings of the first international congress of the international association of the microbiological society, 1975 Japan, Tokyo. 297.

BUAN, N., KULKARNI, G. & METCALF, W. 2011. Genetic methods for methanosarcina species. *Methods Enzymol,* 494**,** 23-42.

CABELLO, P., ROLDAN, M. D. & MORENO-VIVIAN, C. 2004. Nitrate reduction and the nitrogen cycle in archaea. *Microbiology,* 150**,** 3527-46.

CARRERO, J. J., STENVINKEL, P., CUPPARI, L., IKIZLER, T. A., KALANTAR-ZADEH, K., KAYSEN, G., MITCH, W. E., PRICE, S. R., WANNER, C., WANG, A. Y. M., TER WEE, P. & FRANCH, H. A. 2013. Etiology of the Protein-Energy Wasting Syndrome in Chronic Kidney Disease: A Consensus Statement From the International Society of Renal Nutrition and Metabolism (ISRNM). *Journal of Renal Nutrition,* 23**,** 77-90.

CĂTANĂ, C.-S., BERINDAN NEAGOE, I., COZMA, V., MAGDAŞ, C., TĂBĂRAN, F. & DUMITRAŞCU, D. L. 2015. Contribution of the IL-17/IL-23 axis to the pathogenesis of inflammatory bowel disease. *World Journal of Gastroenterology : WJG,* 21**,** 5823-5830.

CHATTERJEE, S., PARK, S., LOW, K., KONG, Y. & PIMENTEL, M. 2007. The degree of breath methane production in IBS correlates with the severity of constipation. *Am J Gastroenterol,* 102**,** 837-41.

CHAUDHARY, P. P., GACI, N., BORREL, G., O'TOOLE, P. W. & BRUGERE, J. F. 2015. Molecular methods for studying methanogens of the human gastrointestinal tract: current status and future directions. *Appl Microbiol Biotechnol,* 99**,** 5801-15.

CHAUDHURI, R. R., LOMAN, N. J., SNYDER, L. A., BAILEY, C. M., STEKEL, D. J. & PALLEN, M. J. 2008. xBASE2: a comprehensive resource for comparative bacterial genomics. *Nucleic Acids Research,* 36**,** D543-6.

CONWAY DE MACARIO, E. & MACARIO, A. J. 2009. Methanogenic archaea in health and disease: a novel paradigm of microbial pathogenesis. *Int J Med Microbiol,* 299**,** 99-108.

CONWAY DE MACARIO, E., MACARIO, A. J. L. & PASTINI, A. 1985. The superficial antigenic mosaic of Methanobrevibacter smithii. *Archives of Microbiology,* 142**,** 311-316.

CRUICKSHANK, S. M., DESCHOOLMEESTER, M. L., SVENSSON, M., HOWELL, G., BAZAKOU, A., LOGUNOVA, L., LITTLE, M. C., ENGLISH, N., MACK, M., GRENCIS, R. K., ELSE, K. J. & CARDING, S. R. 2009. Rapid dendritic cell mobilization to the large intestinal epithelium is associated with resistance to Trichuris muris infection. *J Immunol,* 182**,** 3055-62.

DARLING, A. E., JOSPIN, G., LOWE, E., MATSEN, F. A., BIK, H. M. & EISEN, J. A. 2014. PhyloSift: phylogenetic analysis of genomes and metagenomes. *PeerJ,* 2**,** e243.

DARLING, A. E., MAU, B. & PERNA, N. T. 2010. Progressive Mauve: multiple genome alignment with gene gain, loss and rearrangement. *PLoS One,* 5**,** e11147.

DEAN, J. A. (ed.) 1978. *Lange's handbook of chemistry,* New York, NY 10020: McGraw-Hill.

DELLOW, D., HUME, I., CLARKE, R. & BAUCHOP, T. 1988. Microbial Activity in the Forestomach of Free-Living Macropodid Marsupials - Comparisons With Laboratory Studies. *Australian Journal of Zoology* 36 383 - 395

DELONG, E. F. 1992. Archaea in coastal marine environments. *Proceedings of the National Academy of Science of the United States of America,* 89**,** 5685-9.

DENMAN, S. E., TOMKINS, N. W. & MCSWEENEY, C. S. 2007. Quantitation and diversity analysis of ruminal methanogenic populations in response to the antimethanogenic compound bromochloromethane. *FEMS Microbiology Ecology,* 62**,** 313-322.

DRIDI, B., FARDEAU, M. L., OLLIVIER, B., RAOULT, D. & DRANCOURT, M. 2012. Methanomassiliicoccus luminyensis gen. nov., sp. nov., a methanogenic archaeon isolated from human faeces. *Int J Syst Evol Microbiol,* 62**,** 1902-7.

DRIDI, B., RAOULT, D. & DRANCOURT, M. 2011. Archaea as emerging organisms in complex human microbiomes. *Anaerobe,* 17**,** 56-63.

ECKBURG, P. B., BIK, E. M., BERNSTEIN, C. N., PURDOM, E., DETHLEFSEN, L., SARGENT, M., GILL, S. R., NELSON, K. E. & RELMAN, D. A. 2005. Diversity of the Human Intestinal Microbial Flora. *Science,* 308**,** 1635-1638.

EDWARDS, T. & MCBRIDE, B. C. 1975. New method for the isolation and identification of methanogenic bacteria. *Applied Microbiology,* 29**,** 540-5.

ENGELHARDT, W. V., WOLTER, S., LAWRENZ, H. & HEMSLEY, J. A. 1978. Production of methane in two non-ruminant herbivores *Comparative Biochemistry and Physiology Part A: Physiology,* 60**,** 309-311.

EVANS, P. N., HINDS, L. A., SLY, L. I., MCSWEENEY, C. S., MORRISON, M. & WRIGHT, A. D. 2009. Community composition and density of methanogens in the foregut of the Tammar wallaby (*Macropus eugenii*). *Applied and Environmental Microbiology,* 75**,** 2598-602.

FAO 2012. *Economic growth is necessary but not suffcient to accelerate reduction of hunger and malnutrition,* Italy, Food and Agriculture Organization of the United Nations (FAO).

FARACHE, J., KOREN, I., MILO, I., GUREVICH, I., KIM, K. W., ZIGMOND, E., FURTADO, G. C., LIRA, S. A. & SHAKHAR, G. 2013. Luminal bacteria recruit CD103+ dendritic cells into the intestinal epithelium to sample bacterial antigens for presentation. *Immunity,* 38**,** 581-95.

FIEVEZ, V., MBANZAMIHIGO, L., PIATTONI, F. & DEMEYER, D. 2001. Evidence for reductive acetogenesis and its nutritional significance in ostrich hindgut as estimated from in vitro incubations. *Journal of Animal Physiology and Animal Nutrition,* 85**,** 271-280.

FRANCHI, L., WARNER, N., VIANI, K. & NUÑEZ, G. 2009. Function of Nod-like Receptors in Microbial Recognition and Host Defense. *Immunological reviews,* 227**,** 106-128.

FRANCOLEON, D. R., BOONTHEUNG, P., YANG, Y., KIM, U., YTTERBERG, A. J., DENNY, P. A., DENNY, P. C., LOO, J. A., GUNSALUS, R. P. & OGORZALEK LOO, R. R. 2009. S-layer Surface-Accessible and Concanavalin A Binding Proteins of Methanosarcina acetivorans and Methanosarcina mazei. *Journal of proteome research,* 8**,** 1972-1982.

FRICKE, W. F., SEEDORF, H., HENNE, A., KRUER, M., LIESEGANG, H., HEDDERICH, R., GOTTSCHALK, G. & THAUER, R. K. 2006. The genome sequence of *Methanosphaera stadtmanae* reveals why this human intestinal archaeon is restricted to methanol and H2 for methane formation and ATP synthesis. *Journal of Bacteriology,* 188**,** 642-58.

GACI, N., BORREL, G., TOTTEY, W., O'TOOLE, P. W. & BRUGERE, J. F. 2014. Archaea and the human gut: New beginning of an old story. *World J Gastroenterol,* 20**,** 16062-16078.

GAGEN, E. J., DENMAN, S. E., PADMANABHA, J., ZADBUKE, S., AL JASSIM, R., MORRISON, M. & MCSWEENEY, C. S. 2010. Functional gene analysis suggests different acetogen populations in the bovine rumen and tammar wallaby forestomach. *Applied and Environmental Microbiology,* 76**,** 7785-95.

GAGEN, E. J., WANG, J., PADMANABHA, J., LIU, J., DE CARVALHO, I. P., LIU, J., WEBB, R. I., AL JASSIM, R., MORRISON, M., DENMAN, S. E. & MCSWEENEY, C. S. 2014. Investigation of a new acetogen isolated from an enrichment of the tammar wallaby forestomach. *BMC Microbiol,* 14**,** 314.

GARNAUT, R. 2008. The Garnaut Climate Change Review. New York: Cambridge University Press.

GEREMIA, A. & JEWELL, D. P. 2012. The IL-23/IL-17 pathway in inflammatory bowel disease. *Expert Rev Gastroenterol Hepatol,* 6**,** 223-37.

GODWIN, S., KANG, A., GULINO, L.-M., MANEFIELD, M., GUTIERREZ-ZAMORA, M.-L., KIENZLE, M., OUWERKERK, D., DAWSON, K. & KLIEVE, A. V. 2014. Investigation of the microbial metabolism of carbon dioxide and hydrogen in the kangaroo foregut by stable isotope probing. *ISME J,* 8**,** 1855-1865.

GOTTLIEB, K., WACHER, V., SLIMAN, J. & PIMENTEL, M. 2016. Review article: inhibition of methanogenic archaea by statins as a targeted management strategy for constipation and related disorders. *Aliment Pharmacol Ther,* 43**,** 197-212.

HAINES, A., METZ, G., DILAWARI, J., BLENDIS, L. & WIGGINS, H. 1977. Breath-methane in patients with cancer of the large bowel. *Lancet,* 2**,** 481-3.

HANSEN, E. E., LOZUPONE, C. A., REY, F. E., WU, M., GURUGE, J. L., NARRA, A., GOODFELLOW, J., ZANEVELD, J. R., MCDONALD, D. T., GOODRICH, J. A., HEATH, A. C., KNIGHT, R. & GORDON, J. I. 2011. Pan-genome of the dominant human gut-associated archaeon, Methanobrevibacter smithii, studied in twins. *Proc Natl Acad Sci U S A,* 108 Suppl 1**,** 4599-606.

HESS, M., SCZYRBA, A., EGAN, R., KIM, T.-W., CHOKHAWALA, H., SCHROTH, G., LUO, S., CLARK, D. S., CHEN, F., ZHANG, T., MACKIE, R. I., PENNACCHIO, L. A., TRINGE, S. G., VISEL, A., WOYKE, T., WANG, Z. & RUBIN, E. M. 2011. Metagenomic Discovery of Biomass-Degrading Genes and Genomes from Cow Rumen. *Science,* 331**,** 463-467.

HOBSON, P. N. (ed.) 1988. *The rumen microbial ecosystem,* New York: Elsevier Applied Science.

HOBSON, P. N. & STEWART, C. S. (eds.) 1997. *The rumen microbial ecosystem,* London: Blackie Academic & Professional.

HORZ, H. P. & CONRADS, G. 2011. Methanogenic Archaea and oral infections - ways to unravel the black box. *J Oral Microbiol,* 3.

HUME, D. A., UNDERHILL, D. M., SWEET, M. J., OZINSKY, A. O., LIEW, F. Y. & ADEREM, A. 2001. Macrophages exposed continuously to lipopolysaccharide and other agonists that act via toll-like receptors exhibit a sustained and additive activation state. *BMC Immunology,* 2**,** 1-12.

HUME, I. 1984. Microbial fermentation in herbivorous marsupials. *BioScience,* 34**,** 435-440.

HWANG, K., SHIN, S. G., KIM, J. & HWANG, S. 2008. Methanogenic profiles by denaturing gradient gel electrophoresis using order-specific primers in anaerobic sludge digestion. *Applied Microbiology and Biotechnology,* 80**,** 269-76.

INOHARA, N. & NUNEZ, G. 2001. The NOD: a signaling module that regulates apoptosis and host defense against pathogens. *Oncogene,* 20**,** 6473-81.

IPCC 2007. Climate Change 2007: The Physical Science Basis, Contribution of Working Group I to the Fourth Assessment Report of the Intergovernmental Panel on Climate Change. Cambridge: Cambridge University Press.

JAEKAL, J., ABRAHAM, E., AZAM, T., NETEA, M. G., DINARELLO, C. A., LIM, J. S., YANG, Y., YOON, D. Y. & KIM, S. H. 2007. Individual LPS responsiveness depends on the variation of toll-like receptor (TLR) expression level. *J Microbiol Biotechnol,* 17**,** 1862-7.

JANSSEN, P. H. 2010. Influence of hydrogen on rumen methane formation and fermentation balances through microbial growth kinetics and fermentation thermodynamics. *Animal Feed Science and Technology,* 160**,** 1-22.

JANSSEN, P. H. & KIRS, M. 2008. Structure of the Archaeal Community of the Rumen. *Applied and Environmental Microbiology,* 74**,** 3619-3625.

JARRELL, K. F., JONES, G. M. & NAIR, D. B. 2010. Biosynthesis and Role of N-Linked Glycosylation in Cell Surface Structures of Archaea with a Focus on Flagella and S Layers. *International Journal of Microbiology,* 2010**,** 20.

JARVIS, G. N., STROMPL, C., BURGESS, D. M., SKILLMAN, L. C., MOORE, E. R. & JOBLIN, K. N. 2000. Isolation and identification of ruminal methanogens from grazing cattle. *Current Microbiology,* 40**,** 327-32.

JOBLIN, K. N., NAYLOR, G. E. & WILLIAMS, A. G. 1990. Effect of *Methanobrevibacter smithii* on xylanolytic activity of anaerobic ruminal fungi. *Applied and Environmental Microbiology,* 56**,** 2287-2295.

JOHNSON, K. A. & GOODY, R. S. 2011. The Original Michaelis Constant: Translation of the 1913 Michaelis–Menten Paper. *Biochemistry,* 50**,** 8264-8269.

JOHNSON, K. A. & JOHNSON, D. E. 1995. Methane emissions from cattle. *Journal of Animal Science,* 73**,** 2483-92.

JOHNSTON, C., UFNAR, J. A., GRIFFITH, J. F., GOOCH, J. A. & STEWART, J. R. 2010. A real-time qPCR assay for the detection of the nifH gene of Methanobrevibacter smithii, a potential indicator of sewage pollution. *J Appl Microbiol,* 109**,** 1946-56.

KANEHISA, M. & GOTO, S. 2000. KEGG: Kyoto encyclopedia of genes and genomes. *Nucleic Acids Research,* 28**,** 27-30.

KANEHISA, M., GOTO, S., FURUMICHI, M., TANABE, M. & HIRAKAWA, M. 2010. KEGG for representation and analysis of molecular networks involving diseases and drugs. *Nucleic Acids Research,* 38**,** D355-60.

KANEHISA, M., GOTO, S., HATTORI, M., AOKI-KINOSHITA, K. F., ITOH, M., KAWASHIMA, S., KATAYAMA, T., ARAKI, M. & HIRAKAWA, M. 2006. From genomics to chemical genomics: new developments in KEGG. *Nucleic Acids Research,* 34**,** D354-7.

KANG, D. D., FROULA, J., EGAN, R. & WANG, Z. 2014. A robust statistical framework for reconstructing genomes from metagenomic data. *bioRxiv*.

KANG, J. Y. 1993. The gastrointestinal tract in uremia. *Digestive Diseases and Sciences,* 38**,** 257-268.

KARASOV, W. H. & CAREY, H. V. 2009. Metabolic teamwork between gut microbes and hosts. *Microbe,* 4**,** 323-328.

KARLSSON, F. H., TREMAROLI, V., NOOKAEW, I., BERGSTROM, G., BEHRE, C. J., FAGERBERG, B., NIELSEN, J. & BACKHED, F. 2013. Gut metagenome in European women with normal, impaired and diabetic glucose control. *Nature,* 498**,** 99-103.

KEMPTON, T. J., MURRAY, R. M. & LENG, R. A. 1976. Methane production and digestability measurements in the grey kangaroo and sheep. *Australian Journal of Biological Sciences* 29**,** 209-214.

KIM, M., OH, H. S., PARK, S. C. & CHUN, J. 2014. Towards a taxonomic coherence between average nucleotide identity and 16S rRNA gene sequence similarity for

species demarcation of prokaryotes. *International Journal of Systematic and Evolutionary Microbiology,* 64**,** 346-51.

KIMURA, M. 1980. A simple method for estimating evolutionary rates of base substitutions through comparative studies of nucleotide sequences. *Journal of Molecular Evolution,* 16**,** 111-20.

KITTELMANN, S., PINARES-PATIÑO, C. S., SEEDORF, H., KIRK, M. R., GANESH, S., MCEWAN, J. C. & JANSSEN, P. H. 2014. Two Different Bacterial Community Types Are Linked with the Low-Methane Emission Trait in Sheep. *PLoS ONE,* 9**,** e103171.

KONSTANTINIDIS, K. T., RAMETTE, A. & TIEDJE, J. M. 2006. The bacterial species definition in the genomic era. *Philosophical Transactions of the Royal Society B: Biological Sciences,* 361**,** 1929-1940.

KOVAROVA-KOVAR, K. & EGLI, T. 1998. Growth kinetics of suspended microbial cells: from single-substrate-controlled growth to mixed-substrate kinetics. *Microbiol Mol Biol Rev,* 62**,** 646-66.

KRAMER, J. K. G. & SAUER, F. D. 1991. Changes in the diether-to-tetraether-lipid ratio during cell growth in Methanobacterium thermoautotrophicum. *FEMS Microbiology Letters,* 83**,** 45-50.

LANE, D. J., PACE, B., OLSEN, G. J., STAHL, D. A., SOGIN, M. L. & PACE, N. R. 1985. Rapid determination of 16S ribosomal RNA sequences for phylogenetic analyses. *Proceedings of the National Academy of Sciences USA,* 82**,** 6955-9.

LASSEY, K. R. 2007. Livestock methane emission: From the individual grazing animal through national inventories to the global methane cycle. *Agricultural and Forest Meteorology,* 142**,** 120-132.

LASSEY, K. R., ULYATT, M. J., MARTIN, R. J., WALKER, C. F. & DAVID SHELTON, I. 1997. Methane emissions measured directly from grazing livestock in New Zealand. *Atmospheric Environment,* 31**,** 2905-2914.

LAU, E., CARVALHO, D. & FREITAS, P. 2015. Gut Microbiota: Association with NAFLD and Metabolic Disturbances. *BioMed Research International,* 2015**,** 9.

LEAHY, S. C., KELLY, W. J., ALTERMANN, E., RONIMUS, R. S., YEOMAN, C. J., PACHECO, D. M., LI, D., KONG, Z., MCTAVISH, S., SANG, C., LAMBIE, S. C., JANSSEN, P. H., DEY, D. & ATTWOOD, G. T. 2010. The genome sequence of the rumen methanogen *Methanobrevibacter ruminantium* reveals new possibilities for controlling ruminant methane emissions. *PLoS One,* 5**,** e8926.

LEAHY, S. C., KELLY, W. J., LI, D., LI, Y., ALTERMANN, E., LAMBIE, S. C., COX, F. & ATTWOOD, G. T. 2013. The Complete Genome Sequence of Methanobrevibacter sp. AbM4. *Stand Genomic Sci,* 8**,** 215-27.

LEE, H. J., PAHL, M. V., VAZIRI, N. D. & BLAKE, D. R. 2012. Effect of hemodialysis and diet on the exhaled breath methanol concentration in patients with ESRD. *J Ren Nutr,* 22**,** 357-64.

LIDE, D. R. (ed.) 2003. *CRC handbook of chemistry and physics,* Boca Raton, Florida: CRC Press.

LIEBREGTS, T., ADAM, B., BREDACK, C., RÖTH, A., HEINZEL, S., LESTER, S., DOWNIE–DOYLE, S., SMITH, E., DREW, P., TALLEY, N. J. & HOLTMANN, G. 2007. Immune Activation in Patients With Irritable Bowel Syndrome. *Gastroenterology,* 132**,** 913-920.

LINEWEAVER, H. & BURK, D. 1934. The Determination of Enzyme Dissociation Constants. *Journal of the American Chemical Society,* 56**,** 658-666.

LIU, Y. & WHITMAN, W. B. 2008. Metabolic, phylogenetic, and ecological diversity of the methanogenic archaea. *Annals of the New York Academy of Sciences,* 1125**,** 171-89.

LOWE, D. C. 2006. Global change: a green source of surprise. *Nature,* 439**,** 148-9.

LUDWIG, W., STRUNK, O., WESTRAM, R., RICHTER, L., MEIER, H., YADHUKUMAR, BUCHNER, A., LAI, T., STEPPI, S., JOBB, G., FORSTER, W., BRETTSKE, I., GERBER, S., GINHART, A. W., GROSS, O., GRUMANN, S., HERMANN, S., JOST, R., KONIG, A., LISS, T., LUSSMANN, R., MAY, M., NONHOFF, B., REICHEL, B., STREHLOW, R., STAMATAKIS, A., STUCKMANN, N., VILBIG, A., LENKE, M., LUDWIG, T., BODE, A. & SCHLEIFER, K. H. 2004. ARB: a software environment for sequence data. *Nucleic Acids Research,* 32**,** 1363-71.

LUO, Y. H., WRIGHT, A. D., LI, Y. L., LI, H., YANG, Q. H., LUO, L. J. & YANG, M. X. 2013. Diversity of methanogens in the hindgut of captive white rhinoceroses, Ceratotherium simum. *BMC Microbiol,* 13**,** 207.

MADSEN, J. & BERTELSEN, M. F. 2012. Methane production by red-necked wallabies (*Macropus rufogriseus*). *Journal of Animal Science,* 4.

MAGIDOVICH, H. & EICHLER, J. 2009. Glycosyltransferases and oligosaccharyltransferases in Archaea: putative components of the N-glycosylation pathway in the third domain of life. *FEMS Microbiology Letters,* 300**,** 122-130.

MAO, S. Y., YANG, C. F. & ZHU, W. Y. 2011. Phylogenetic analysis of methanogens in the pig feces. *Current Microbiology,* 62**,** 1386-9.

MARIC, I., HOLT, P. G., PERDUE, M. H. & BIENENSTOCK, J. 1996. Class II MHC antigen (Ia)-bearing dendritic cells in the epithelium of the rat intestine. *J Immunol,* 156**,** 1408-14.

MARKOWITZ, V. M., CHEN, I.-M. A., PALANIAPPAN, K., CHU, K., SZETO, E., GRECHKIN, Y., RATNER, A., JACOB, B., HUANG, J., WILLIAMS, P., HUNTEMANN, M., ANDERSON, I., MAVROMATIS, K., IVANOVA, N. N. & KYRPIDES, N. C. 2012. IMG: the integrated microbial genomes database and comparative analysis system. *Nucleic Acids Research,* 40**,** D115-D122.

MATHUR, R., AMICHAI, M., CHUA, K. S., MIROCHA, J., BARLOW, G. M. & PIMENTEL, M. 2013. Methane and hydrogen positivity on breath test is associated with greater body mass index and body fat. *J Clin Endocrinol Metab,* 98**,** E698-702.

MILLER, T. L. & LIN, C. 2002. Description of Methanobrevibacter gottschalkii sp. nov., Methanobrevibacter thaueri sp. nov., Methanobrevibacter woesei sp. nov. and Methanobrevibacter wolinii sp. nov. *Int J Syst Evol Microbiol,* 52**,** 819-22.

MILLER, T. L. & WOLIN, M. J. 1983. Oxidation of hydrogen and reduction of methanol to methane is the sole energy source for a methanogen isolated from human feces. *Journal of Bacteriology,* 153**,** 1051-5.

MILLER, T. L. & WOLIN, M. J. 1985. *Methanosphaera stadtmaniae* gen. nov., sp. nov.: a species that forms methane by reducing methanol with hydrogen. *Archives of Microbiology,* 141**,** 116-22.

MILLER, T. L., WOLIN, M. J., CONWAY DE MACARIO, E. & MACARIO, A. J. 1982. Isolation of Methanobrevibacter smithii from human feces. *Appl Environ Microbiol,* 43**,** 227-32.

MORRISON, M. 2013. Looking large, to make more, out of gut metagenomics. *Current Opinion in Microbiology,* 16**,** 630-635.

MOWAT, A. M. & BAIN, C. C. 2011. Mucosal macrophages in intestinal homeostasis and inflammation. *J Innate Immun,* 3**,** 550-64.

MUDTER, J. & NEURATH, M. F. 2007. Il-6 signaling in inflammatory bowel disease: pathophysiological role and clinical relevance. *Inflamm Bowel Dis,* 13**,** 1016-23.

MURTAGH, F. E. M., ADDINGTON-HALL, J. & HIGGINSON, I. J. 2007. The Prevalence of Symptoms in End-Stage Renal Disease: A Systematic Review. *Advances in Chronic Kidney Disease,* 14**,** 82-99.

NALLU, A., SHARMA, S., RAMEZANI, A., MURALIDHARAN, J. & RAJ, D. 2016. Gut microbiome in chronic kidney disease: challenges and opportunities. *Translational Research*.

NAVA, G. M., CARBONERO, F., OU, J., BENEFIEL, A. C., O'KEEFE, S. J. & GASKINS, H. R. 2012. Hydrogenotrophic microbiota distinguish native Africans from African and European Americans. *Environmental Microbiology Reports,* 4**,** 307-315.

NOTTINGHAM, P. M. & HUNGATE, R. E. 1968. Isolation of methanogenic bacteria from feces of man. *J Bacteriol,* 96**,** 2178-9.

O'KEEFE, S. J., CHUNG, D., MAHMOUD, N., SEPULVEDA, A. R., MANAFE, M., ARCH, J., ADADA, H. & VAN DER MERWE, T. 2007. Why do African Americans get more colon cancer than Native Africans? *J Nutr,* 137**,** 175S-182S.

OCHMAN, H. & MORAN, N. A. 2001. Genes Lost and Genes Found: Evolution of Bacterial Pathogenesis and Symbiosis. *Science,* 292**,** 1096-1099.

OREN, A. & GARRITY, G. M. 2013. List of new names and new combinations previously effectively, but not validly, published. *International Journal of Systematic and Evolutionary Microbiology,* 63**,** 3931-3934.

OUWERKERK, D., MAGUIRE, A. J., KLIEVE, A. V. & MCMILLENA, L. 2009. Hydrogen utilising bacteria from the forestomach of eastern grey (*Macropus giganteus*) and red (*Macropus rufus*) kangaroos. *Animal Production Science,* 49**,** 1043–1051.

OUWERKERK, D., TURNER, A. F. & KLIEVE, A. V. 2008. Diversity of methanogens in ruminants in Queensland. *Australian Journal of Experimental Agriculture* 48**,** 722-725.

PARKS, D. H., IMELFORT, M., SKENNERTON, C. T., HUGENHOLTZ, P. & TYSON, G. W. 2015. CheckM: assessing the quality of microbial genomes recovered from isolates, single cells, and metagenomes. *Genome Res,* 25**,** 1043-55.

PAUL, K., NONOH, J. O., MIKULSKI, L. & BRUNE, A. 2012. "*Methanoplasmatales*," *Thermoplasmatales*-related archaea in termite guts and other environments, are the seventh order of methanogens. *Applied and Environmental Microbiology,* 78**,** 8245-53.

PEI, C.-X., MAO, S.-Y., CHENG, Y.-F. & ZHU, W.-Y. 2009. Diversity, abundance and novel 16S rRNA gene sequences of methanogens in rumen liquid, solid and epithelium fractions of Jinnan cattle. *Animal,* FirstView**,** 1-10.

PFAFFL, M. W. 2001. A new mathematical model for relative quantification in real-time RT–PCR. *Nucleic Acids Research,* 29**,** e45-e45.

PIMENTEL, M., LIN, H. C., ENAYATI, P., VAN DEN BURG, B., LEE, H. R., CHEN, J. H., PARK, S., KONG, Y. & CONKLIN, J. 2006. Methane, a gas produced by enteric bacteria, slows intestinal transit and augments small intestinal contractile activity. *Am J Physiol Gastrointest Liver Physiol,* 290**,** G1089-95.

PINARES-PATIÑO, C. S., EBRAHIMI, S. H., MCEWAN, J. C., DODDS, K. G., CLARK, H. & LUO, D. 2011a. *Is rumen retention time implicated in sheep differences in methane emission?,* New Zealand Society of Animal Production.

PINARES-PATINO, C. S., HICKEY, S. M., YOUNG, E. A., DODDS, K. G., MACLEAN, S., MOLANO, G., SANDOVAL, E., KJESTRUP, H., HARLAND, R., HUNT, C., PICKERING, N. K. & MCEWAN, J. C. 2013. Heritability estimates of methane emissions from sheep. *Animal,* 7 Suppl 2**,** 316-21.

PINARES-PATIÑO, C. S., LASSEY, K. R., MARTIN, R. J., MOLANO, G., FERNANDEZ, M., MACLEAN, S., SANDOVAL, E., LUO, D. & CLARK, H. 2011b. Assessment of the sulphur hexafluoride (SF6) tracer technique using respiration chambers for estimation of methane emissions from sheep. *Animal Feed Science and Technology,* 166**,** 201-209.

PONTES, H., GUEDES DE PINHO, P., CASAL, S., CARMO, H., SANTOS, A., MAGALHAES, T., REMIAO, F., CARVALHO, F. & LOURDES BASTOS, M. 2009. GC determination of acetone, acetaldehyde, ethanol, and methanol in biological matrices and cell culture. *Journal of Chromatographic Science,* 47**,** 272-8.

POPE, P. B., SMITH, W., DENMAN, S. E., TRINGE, S. G., BARRY, K., HUGENHOLTZ, P., MCSWEENEY, C. S., MCHARDY, A. C. & MORRISON, M. 2011. Isolation of Succinivibrionaceae implicated in low methane emissions from Tammar wallabies. *Science,* 333**,** 646-8.

POULSEN, M., SCHWAB, C., BORG JENSEN, B., ENGBERG, R. M., SPANG, A., CANIBE, N., HØJBERG, O., MILINOVICH, G., FRAGNER, L., SCHLEPER, C., WECKWERTH, W., LUND, P., SCHRAMM, A. & URICH, T. 2013. Methylotrophic methanogenic Thermoplasmata implicated in reduced methane emissions from bovine rumen. *Nat Commun,* 4**,** 1428.

PRICE, M. N., DEHAL, P. S. & ARKIN, A. P. 2010. FastTree 2 – Approximately Maximum-Likelihood Trees for Large Alignments. *PLoS ONE,* 5**,** e9490.

PRIEFERT, H. & STEINBUCHEL, A. 1992. Identification and molecular characterization of the acetyl coenzyme A synthetase gene (acoE) of Alcaligenes eutrophus. *J Bacteriol,* 174**,** 6590-9.

RASKIN, L., STROMLEY, J. M., RITTMANN, B. E. & STAHL, D. A. 1994. Group-specific 16S rRNA hybridization probes to describe natural communities of methanogens. *Applied and Environmental Microbiology,* 60**,** 1232-40.

RASMUSSEN, R. 2001. Quantification on the LightCycler. *In:* MEUER, S., WITTWER, C. & NAKAGAWARA, K.-I. (eds.) *Rapid Cycle Real-Time PCR.* Springer Berlin Heidelberg.

REA, S., BOWMAN, J. P., POPOVSKI, S., PIMM, C. & WRIGHT, A.-D. G. 2007. Methanobrevibacter millerae sp. nov. and Methanobrevibacter olleyae sp. nov., methanogens from the ovine and bovine rumen that can utilize formate for growth. *International Journal of Systematic and Evolutionary Microbiology,* 57**,** 450-456.

RESCIGNO, M., URBANO, M., VALZASINA, B., FRANCOLINI, M., ROTTA, G., BONASIO, R., GRANUCCI, F., KRAEHENBUHL, J. P. & RICCIARDI-CASTAGNOLI, P. 2001. Dendritic cells express tight junction proteins and penetrate gut epithelial monolayers to sample bacteria. *Nat Immunol,* 2**,** 361-7.

ROHLIN, L., LEON, D. R., KIM, U., LOO, J. A., OGORZALEK LOO, R. R. & GUNSALUS, R. P. 2012. Identification of the major expressed S-layer and cell surface-layer-related proteins in the model methanogenic archaea: Methanosarcina barkeri Fusaro and Methanosarcina acetivorans C2A. *Archaea,* 2012**,** 873589.

ROSSET, S. 2007. Efficient inference on known phylogenetic trees using Poisson regression. *Bioinformatics,* 23**,** e142-e147.

ROSSI, M., JOHNSON, D. W., MORRISON, M., PASCOE, E., COOMBES, J. S., FORBES, J. M., MCWHINNEY, B. C., UNGERER, J. P. J., DIMESKI, G. & CAMPBELL, K. L. 2014. SYNbiotics Easing Renal failure by improving Gut microbiologY (SYNERGY): a protocol of placebo-controlled randomised cross-over trial. *BMC Nephrology,* 15**,** 106-106.

ROSSI, M., JOHNSON, D. W., MORRISON, M., PASCOE, E. M., COOMBES, J. S., FORBES, J. M., SZETO, C. C., MCWHINNEY, B. C., UNGERER, J. P. & CAMPBELL, K. L. 2016. Synbiotics Easing Renal Failure by Improving Gut Microbiology (SYNERGY): A Randomized Trial. *Clin J Am Soc Nephrol,* 11**,** 223-31.

ROZEN, S. & SKALETSKY, H. 2000. Primer3 on the WWW for general users and for biologist programmers. *Methods Mol Biol,* 132**,** 365-86.

RUTHERFORD, K., PARKHILL, J., CROOK, J., HORSNELL, T., RICE, P., RAJANDREAM, M. A. & BARRELL, B. 2000. Artemis: sequence visualization and annotation. *Bioinformatics,* 16**,** 944-5.

SAKAI, S., IMACHI, H., HANADA, S., OHASHI, A., HARADA, H. & KAMAGATA, Y. 2008. Methanocella paludicola gen. nov., sp. nov., a methane-producing archaeon, the first isolate of the lineage 'Rice Cluster I', and proposal of the new archaeal order Methanocellales ord. nov. *International Journal of Systematic and Evolutionary Microbiology,* 58**,** 929-936.

SAMUEL, B. S., HANSEN, E. E., MANCHESTER, J. K., COUTINHO, P. M., HENRISSAT, B., FULTON, R., LATREILLE, P., KIM, K., WILSON, R. K. & GORDON, J. I. 2007. Genomic and metabolic adaptations of *Methanobrevibacter smithii* to the human gut. *Proc Natl Acad Sci U S A,* 104**,** 10643-8.

SCANLAN, P. D., SHANAHAN, F. & MARCHESI, J. R. 2008. Human methanogen diversity and incidence in healthy and diseased colonic groups using mcrA gene analysis. *BMC Microbiol,* 8**,** 79.

SEEDORF, H., KITTELMANN, S. & JANSSEN, P. H. 2015. Few highly abundant operational taxonomic units dominate within rumen methanogenic archaeal species in New Zealand sheep and cattle. *Appl Environ Microbiol,* 81**,** 986-95.

SHAKHOV, A. N., COLLART, M. A., VASSALLI, P., NEDOSPASOV, S. A. & JONGENEEL, C. V. 1990. Kappa B-type enhancers are involved in lipopolysaccharide-mediated transcriptional activation of the tumor necrosis factor alpha gene in primary macrophages. *The Journal of Experimental Medicine,* 171**,** 35-47.

SHAMES, B. D., SELZMAN, C. H., PULIDO, E. J., MENG, X., MELDRUM, D. R., MCINTYRE, R. C., HARKEN, A. H. & BANERJEE, A. 1999. LPS-Induced NF-κB Activation and TNF-α Release in Human Monocytes Are Protein Tyrosine Kinase Dependent and Protein Kinase C Independent. *Journal of Surgical Research,* 83**,** 69-74.

SHI, W., MOON, C. D., LEAHY, S. C., KANG, D., FROULA, J., KITTELMANN, S., FAN, C., DEUTSCH, S., GAGIC, D., SEEDORF, H., KELLY, W. J., ATUA, R., SANG, C., SONI, P., LI, D., PINARES-PATINO, C. S., MCEWAN, J. C., JANSSEN, P. H., CHEN, F., VISEL, A., WANG, Z., ATTWOOD, G. T. & RUBIN, E. M. 2014.

Methane yield phenotypes linked to differential gene expression in the sheep rumen microbiome. *Genome Res,* 24**,** 1517-25.

SMITH, J. A. 2009. Macropod nutrition. *Vet Clin North Am Exot Anim Pract,* 12**,** 197-208, xiii.

ST-PIERRE, B. & WRIGHT, A. D. 2013. Diversity of gut methanogens in herbivorous animals. *Animal,* 7 Suppl 1**,** 49-56.

SUBHARAT, S., SHU, D., ZHENG, T., BUDDLE, B. M., JANSSEN, P. H., LUO, D. & WEDLOCK, D. N. 2015. Vaccination of cattle with a methanogen protein produces specific antibodies in the saliva which are stable in the rumen. *Veterinary Immunology and Immunopathology,* 164**,** 201-207.

SULLIVAN, M. J., BEN ZAKOUR, N. L., FORDE, B. M., STANTON-COOK, M. & BEATSON, S. A. 2015. Contiguity: Contig adjacency graph construction and visualisation. *PeerJ PrePrints,* 3**,** e1273.

TAKAHASHI-IWANAGA, H., IWANAGA, T. & ISAYAMA, H. 1999. Porosity of the epithelial basement membrane as an indicator of macrophage-enterocyte interaction in the intestinal mucosa. *Arch Histol Cytol,* 62**,** 471-81.

TAMURA, K., PETERSON, D., PETERSON, N., STECHER, G., NEI, M. & KUMAR, S. 2011. MEGA5: Molecular Evolutionary Genetics Analysis Using Maximum Likelihood, Evolutionary Distance, and Maximum Parsimony Methods. *Molecular Biology and Evolution,* 28**,** 2731-9.

TANG, W. H. W., WANG, Z., KENNEDY, D. J., WU, Y., BUFFA, J., AGATISA-BOYLE, B., LI, X. S., LEVISON, B. S. & HAZEN, S. L. 2014. Gut Microbiota-Dependent Trimethylamine N-oxide (TMAO) Pathway Contributes to Both Development of Renal Insufficiency and Mortality Risk in Chronic Kidney Disease. *Circulation Research*.

THAUER, R. K., KASTER, A. K., SEEDORF, H., BUCKEL, W. & HEDDERICH, R. 2008. Methanogenic archaea: ecologically relevant differences in energy conservation. *Nature Reviews Microbiology,* 6**,** 579-91.

THOMPSON, J. D., HIGGINS, D. G. & GIBSON, T. J. 1994. CLUSTAL W: improving the sensitivity of progressive multiple sequence alignment through sequence weighting, position-specific gap penalties and weight matrix choice. *Nucleic Acids Research,* 22**,** 4673-4680.

VANDERHAEGHEN, S., LACROIX, C. & SCHWAB, C. 2015. Methanogen communities in stools of humans of different age and health status and co-occurrence with bacteria. *FEMS Microbiol Lett,* 362**,** fnv092.

VETRIANI, C., JANNASCH, H. W., MACGREGOR, B. J., STAHL, D. A. & REYSENBACH, A. L. 1999. Population structure and phylogenetic characterization of marine benthic Archaea in deep-sea sediments. *Applied and Environmental Microbiology,* 65**,** 4375-84.

WALLACE, R. J., ROOKE, J. A., MCKAIN, N., DUTHIE, C. A., HYSLOP, J. J., ROSS, D. W., WATERHOUSE, A., WATSON, M. & ROEHE, R. 2015. The rumen microbial metagenome associated with high methane production in cattle. *BMC Genomics,* 16**,** 839.

WANG, Z., KLIPFELL, E., BENNETT, B. J., KOETH, R., LEVISON, B. S., DUGAR, B., FELDSTEIN, A. E., BRITT, E. B., FU, X., CHUNG, Y. M., WU, Y., SCHAUER, P., SMITH, J. D., ALLAYEE, H., TANG, W. H., DIDONATO, J. A., LUSIS, A. J. & HAZEN, S. L. 2011. Gut flora metabolism of phosphatidylcholine promotes cardiovascular disease. *Nature,* 472**,** 57-63.

WELANDER, P. V. & METCALF, W. W. 2005. Loss of the mtr operon in Methanosarcina blocks growth on methanol, but not methanogenesis, and reveals an unknown methanogenic pathway. *Proc Natl Acad Sci U S A,* 102**,** 10664-9.

WEYAND, C. M., YOUNGE, B. R. & GORONZY, J. J. 2011. IFN-γ and IL-17 - The Two Faces of T Cell Pathology in Giant Cell Arteritis. *Current opinion in rheumatology,* 23**,** 43-49.

WHITEHOUSE, N. L., OLSON, V. M., SCHWAB, C. G., CHESBRO, W. R., CUNNINGHAM, K. D. & LYKOS, T. 1994. Improved techniques for dissociating particle-associated mixed ruminal microorganisms from ruminal digesta solids. *Journal of Animal Science,* 72**,** 1335-43.

WRIGHT, A. D., AUCKLAND, C. H. & LYNN, D. H. 2007. Molecular diversity of methanogens in feedlot cattle from Ontario and Prince Edward Island, Canada. *Applied and Environmental Microbiology,* 73**,** 4206-10.

WRIGHT, A. D. & PIMM, C. 2003. Improved strategy for presumptive identification of methanogens using 16S riboprinting. *Journal of Microbiological Methods,* 55**,** 337-49.

YAMABE, K., MAEDA, H., KOKEGUCHI, S., TANIMOTO, I., SONOI, N., ASAKAWA, S. & TAKASHIBA, S. 2008. Distribution of Archaea in Japanese patients with

periodontitis and humoral immune response to the components. *FEMS Microbiol Lett,* 287**,** 69-75.

YAO, J., MACKMAN, N., EDGINGTON, T. S. & FAN, S. T. 1997. Lipopolysaccharide induction of the tumor necrosis factor-alpha promoter in human monocytic cells. Regulation by Egr-1, c-Jun, and NF-kappaB transcription factors. *J Biol Chem,* 272**,** 17795-801.

YIN, Y., MAO, X., YANG, J., CHEN, X., MAO, F. & XU, Y. 2012. dbCAN: a web resource for automated carbohydrate-active enzyme annotation. *Nucleic Acids Res,* 40**,** W445-51.

YOUNGLESON, J. S., JONES, W. A., JONES, D. T. & WOODS, D. R. 1989. Molecular analysis and nucleotide sequence of the adh1 gene encoding an NADPH-dependent butanol dehydrogenase in the Gram-positive anaerobe Clostridium acetobutylicum. *Gene,* 78**,** 355-64.

YU, Z. & MORRISON, M. 2004. Improved extraction of PCR-quality community DNA from digesta and fecal samples. *BioTechniques,* 36**,** 808-12.

ZERBINO, D. R. & BIRNEY, E. 2008. Velvet: algorithms for de novo short read assembly using de Bruijn graphs. *Genome Res,* 18**,** 821-9.

ZHAO, Y., JIA, X., YANG, J., LING, Y., ZHANG, Z., YU, J., WU, J. & XIAO, J. 2014. PanGP: A tool for quickly analyzing bacterial pan-genome profile. *Bioinformatics*.

ZHAO, Y., WU, J., YANG, J., SUN, S., XIAO, J. & YU, J. 2012. PGAP: pan-genomes analysis pipeline. *Bioinformatics,* 28**,** 416-8.

ZHU, L., BAKER, S. S., GILL, C., LIU, W., ALKHOURI, R., BAKER, R. D. & GILL, S. R. 2013. Characterization of gut microbiomes in nonalcoholic steatohepatitis (NASH) patients: a connection between endogenous alcohol and NASH. *Hepatology,* 57**,** 601-9.